Geologic Mapping of the Franklin Volcanic Field Western Ross Sea, Antarctica

A Senior Honors Thesis

Submitted in Partial Fulfillment of the Requirements for graduation with distinction in Geological Sciences in the undergraduate colleges of The Ohio State University

by

Adrienne E. Smith

The Ohio State University
December 2004

Project Advisor: Terry J. Wilson, Department of Geological Sciences

Approved by

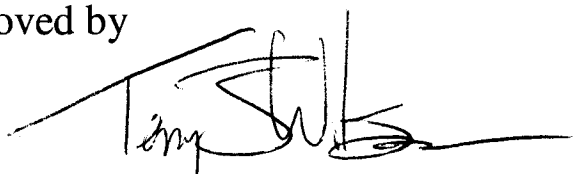

Terry J Wilson

Acknowledgements

I would like to thank Terry Wilson for allowing me to be part of the NBP 04-01 research expedition and for her perpetual guidance thereafter.

A great deal of credit is due to Marcy Davis, Stuart Henrys, Jerome Hall and other members of the NBP 04-01 cruise research team.

This work would also not be possible without the support of my committee members, parents, sisters, fellow geology students and Michael A. Block.

This research was funded by a grant from the National Science Foundation and the Research Experience for Undergraduates Initiative.

Abstract

The RVIB N. B. Palmer collected bathymetric and seismic data in the western Ross Sea in January/February 2004 with the specific purpose of mapping neotectonic structural and volcanic features on and beneath the seafloor. The Franklin Volcanic Field (FVF) is an important feature revealed by the bathymetric data. The volcanic field, which is expressed as a regional bathymetric high, is a minimum of 80 km long and up to 40 km wide. As one moves north, the overall trend of the volcanic field appears to curve from N-S to NE. Superimposed on the regional high are the subaerial portion of Franklin Island and clusters of submarine volcanic cones. Franklin Island has been interpreted as the western remnant of a shield volcano and has a single K-Ar date of 4.8+2 Ma. Its submarine morphology is characterized by a steep western flank and an eastern flank that, within the limits of the mapped region, appears to have a shallower slope. North of the island, there are 8 discrete cones, three of which were dredged, yielding basaltic lava, hyaloclastite and tuff. The seafloor morphology in the northern sector of the field is characterized by lineations at several scales, some hummocky terrain marked by circular to oval depressions, and superimposed iceberg scours. Based on morphology alone, the linear features could reflect volcanic ridges, faults, or glacial lineations, or may have formed by a combination of these processes. The origin of the seafloor features within the FVF has been determined through integrated analysis of magnetic, gravimetric and seismic data. Using the spatial associations of the features, this work proposes a reconstruction of the direction of glacial flow during the Last Glacial Maximum as well as maximum and minimum crustal stress directions during the formation of the Franklin Volcanic Field.

Table of Contents

Introduction

Within the western Ross Sea, Antarctica, abundant faulting and volcanism have long been known and recently interpreted as the manifestation of extension in the West Antarctic rift system. The rift system has been the site of Mesozoic to Cenozoic extension and Cenozoic volcanism including that responsible for the formation of Franklin Island. In the last two decades, marine geophysical surveys had begun to display the regional structures, including tectonically formed basins and basement highs underlying the western Ross Sea (Figure 1). However, detailed regional surveys had not been undertaken. In January - February 2004 a geophysical survey was completed aboard the RVIB Nathaniel B. Palmer (NBP 04-01) during which 7000 km of multibeam bathymetric, magnetic and gravity data were obtained (Figure 2 and 3). In addition, extensive new multichannel (2000 km) and single-channel (500 km) seismic reflection profiles were acquired. During the course of this survey, mapping of the seafloor features adjacent to Franklin Island revealed clusters of submarine volcanoes, possible volcanic ridges, curvilinear escarpments and probable glacial features on the seafloor. Due to these discoveries, this region became a focus for more continuous bathymetric mapping of the seafloor and seven seismic profiles were collected across the northern part of the field. Because of the wealth of diverse features, and abundant data, this region then became the focus of this study. This region is referred to here as the Franklin Volcanic Field after the emergent Franklin Island.

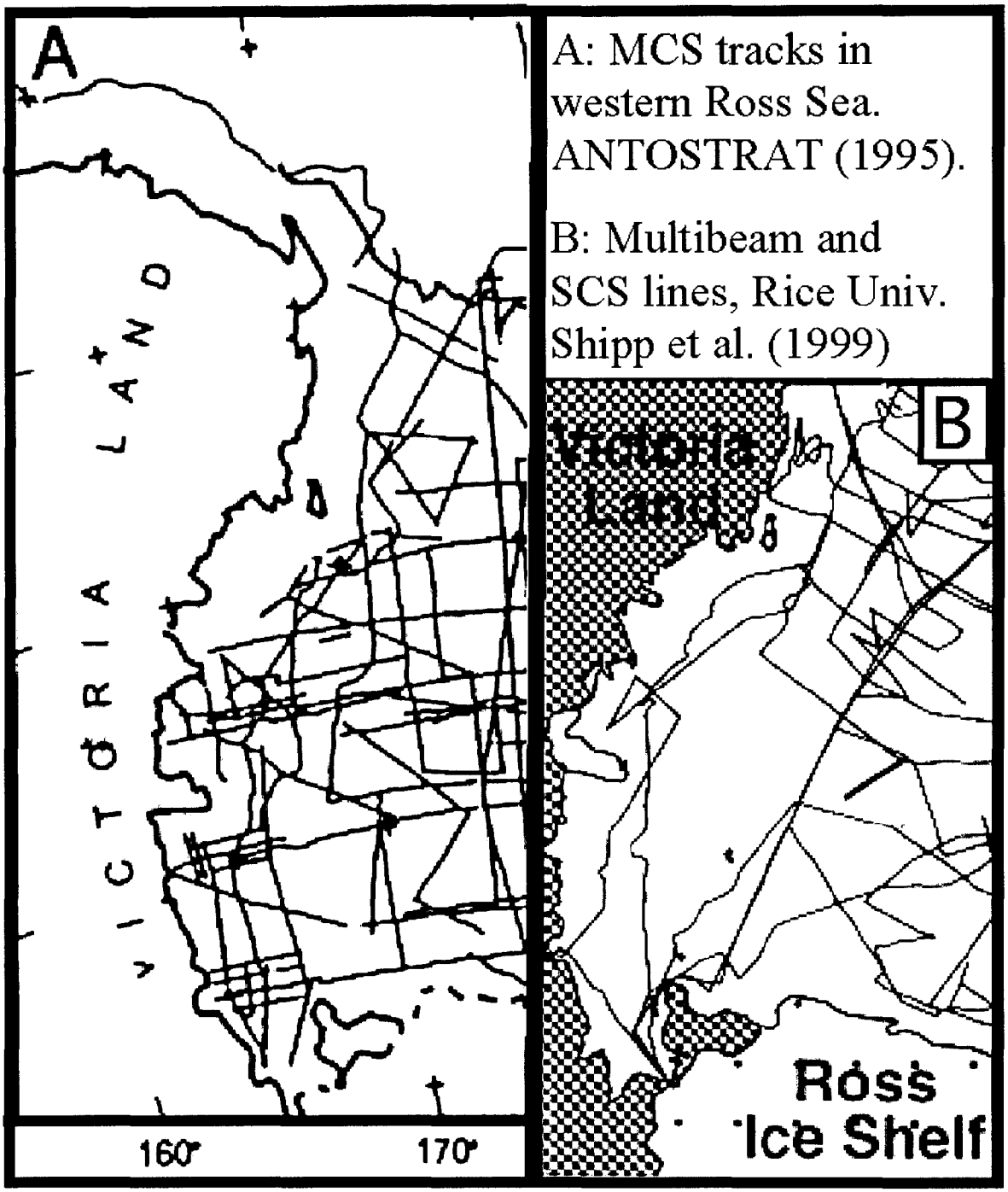

Figure 1: A) Previous multichannel seismic surveys. B) Pre-existing multibeam survey. Note the wide spacing observations within these geophysical data sets.

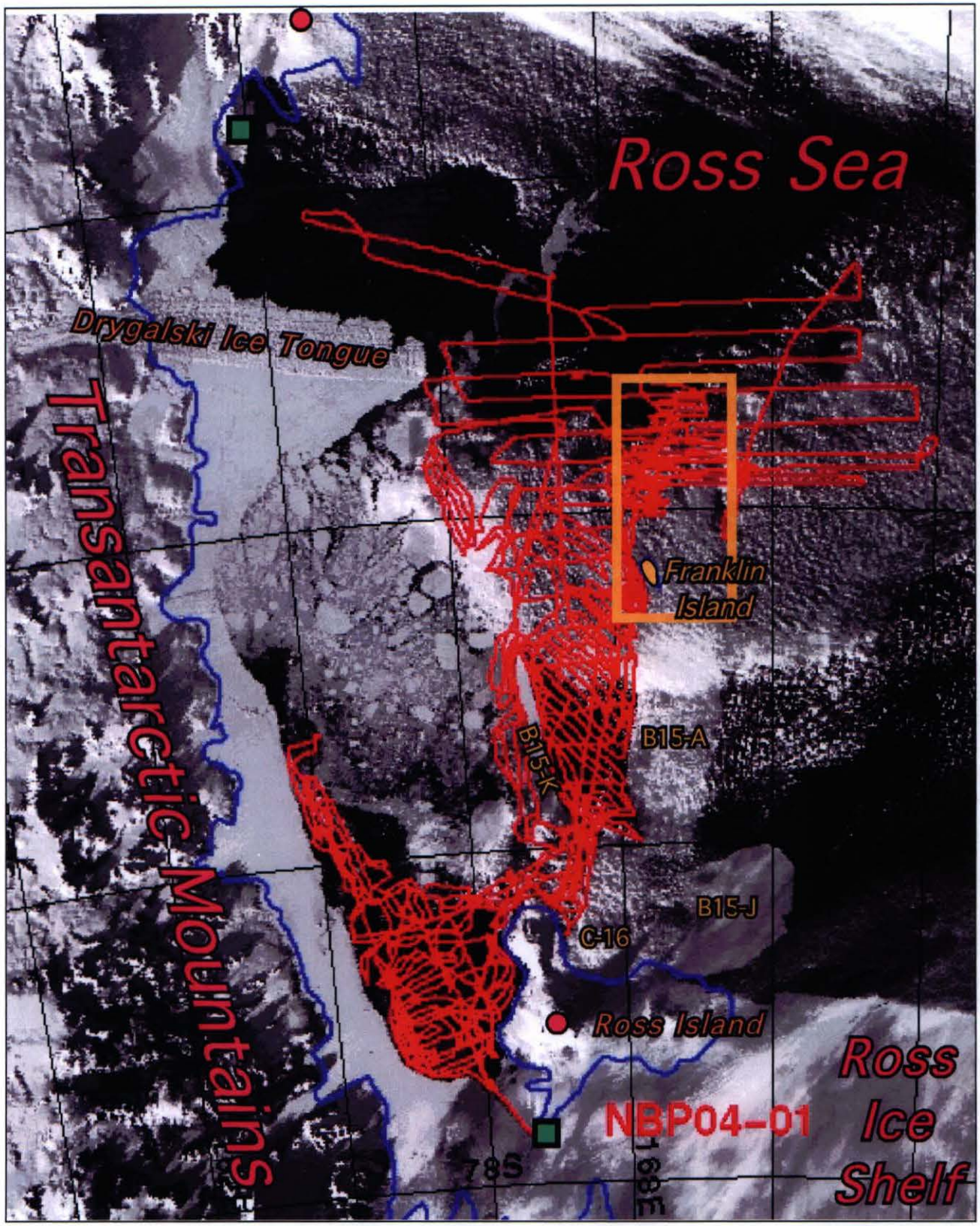

Figure 2: Satellite image of NBP 04-01survey area. Ship tracks are in red. Note the location of Franklin Island and large icebergs which inhibited further data collection.

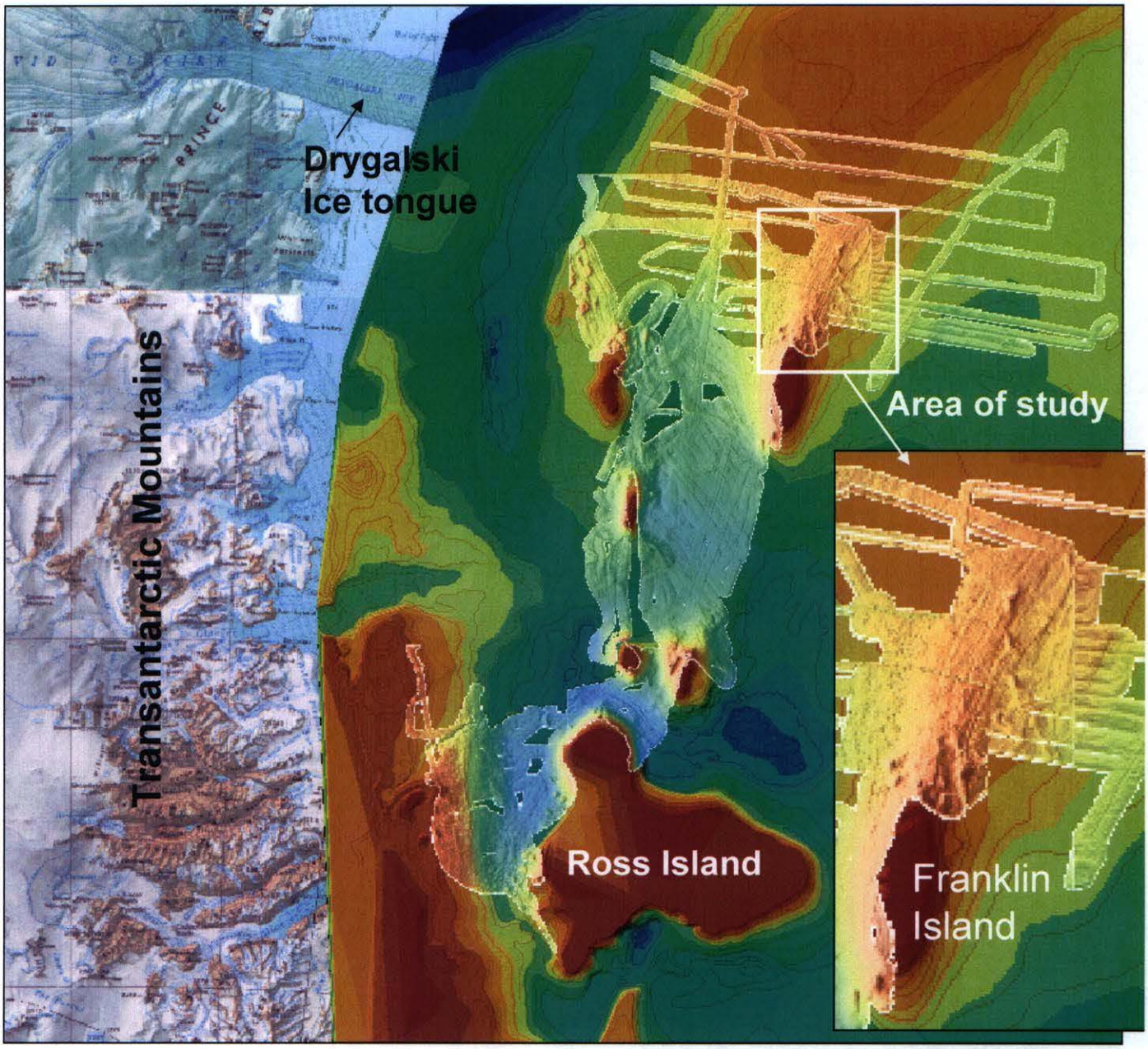

Figure 3: Position of Franklin Island in the Western Ross Sea. NBP 04-01 swath bathymetry superimposed on seafloor topography, shown by color gradient at 40 meter intervals.

Objectives and Scope of the study

Franklin Island is the western remnant of a shield volcano dating 4.8 +/- 2.0 Ma (Kyle, 1990) and the surface expression of an otherwise submarine volcanic field. On the northern flank of the island, there are diverse seafloor features which could be of tectonic, glacial or volcanic origin. The features formed by each mode of origin provide information about a distinctive aspect of the geologic evolution of the region. This study focuses on distinguishing features of different origin using observations from the geophysical data sets obtained during the NBP 04-01 cruise. Observations of bathymetric data, which lead to the interest in the region, will be integrated with magnetic, gravity and seismic data and compared to analogous features. Once the origin of the features has been determined, their spatial associations will be used to reconstruct conditions of their formation. Features of glacial origin are used to determine the direction of ice sheet movement during the Last Glacial Maximum. Features of volcanic and tectonic origin are used to reconstruct the principal stress directions that acted in the lithosphere during the observed deformation. Cross-cutting relationships are used to constrain the relative timing of events in the Franklin Volcanic Field. These results contribute to a greater understanding of the temporal and spatial constraints of recent and active(?) extensional tectonism in this part of the West Antarctic rift system.

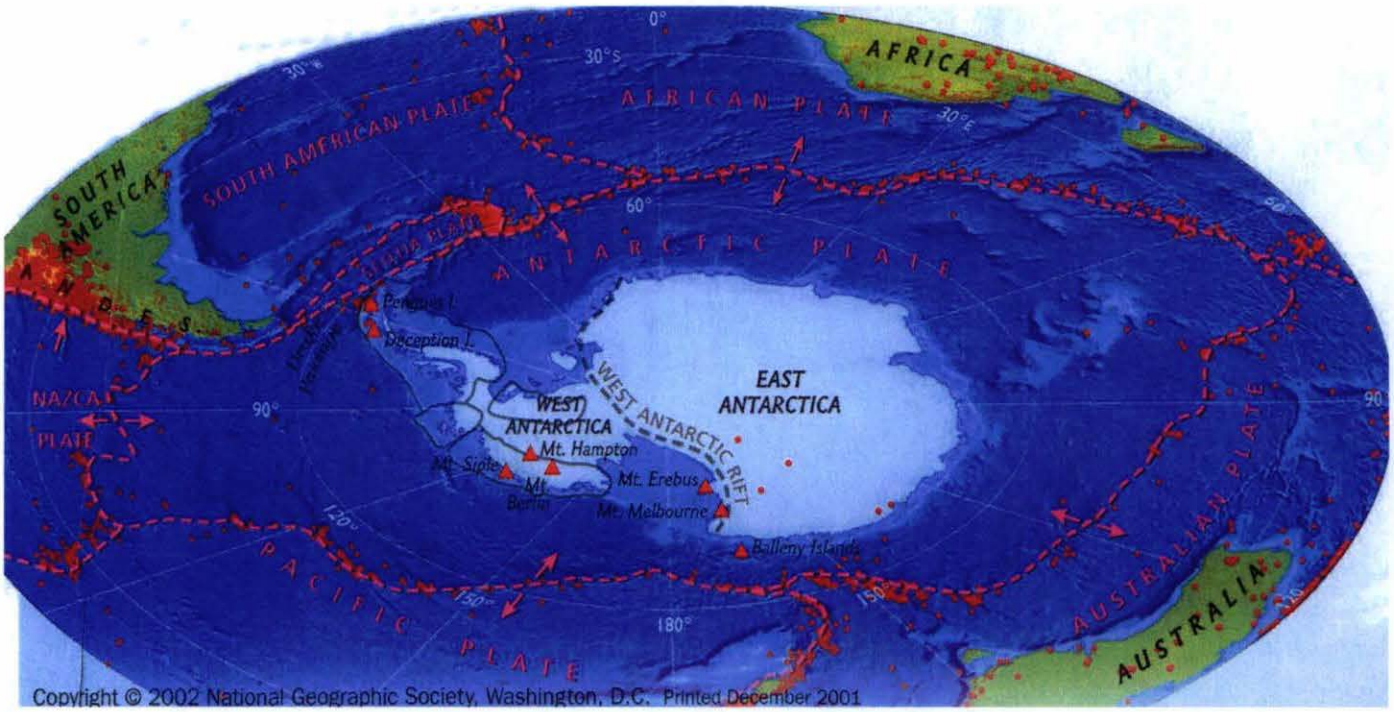

Figure 4: Tectonic setting of the Antarctic Continent. Tectonic plate boundaries represented by dashed pink line. All margins are divergent boundaries.

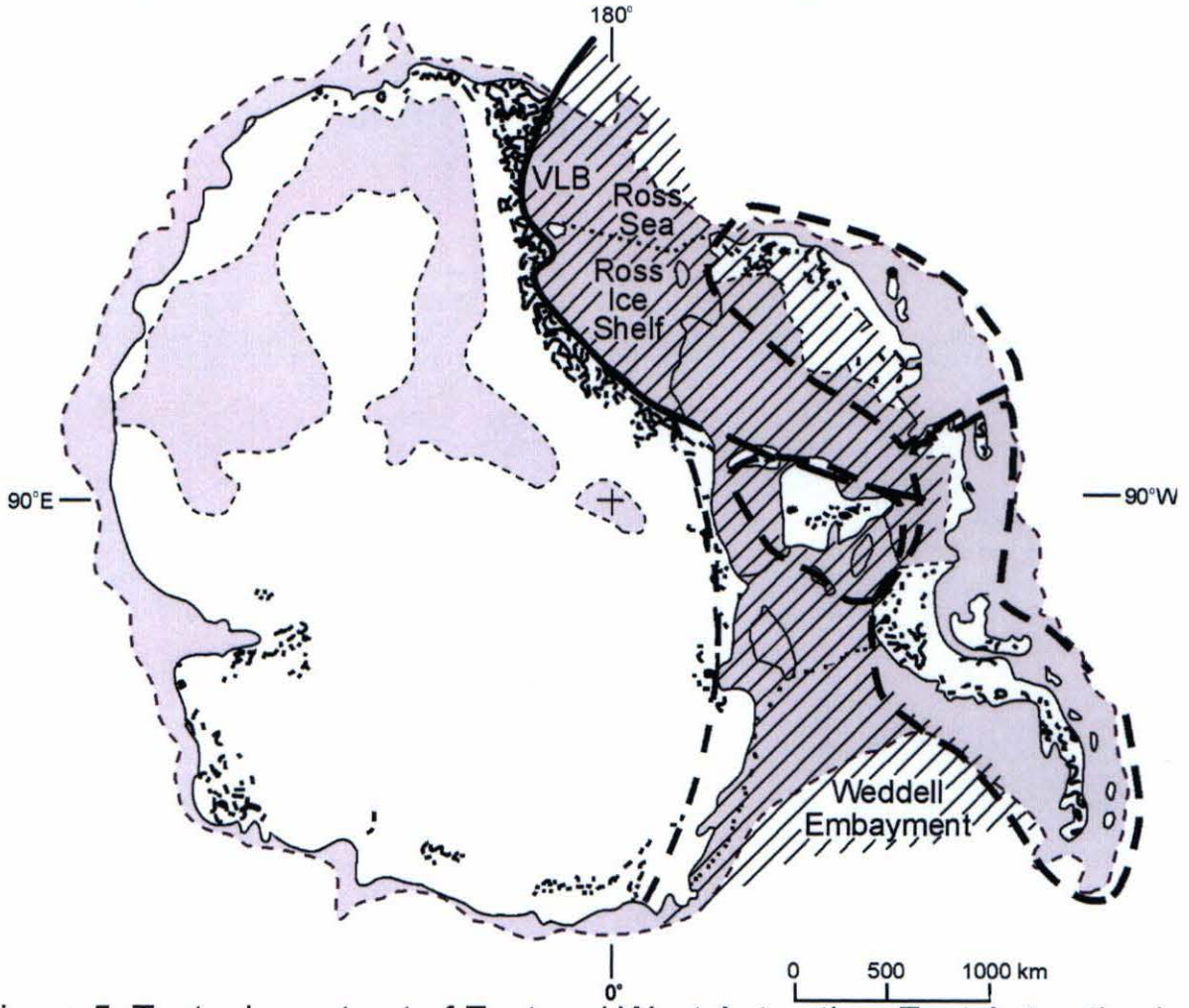

Figure 5: Tectonic contrast of East and West Antarctica. East Antarctica is Precambrian Craton. West Antarctica is divided into crustal blocks.

Geologic setting

Antarctic Plate Setting

The Antarctic continent is centered on a tectonic plate which is surrounded by submarine divergent plate margins (Fitzgerald, 2002. See Figure 4 for the tectonic setting of the Antarctic continent). The continent is segregated into two geologically diverse provinces, East and West Antarctica (Figure 5). East Antarctica is underlain by Precambrian cratonic crust (Dalziel and Elliot, 1982). West Antarctica is an assemblage of continental blocks which moved with respect to East Antarctica and with respect to each other during the Mesozoic and Cenozoic (Fitzgerald, 2002). The boundary between East and West Antarctica is believed to lie between the Transantarctic Mountains and West Antarctic Rift system, or within the West Antarctic Rift System itself. Evidence of Mesozoic to Cenozoic deformation has been found in West Antarctica and along the Transantarctic Mountains at the edge of the East Antarctic craton, with the dominant phase of rifting in West Antarctica occurring during the Cretaceous, coeval with breakup of the Gondwanaland supercontinent (Davey and Brancolini, 1995; Fizgerald, 2002; Stock et al., 2002). Extension and crustal thinning have been concentrated in the West Antarctic Rift system and may be active today in the Terror Rift (Wilson and Lawver, unpublished).

West Antarctic Rift System – Transantarctic Mountains

The West Antarctic Rift System (WARS) is a minimum of 3200km long and 800 km wide. The true extent of the rift system is unknown because it is entirely below sea level and is covered by the Ross Sea, West Antarctic Ice Sheet and Weddell Sea.

Volcanism and extensional strain have repeatedly focused in the WARS due to the lithospheric weakness of the region. The underlying crust has been thinned to a minimum of 17km thick beneath the Victoria Land Basin in the western Ross Sea but thickens regionally to 36 km in the Transantarctic Mountains. Where sufficient data exists, discrete rift basins have been defined within the West Antarctic Rift system (Figure 6). In the Ross Sea, there are four basins formed by WARS extension and separated by basement highs (Davey and Brancolini, 1995). One of these basins is the Victoria Land Basin which is in the westernmost WARS, adjacent to the TAM.

The Transantarctic Mountains (TAM) are a topographic boundary between East and West Antarctica as well as the edge of the West Antarctic Rift System and the western boundary of the Ross Sea. They stretch across the Antarctic continent for approximately 3500km and reach elevations of over 4000m. Their raised topography is derived from the uplift of crustal blocks along a series of normal faults running parallel to the range's length. Exhumation of the range began in the Early Cretaceous, but the major episode of rapid uplift occurred 50-55Ma. The Transantarctic Mountain Front, which faces the Ross Sea, is a zone of major normal faulting along which fault blocks have been downthrown toward the coast as part of the subsidence of the West Antarctic Rift System. (Davey and Brancolini, 1995; Fitzgerald, 2002) Figure 7 shows the known regional structures in the TAM adjacent Ross Sea.

Terror Rift

The Terror Rift is located within the Victoria Land Basin of the Western Ross Sea (Figure 8, Cooper et al., 1987). It is part of a north-south trending fault system which is

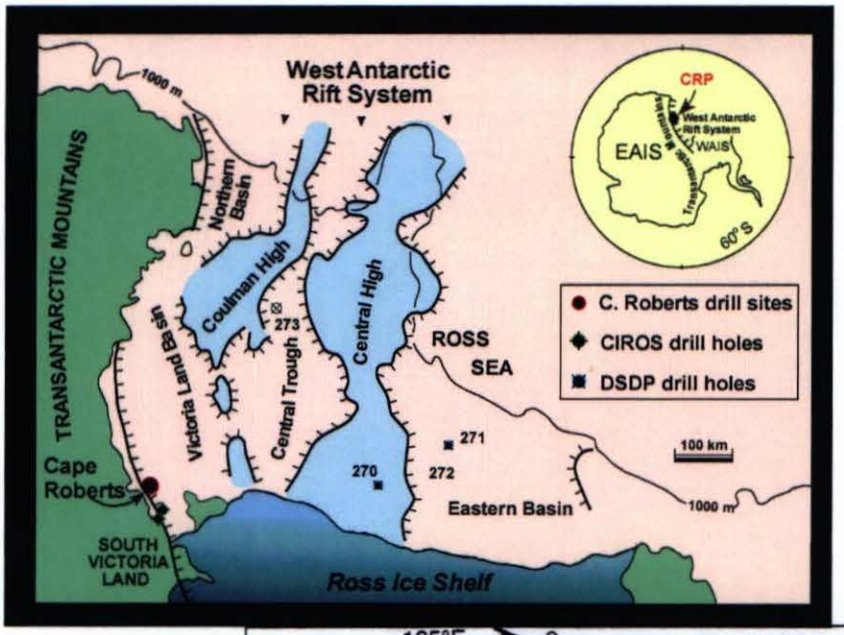

Figure 6: West Antarctic Rift System with basement highs in blue and basement lows in pink. Note the location of the Victoria Land Basin.

Figure 7 : Regional fault patterns within the West Antarctic Rift System and Transantarctic Mountains.

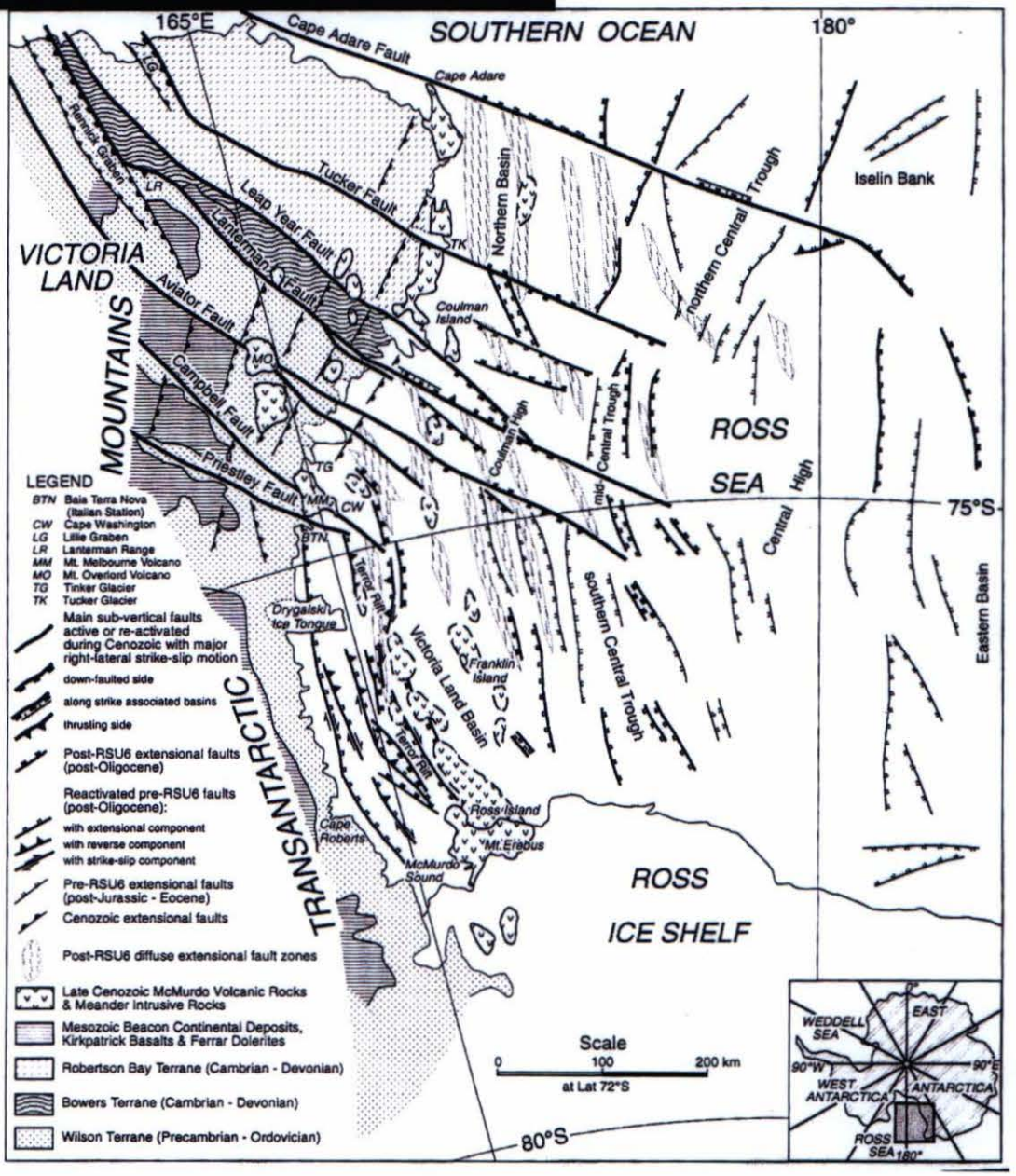

Figure 8

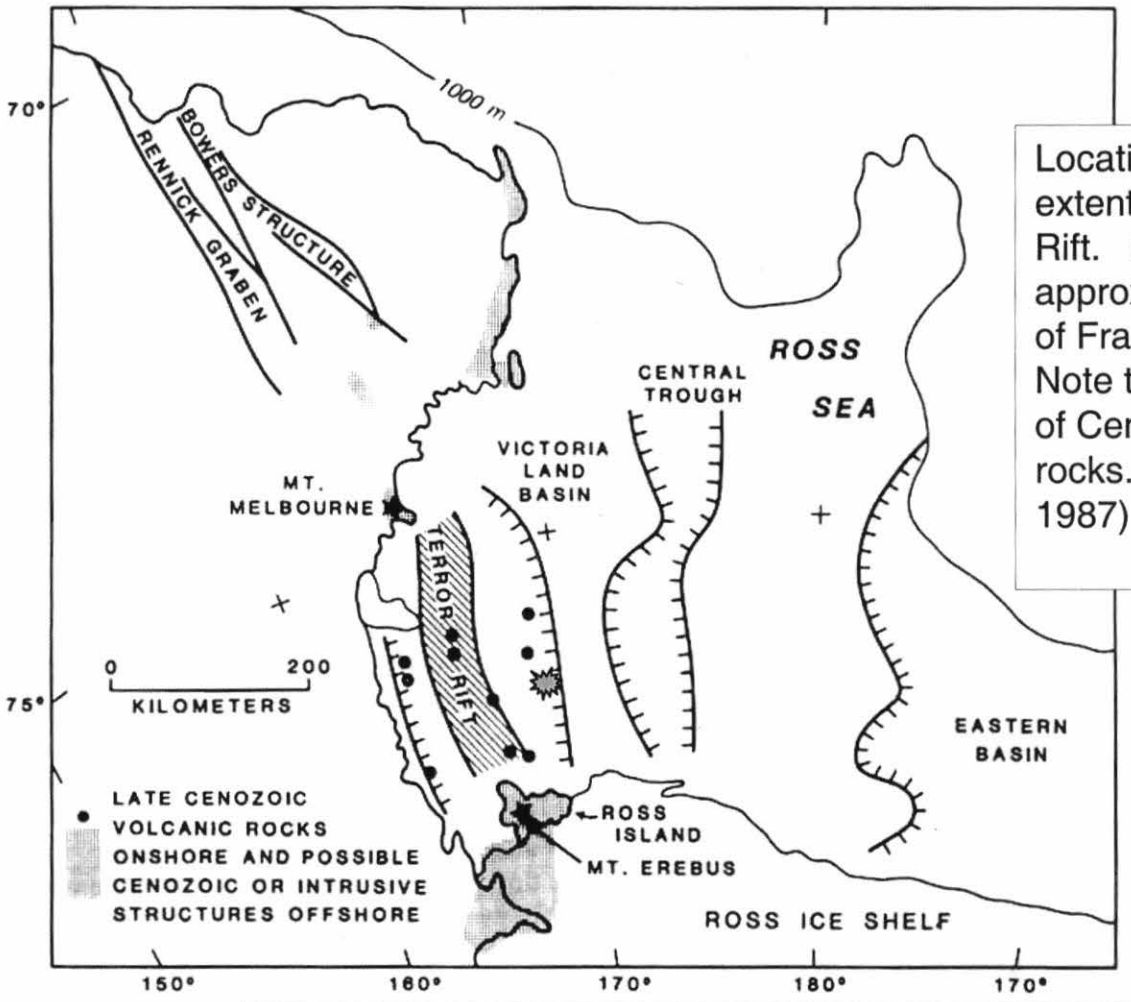

Location and known extent of the Terror Rift. ✹ indicates approximate location of Franklin Island. Note the distribution of Cenozoic volcanic rocks. (Cooper et al., 1987)

Location of known structures in the Terror Rift. (Cooper et al., 1987)

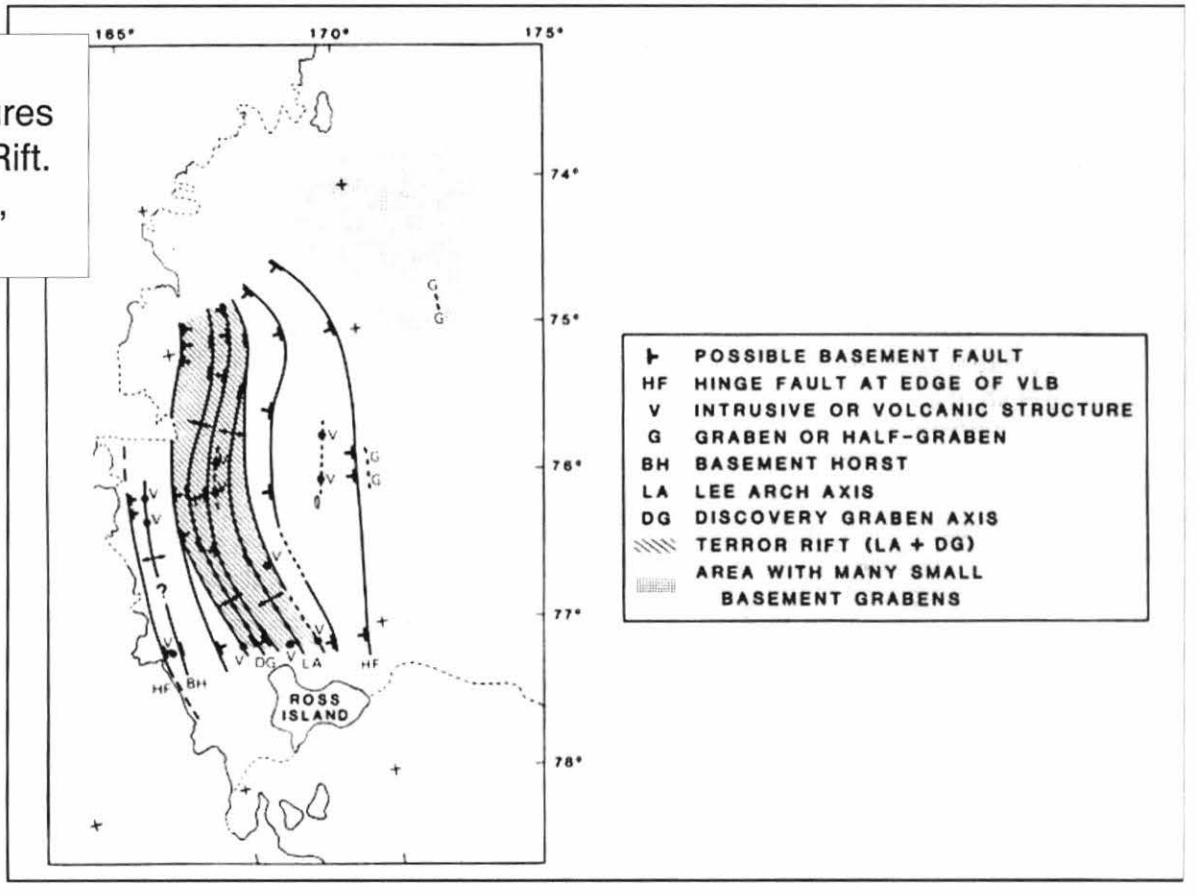

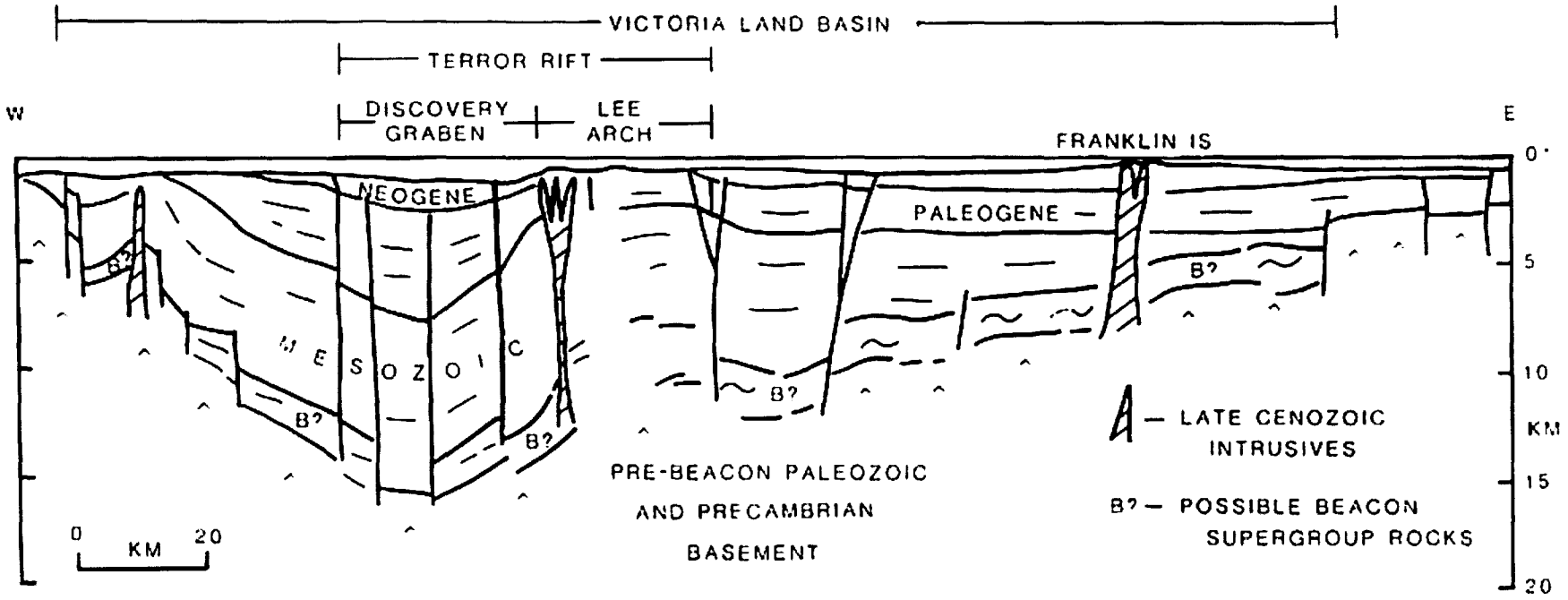

Figure 9: Cartoon cross section Terror Rift as defined from seismic profiles by Cooper et al. (1987).

parallel to the overall trend of the TAM (Salvini, 1997). It is commonly defined to extend between the active volcanoes Mt. Melbourne in the north and Mt Erebus in the south, but may link to onshore faults in the TAM of north Victoria Land and may continue southward beneath the Ross Ice Shelf (Wilson, 1999). The Terror Rift is the youngest location of extensional tectonism in the WARS, and the presence of faults and volcanic rocks reaching the seafloor led Cooper et al. (1987) to suggest that it still may be an active feature. The Terror Rift was defined seismically by Cooper et al (1987) and divided into two structural zones: Lee Arch, which is intruded by volcanic bodies; and Discovery Graben, which is bounded by normal faults with displacements up to 3km (Figure 9). Salvini et .al (1997) note that the tectonic regime reflects both extensional and lateral components, making it a transtensional setting. The detailed geometry of faults and the extent of faulting associated with the Terror Rift are not known due to the sparse spacing of seismic profiles which cross it. A major goal of the NBP 04-01 expedition was to collect denser seismic data as well as bathymetric data over Terror Rift to further constrain its geographic boundaries (Wilson and Lawver, unpublished).

Cenozoic Volcanic Rocks

McMurdo Volcanic Group

The McMurdo Volcanic Group is defined as all Cenozoic volcanic rocks within the Transantarctic Mountains or the Ross Sea Embayment (meaning the sea itself or the adjacent Ross Ice Shelf, Figure 10). It is further subdivided into three provinces which are delineated by their spatial distribution and tectonic setting and which show variable lava compositions. The Mt. Melbourne province is located within the TAM as well as at

Figure 10

Known distribution of terrestrial volcanic rocks proximal to the Terror Rift.

✹ Indicates the approximate location of Franklin Island.

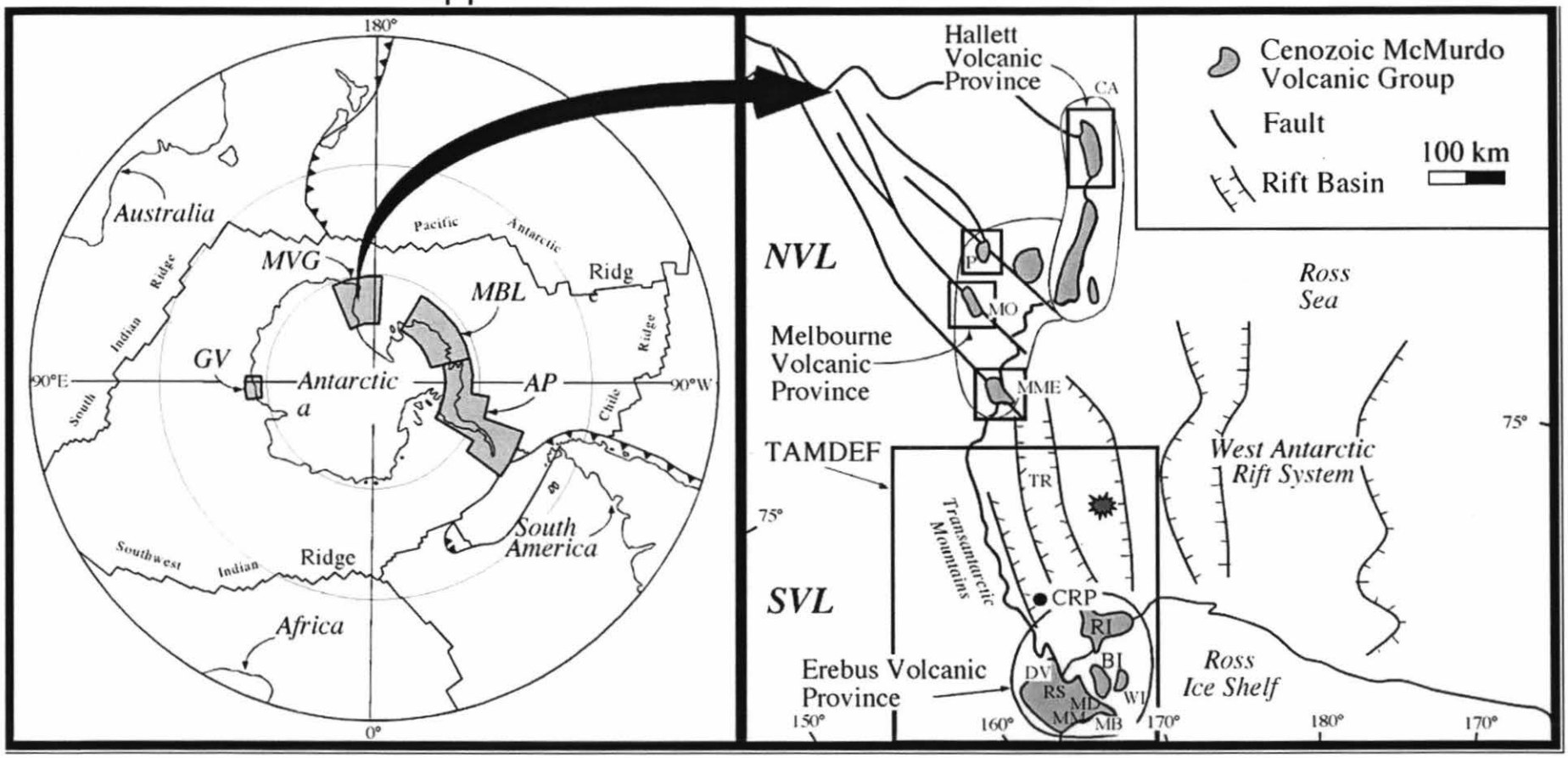

the bounding normal faults separating the TAM and the Ross Sea and lies at the north end of the Terror Rift. (Kyle, 1990) The oldest magmatic intrusions in the province are dated to 50 Ma (Rocchi et. al, 2002) with volcanism extending to the present. The Mt. Erebus volcanic province is located at the intersection of fault zones bounding the TAM, at the southern end of the Ross Sea portion of the Terror Rift. Volcanic activity within this province dates back to about 25 Ma from drill core records, with the oldest volcanic outcrops dated at 19 Ma (Kyle, 1990)

Franklin Island and surrounding seafloor volcanoes

Franklin Island is located approximately 100km NNE of Mt. Erebus and east of the region currently defined as the Terror Rift (76d10'S, 168d23'E). The island has an elongate North-South trend and measures 7.6km long, 2 km wide and 247 meters high. It is interpreted as the western remnant of a shield volcano which deposited the interbedded lava flows and tuffs that are exposed on the Island's steep eastern flank. The olivine-bearing basalt lava on the island yielded a K-Ar date of 4.8Ma +/ – 2.0 Ma. (Kyle, 1990 Ch A.13)

Other volcanoes formed on the western Ross Sea floor were suggested by an aeromagnetic survey in 1984 (Duerbaum and Tessensohn), and some volcanic centers were mapped again during a 1987 marine geophysical survey by Behrendt et. al. (Kyle, 1990). The presence of extensive Cenozoic volcanic rocks on or beneath the seafloor of the western Ross Sea has been interpreted from regional aeromagnetic anomaly patterns (Figure 11, Behrendt et. al, 1996). Anomalies on the seafloor show a roughly North-South elongation and are attributed to basic igneous rocks which have intruded into or

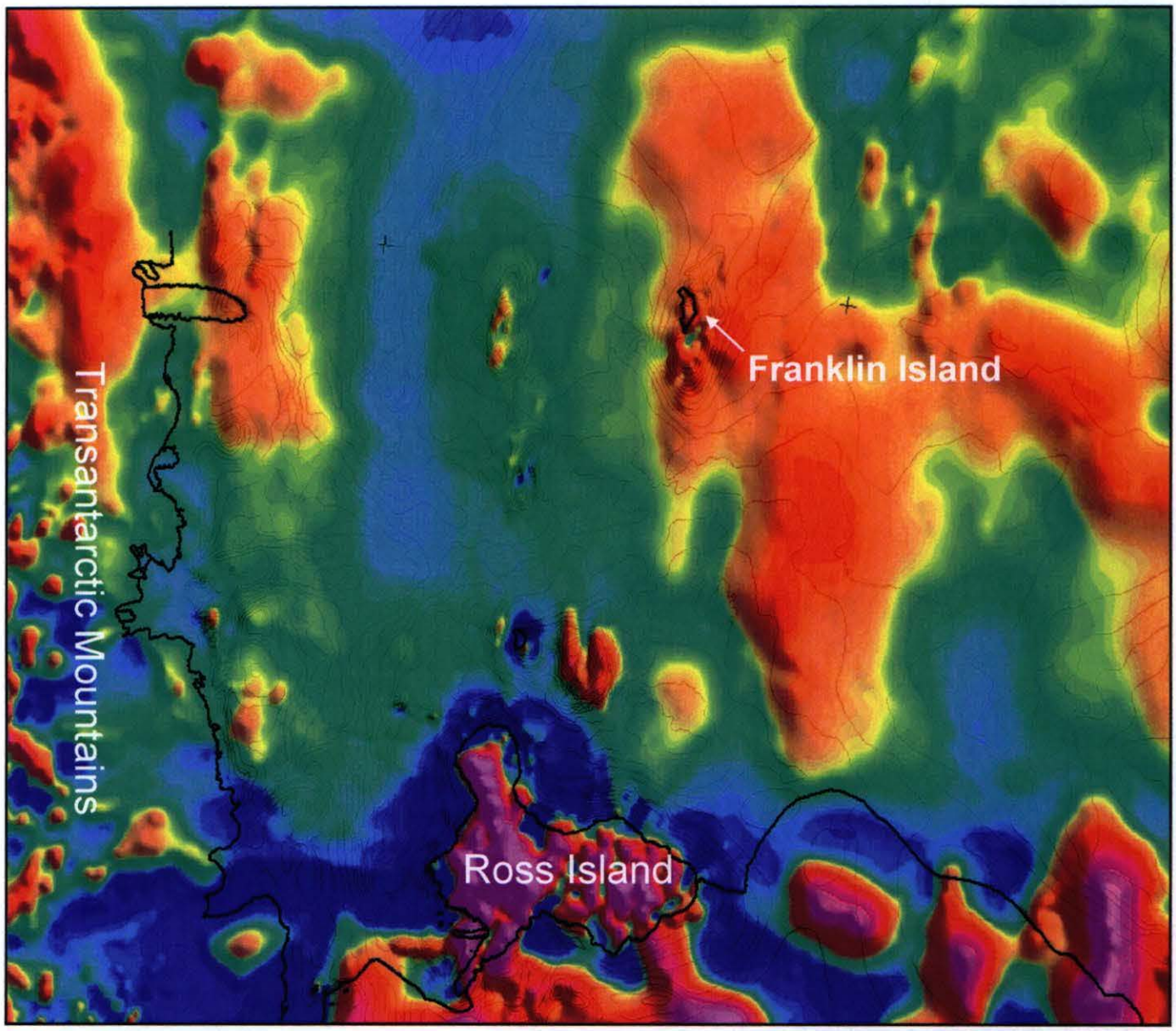

Figure 11: Shaded relief map of aeromagnetic anomalies in the Ross Sea (Data from Chiappini (2001)). Dark blues are magnetic lows grading to red and purple which are magnetic highs. Note location of Franklin Island in broad, positive magnetic anomaly. Coastal boundaries in black.

been extruded onto sedimentary basin rocks. Franklin Island falls within such a magnetic high.

Data on individual volcanic edifices, their alignment relative to each other and on any related faults were collected during the NBP 04-01 cruise.

Glacial History

The West Antarctic Ice Sheet

The West Antarctic Ice Sheet formed due to the amalgamation of ice caps during the Oligocene and early Miocene. Throughout the late Miocene and into the Pleistocene it periodically advanced over the continental shelf of the Ross Sea Embayment, eroding the substrate and creating glacially-carved landforms and extensive unconformities, as well as leaving glacial deposits on the seafloor. During the Last Glacial Maximum, the ice sheet extended to within 100km of the shelf break of the western Ross Sea and to the shelf edge of the central and eastern Ross Sea (Figure 12). Retreat of the ice sheet began between 15,000 and 12,000 yr B.P. and proceeded at an average rate of 100m/ yr. By 11,500 yr B.P. the grounding line was proximal to the Drygalski Ice Tongue and by 7,000 yr B.P. had retreated to Ross Island. Between 7,000 and 5,000 yr B.P. the ice sheet underwent an episode of rapid retreat. (Anderson and Shipp, 2001) Grounding line retreat to the current glacial extent continued through the Holocene to the present (Anderson et al, 2002).

Throughout the embayment, the signature of the ice sheet consists of mega scale glacial lineations up to tens of kilometers in length that result from the deformation of soft subglacial debris under a grounded ice sheet (Figure 13). The lineations indicate

Figure 12

Maximum ice extent at the Last Glacial Maximum

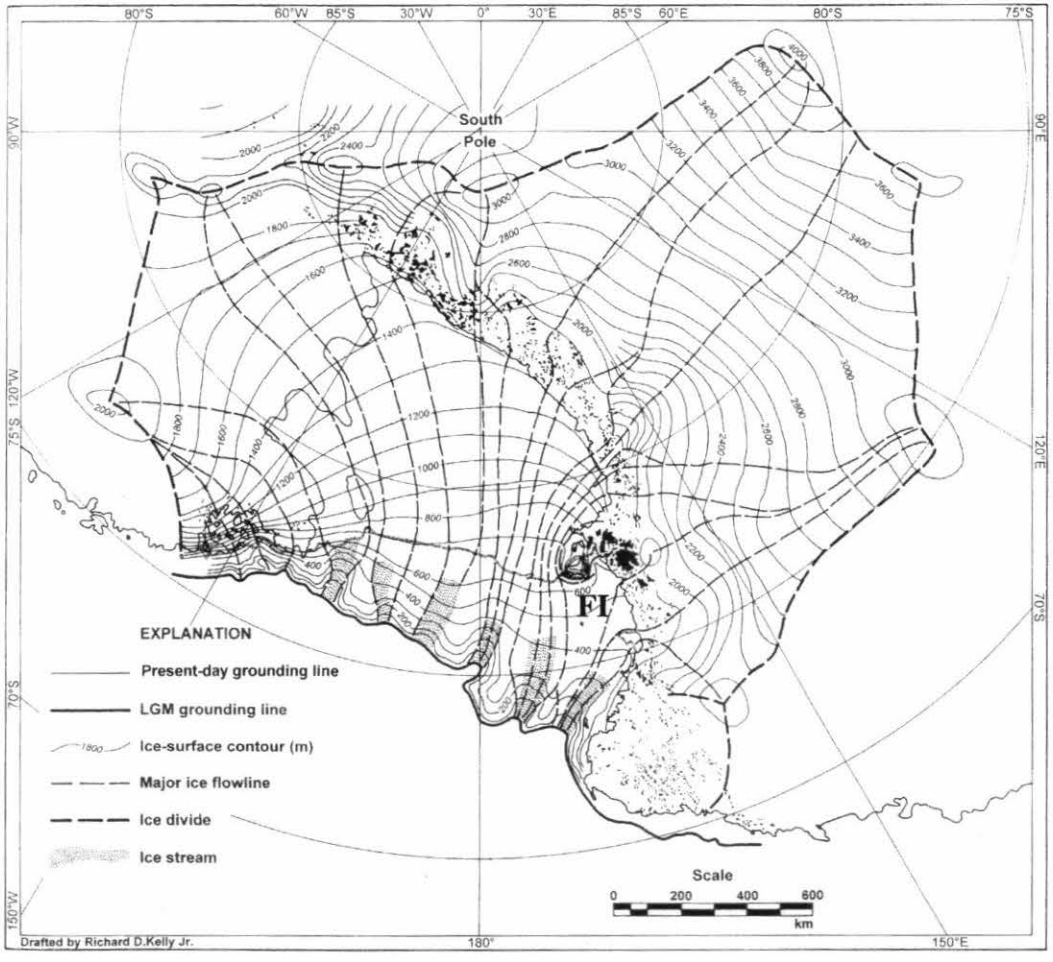

Denton and Hughes, 2000

Retreat of West Antarctic Ice Sheet since LGM

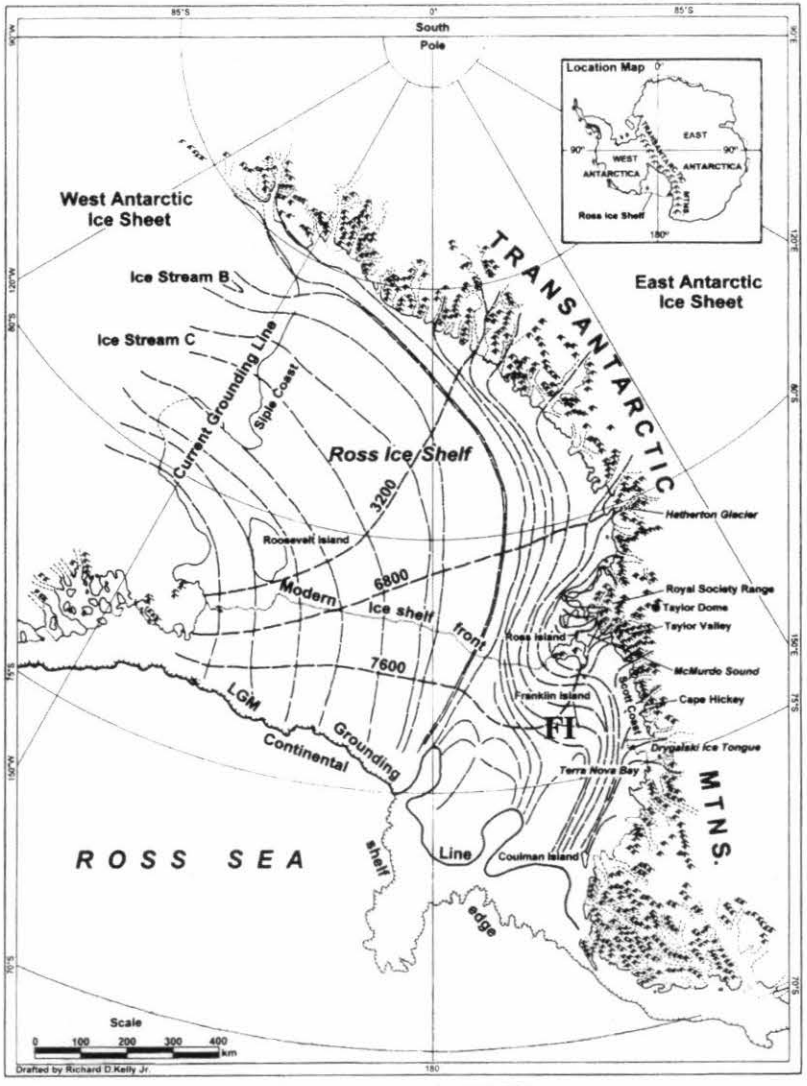

Conway et al., 1999

rapidly moving ice and demonstrate a unidirectional flow regime except where diverted around bathymetric highs. Drumlins and flutes are present at the transition between landward crystalline basement and the sedimentary infilling of the embayment due to the changing velocity of ice advance. (Anderson and Shipp, 2001; Wellner et. al, 2001) The retreat signature of the ice sheet is marked by ridge and groove moraine topography with cross cutting iceberg furrows (Figure 13B). The late stage episode of rapid retreat led to the calving of large icebergs from the glacier front. These icebergs moved offshore cutting iceberg furrows into the shelf at depths up to700m below current sea level. (Anderson and Shipp, 2001)

Figure 13: Retreat signature of the West Antarctic Ice Sheet.

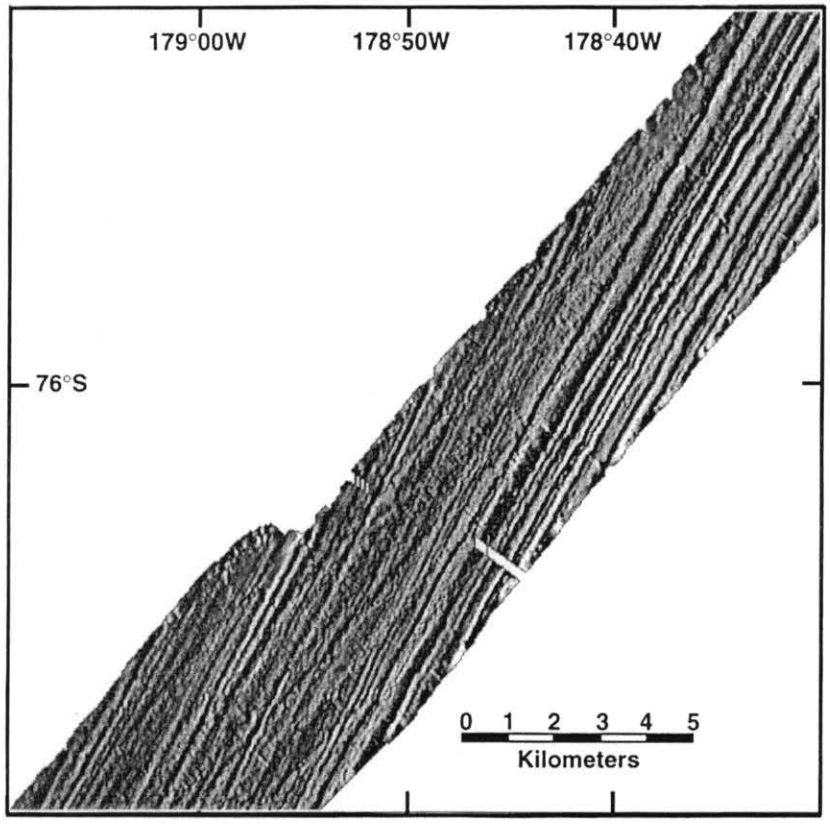

A) Mega scale glacial lineations (Shipp and Anderson, 1997)

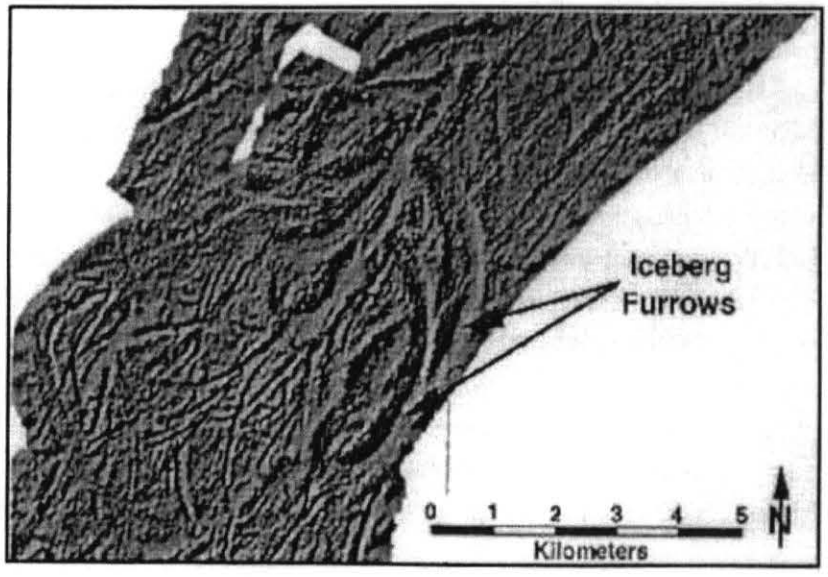

B) Iceberg furrows (Anderson, 1999)

Methods

Discrimination of Seafloor Features

In order to understand the geologic context and significance of the seafloor features in the Franklin Volcanic Field, their mode of origin must be distinguished. Using a basic understanding of geologic processes, a generalized set of criteria for feature origin can be established. Bathymetric data allows the examination of the morphology of the features. Seafloor hills in the Ross Sea region could be either glacially-formed drumlins or volcanic cones. Escarpments could be tectonically formed faults, dikes or glacial erosion surfaces. In most cases, morphologic characteristics are not sufficient to identify the origin of a seafloor feature and additional data types are required.

The NBP 04-01 geophysical data and dredge records provide a means to confirm or delineate the origin of ambiguous bathymetric features. Dredging uses a metal bucket to pluck rocks from the sides of seafloor hills. The lithologies present can then be identified directly. When the depth or relief of seafloor features prevents dredging, geophysical data is used. Magnetic data are used to detect iron bearing rocks, especially basalts, which are associated with volcanic origin. Gravity data allow the detection of subsurface or surface concentrations of dense bodies of mass in volcanic intrusions. Seismic profile data provide a cross sectional view which can be examined for truncation and offset along faults or stratigraphic disruption by volcanic intrusions.

This study first uses the surface expression of features on the seafloor to create hypotheses for their mode of origin. Then through examination of the geophysical data sets, and integration of observations, the origin of the features is constrained based on the expectations outlined in Table A.

Table A : Geophysical characteristics of positive relief sea floor features

		Glacially formed	Volcanically formed	Faults (tectonically formed)
Bathymetric character	**Morphology**	Beveled tops Elongation in glacial flow direction Lee side in up-flow direction Moderate surface relief	Volcanoes: Conical or beveled Elongate or round High surface relief Dikes: Elongate, curvilinear Low surface relief	Linear or curvilinear in map view Low to moderate surface relief
	Distribution	Clustered due to changes in glacier velocity	Potential regional alignment Clusters common Isolated vents common	Parallel, conjugate or branching orientation
Seismic character		Surficial features Lacks internal stratification	Feeder system penetrates at depth disrupting substrate layers Internal stratification above median seafloor surface level	Penetrate at depth Offset of substrate layers
Magnetic character		No signature	High magnetic profile due to natural remnant magnetization and magnetic susceptibility of basic igneous rocks	Potentially high if a magnetic body is closer to the surface due to fault displacement
Gravimetric character		No signature	High locally due to concentration of dense rock Low regionally due to crustal loading and mantle depression	Potentially high or low. Features which concentrate mass will cause positive anomalies.

Interpretation of seafloor features

Glacial Flow Directions

Glaciers have the capacity to carry large volumes of rock debris which can be used to erode the underlying substrate or can be deposited by the glacier on top of the substrate. One mechanism of glacial erosion is abrasion, in which material trapped at the bottom of the glacier cuts scours into the underlying rock units. These features show a variety of scales ranging from inch long striae to the mega scale glacial lineations mapped on the Ross seafloor by Shipp et al. (1999). Abrasive erosion requires the surface lithology to be softer than the material being carried at the base of the glacier. (Hambrey, 1994) Thus, glaciers are more efficient in eroding unlithified or sedimentary rock units than igneous bodies such as basalt lava flows.

Glaciers also act constructively, depositing unsorted debris in drumlins, asymmetric hills which taper in direction of glacial flow, or moraines, ridges of unconsolidated material. The location of drumlins in the Ross Sea has been correlated to the contact between sedimentary and crystalline substrate lithologies by Anderson et al. (2001). The lithologic contrast creates a change in the glacier's basal flow velocity and results in a combination of erosional and depositional processes which create the asymmetric geometry of the drumlins. Moraines are deposits parallel or perpendicular to the direction of glacial flow. Parallel moraines develop in subglacial areas where the base of the glacier is not in direct contact with the substrate and are lineated in the direction of glacier flow (Hambrey, 1994). Thus, the ridge and groove topography of glacial lineations can be either erosional or depositional but both types of lineation constrain glacial flow to be parallel to their elongation direction.

The following section summarizes the method for interpreting stress directions from the alignment of tectonic or volcanic features. Material is referenced from Suppe (1985) unless otherwise noted.

Stress Orientation

Fractures in rock are constrained to geometric patterns that are controlled by the orientation of the stress field in the crust at the time of their formation. The principal components of the stress field are S1, the direction of maximum compression; S3, the direction of least compression and S2; the intermediate principal stress. Because the atmosphere of the Earth is a fluid and incapable of transmitting stress, one principal stress must be oriented perpendicular to the surface of the Earth confining the other two to the horizontal plane which approximates the Earth's surface. Because of the predictable relations between stress orientations and fracture geometry, the orientation of principal stresses can be reconstructed by mapping the orientations of fractures. When examining fractures on a two dimensional surface, only the relative magnitudes of the two horizontal stresses can be determined. Then, the convention of using S1, S2 and S3 is negated and the stresses are referred to as the maximum or minimum horizontal stress.

In homogeneous rock, extension fractures open in the direction of least compressive stress (S3) and propagate parallel to the S1-S2 plane (Figure 14). Dikes and volcanic fissures are extension mode fractures created by magmatic pressure. Thus the opening and elongation directions of tabular magmatic intrusions also correspond to S3 and the S1-S2 plane, respectively. When observing dikes or fissures in map view, the direction of opening in the fractures is parallel to the minimum horizontal stress (i.e.

Figure 14: Structural interpretation of opening mode fractures

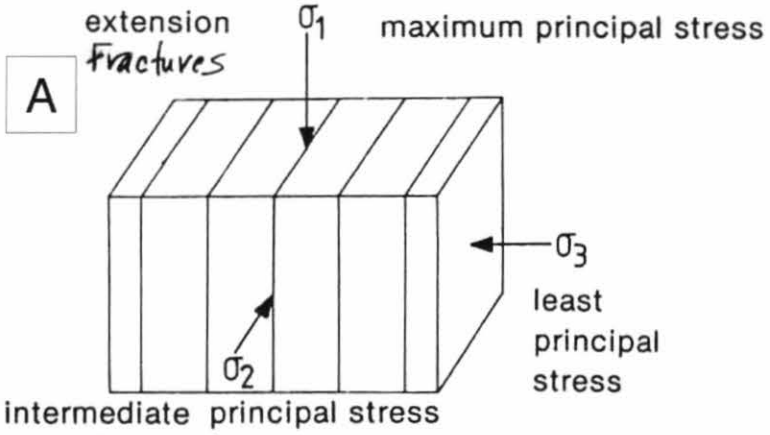

(McClay, 1987)

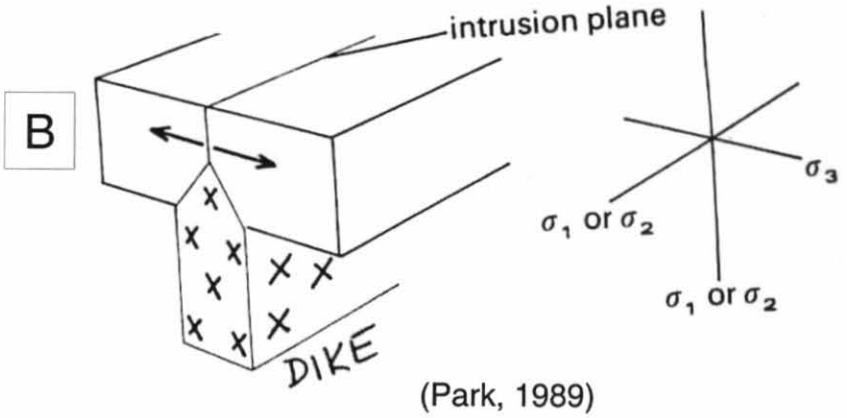

(Park, 1989)

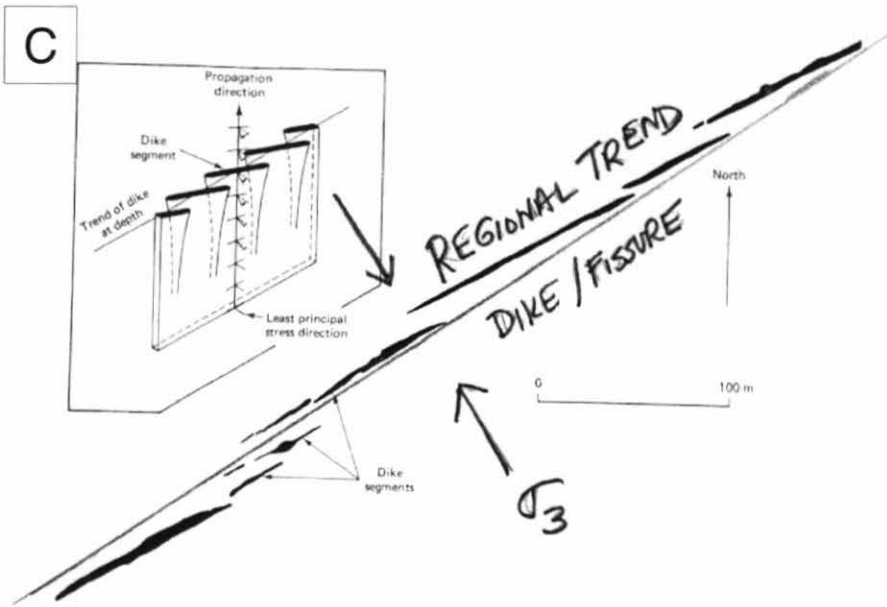

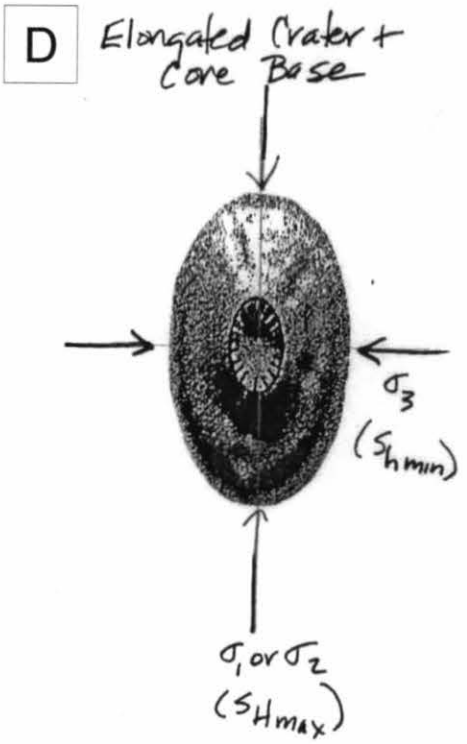

From Suppe (1985)

perpendicular to the dike trend) which could correspond to S3 or S2. The trend of the dike is parallel to the maximum horizontal stress, which could correspond to S1 or S2. Volcanic cones have underlying feeder dikes with an orientation constrained by the stress field. Elongate cones on the surface of the Earth result from parallel, elongate feeder systems in the subsurface (Nakamura, 1977). Therefore, using the elongation direction of volcanic cones, the trend of the underlying feeder system, which parallels the maximum horizontal stress direction, can be mapped (Figure 14D).

Faults are shear fractures along which slip occurs, causing displacement of rock units across the trace of the fault plane. Anderson's theory of faulting predicts the sense of shear which will occur along shear fractures based on the orientation of the three principal stresses in the Earth's crust (Figure 15). Given that the stresses are mutually perpendicular, there are only three unique possibilities for stress component orientation. The following summarizes the predicted orientation and sense of displacement along fault planes relative to the surface of the Earth depending on stress component orientation: when S1 is vertical, faults are inclined at 60 degrees (measured down from the surface) and have normal-sense displacement; when S2 is vertical, faults form vertically and have strike-slip displacement; when S3 is vertical the fractures are inclined at 30 degrees and have thrust displacement. Anderson's theory also predicts the formation of conjugate sets (i.e. two sets of planes formed at the same time, with an internal angle between them of 60 degrees). S1 bisects the acute angle between conjugate fault planes.

The internal pressure inside a cylindrical conduit which feeds magma to the surface at a major volcanic center creates stresses in the surrounding rock that are parallel and perpendicular to the conduit. When the local stress field is dominated by magmatic

Figure 15: Structural interpretation of shear fractures (faults)

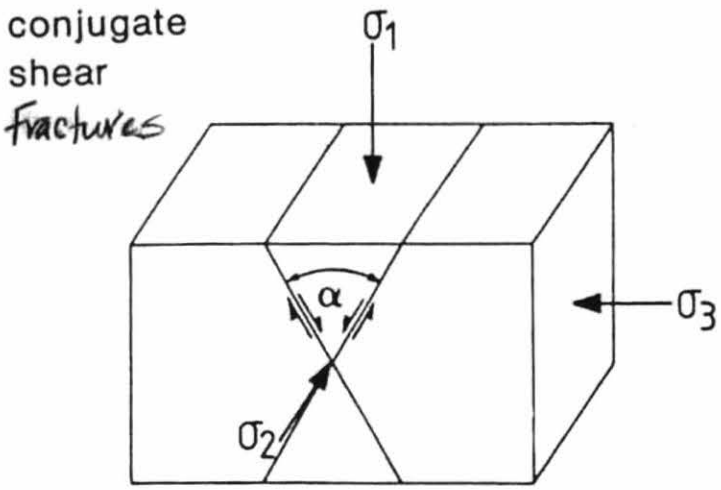

(McClay, 1987)

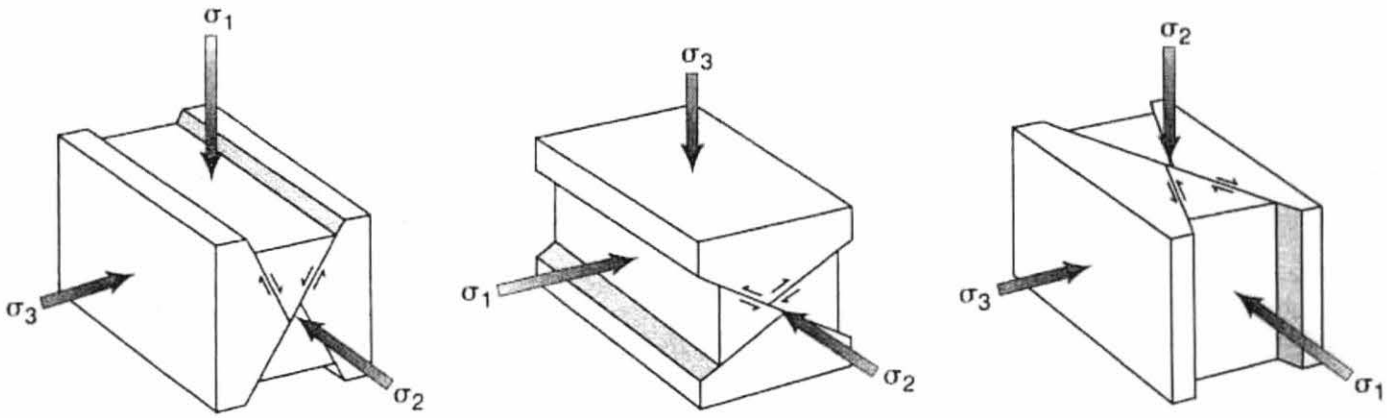

Anderson's Theory of faulting predicts conjugate sets of a) normal faults when S1 is vertical b) thrust faults when S3 is vertical c) strike slip faults when S2 is vertical.

Figure 16: Interpreting stress from regional dike swarms.

RADIAL DIKE SWARM AROUND VOLCANIC CENTER

• Controlled by local stress

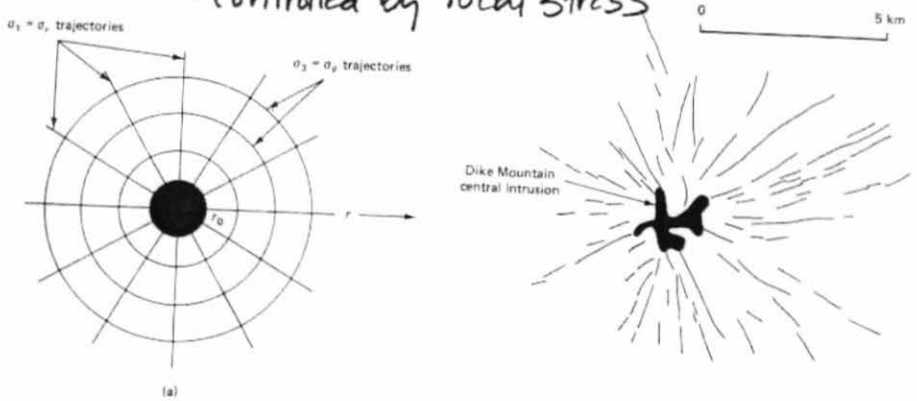

(a)

DIKE SWARM WITH 'HOURGLASS' SHAPE AROUND VOLCANIC CENTER
Controlled by regional stress in crust

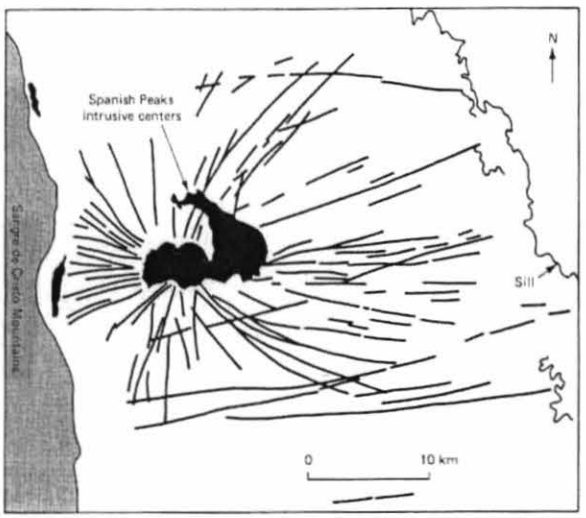

(a)

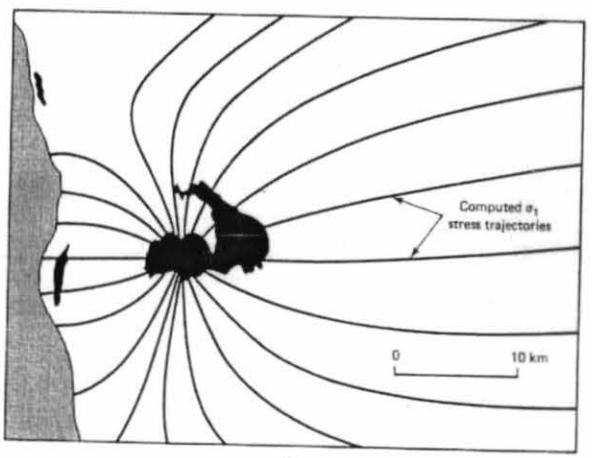

(b)

pressure, a radial pattern of dikes and fissures develops around the volcanic center (Figure 16A). In the presence of a strong regional stress field, the dikes and fissures around the magmatic center may initially be radial, but at distance are reoriented to align with the regional S1-S2 plane (Figure 16B). (Nakamura, 1977)

One can apply the principles outlined above to use existing fractures, faults or volcanic bodies to reconstruct the stress field orientation responsible for their formation. In this application, the timing of the structural deformation must be constrained. The presence of pre-existing faults or fractures creates zones of weakness that may become reactivated by stresses, rather than a new fracture forming (Nakamura, 1977). It is commonly thought that magma may follow pre-existing fault planes, if they are suitably oriented close to the direction in which a new opening-mode fracture would form.

Figures: Bathymetry Data

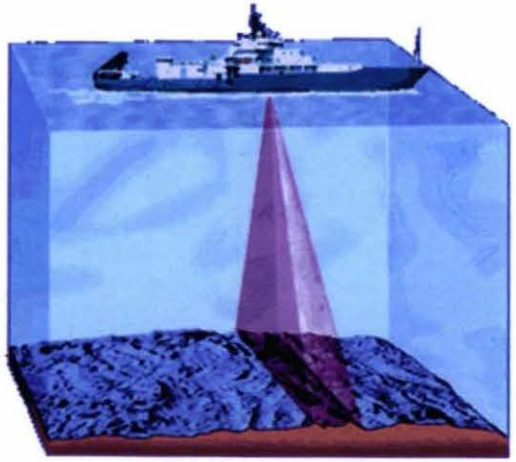

Figure 17: Collection of bathymetry data in a swath beneath the ship.

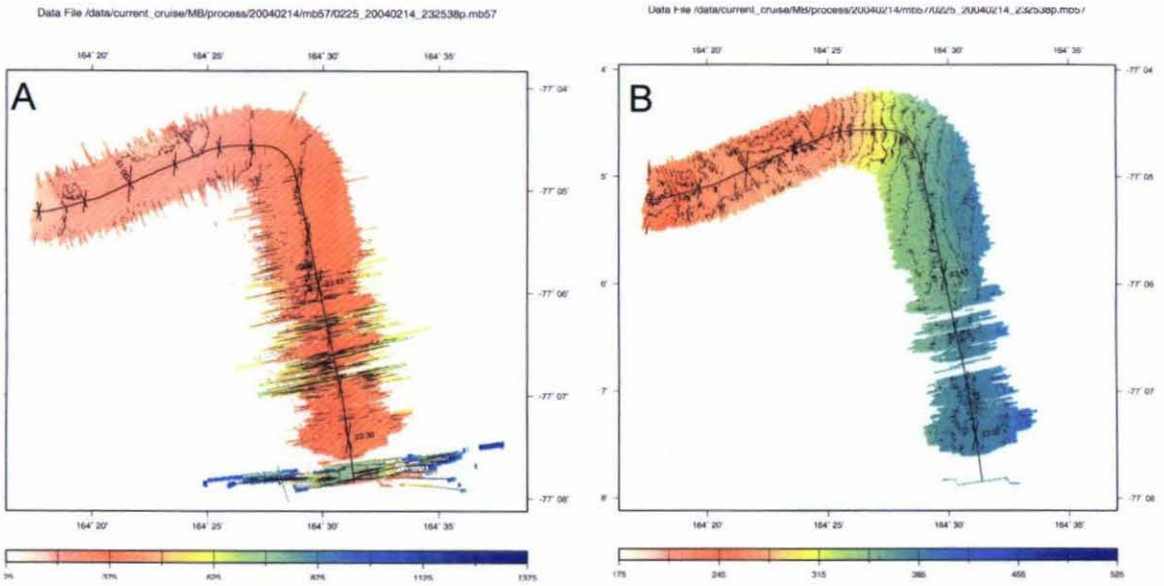

Figure 18: Bathymetric data correction. A) Before editing data are skewed due to a few extreme depth values. B) Edited file better shows the true change in depth for the mapped area. (Files edited by the author)

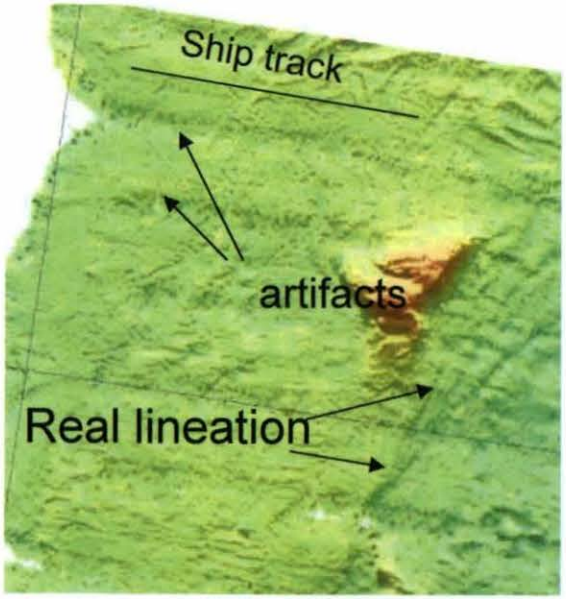

Figure 19: Artifacts in bathymetric data parallel ship tracklines.

Geophysical Data

Bathymetric Data

Bathymetric data were collected continuously during NBP04-01using onboard sonar systems. Sonar uses sound wave propagation to map the topography of a surface. By emitting a sound wave and recording the time until its return, the distance to the reflecting surface can be determined. In marine geophysical surveys, a discrete ping is periodically sounded in the water from instruments mounted on the hull or towed behind the ship. The sound wave from the 'ping' travels through the water column, reflects off the sea floor surface and returns to the ship. Multibeam sonar simultaneously sends multiple sonar beams in a fan-shaped pattern oriented perpendicular to the ship's track, allowing the collection of data in a swath, rather than a single line, beneath the ship (Figure 17). Parts of the wave can be falsely reflected by objects other than the sea floor surface or can be diverted away from the ship due to small variations on the surface. This creates error in the bathymetric record which is processed out through editing using a program called "Mbedit", a component of the "MBsystem" software package.

During the NBP 04-01 cruise, multibeam bathymetry data were collected continuously using the onboard Konigsberg-Simrad EM120 system. When in sea ice, the quality of the data was depleted due to the abundance of false reflectors in the water column. Each hour, the data were complied into a file showing the results from each individual ping. The ping files were then manually edited by members of the science team (Figure 18). As a general rule, minimal editing was applied in order to preserve as much of the correct data as possible. The extreme outer margins of a swath typically have both the least data and the most inconsistent data values. Artifacts remain in the

bathymetric maps, consisting mainly of linear traces parallel to the ship's track, along the center and outer margins of the swath, due to sound wave diffraction and the ping editing process (Figure 19).

During the course of the NBP0401 survey, the discovery of numerous seafloor hills and ridges in the vicinity of Franklin Island led to the decision to carry out a more complete survey in the region. The area to the east of Franklin Island could not be surveyed due to the presence of the B-15A mega-iceberg. The very shallow water to the south of Franklin Island precluded extensive surveying there, as ship procedure mandated surveying in depths greater than 100-200 m below sea level in uncharted areas. We were able to carry out a more complete surveying to the north of Franklin Island, and these data are the focus of this study. The resulting bathymetric map is displayed as Figure 30 and discussed below.

Magnetic Data

The following two sections incorporate background information on the origin, collection and processing of geomagnetic data. This material is referenced from Reynolds (1997) except where otherwise noted.

The Earth's Magnetic Field

The Earth's magnetic field is modeled by a dipole which is the magnetic field surrounding a common bar magnet (See Figure 20). The different orientation of the two poles generates a magnetic flux, or gradient, between the two ends, which then generates a magnetic field surrounding the magnet in a three-dimensional sphere. The analog to this

Figure 20

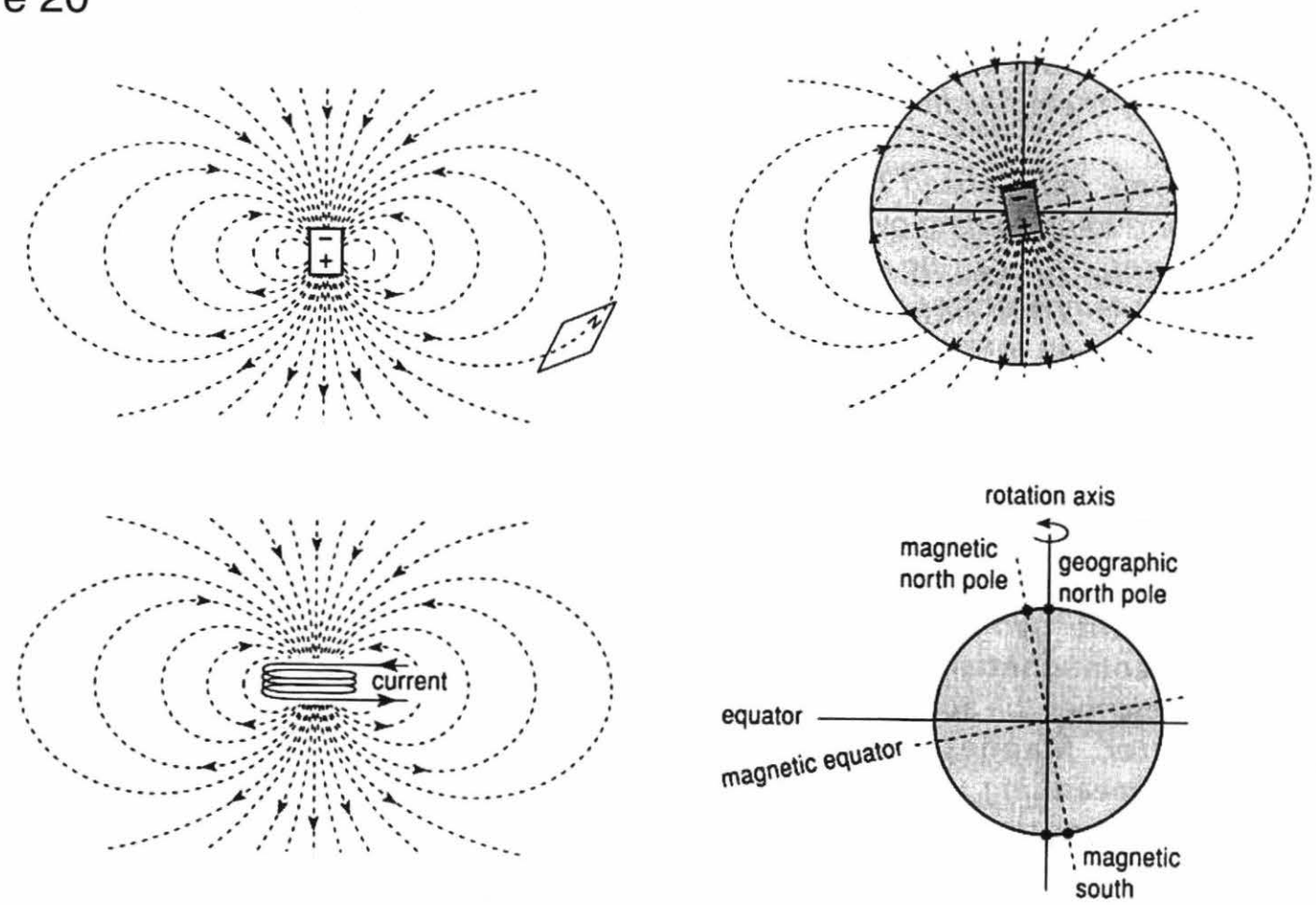

Similarity of the dipole model of the magnetic field of A) a bar magnet B) a current conducting coil and C) the Earth. D) illustrates the inclination of the Earth's magnetic field and the relative locations of the magnetic poles to the "true" or geographic poles. (Musset and Khan, 2001)

process is a hybrid of two more familiar natural processes: a river flowing down its stream gradient and the flow of electricity in a completed circuit.

The Earth's magnetic field is inclined to its axis of rotation by 11.5 degrees. Therefore, the magnetic poles do not correspond to the geographic poles which are referred to as "true" North/South. Since the magnetic field is a vector field, it can be broken down into components. The total force vector, F, has an orientation with respect to North, defined by the declination, D, and an angle from the horizontal, called the inclination, I (Figure 21). The declination angle is the angle between true north and the magnetic north pole. At the magnetic poles, the magnetic field points directly into the Earth in direct contrast to the equator where the magnetic field is oriented parallel to the surface of the Earth. In between these two extreme latitudes, the magnetic field is directed at an acute angle to the surface of the Earth which is termed the inclination angle. Together, the declination and inclination angles relate the orientation of the magnetic field at a point to the location of the magnetic poles. The total force vector, F, can be resolved into an H component, which is directed horizontally along the surface of the Earth and points to magnetic North, and the Z component which is directed perpendicular to the Earth.

The strength of the magnetic field is commonly measured in nanoTesla, a unit equivalent to 10^-9 Tesla and abbreviated "nT." The magnitude of the field is greatest near the magnetic poles, where the field enters or exits the dipole, and measures approximately 60,000 nT. At the magnetic equator, the field is the weakest measuring a minimum of 30,000 nT. Also, since the field is generated inside the Earth, it decreases in strength at greater distance from the Earth's core.

In contrast to the geographic poles, the north and south magnetic poles are drifting around the high latitude regions of the planet and thereby creating periodic variation within the field. From day to day, the Earth's magnetic field sees periods of high and low intensity known as diurnal variations. These can be considered magnetic tides because they occur twice daily and mark the maximum and minimum values of the field strength under normal conditions. In the upper atmosphere of the Earth, in a region known as the ionosphere, charged particles are sometimes liberated from ionic bonds by solar radiation. During periods of intense radiation, such as when sunspots propel large quantities of charged particles into the ionosphere, fluctuations of hundreds of nT are globally observed. (Kearey and Brooks, 1984) This hyperactivity is known as a magnetic storm and often prevents the collection of usable data for the day or days on which it persists.

Based on measuring and modeling of the global magnetic field over time, the International Geomagnetic Reference Field, or IGRF, has been developed. This model predicts the undisturbed strength of the magnetic field at a given location for a given time. (Kearey and Brooks, 1984) Localized divergence from these predicted values of magnetic field strength can be caused by geological features, in addition to the natural variation of the Earth's magnetic field. Some igneous rocks contain an abundance of iron bearing minerals, which may have a high magnetic susceptibility meaning that the rock has a greater propensity to record the magnetic field orientation and strength at the time of its formation (known as natural remnant magnetization) as well as being more responsive to the current magnetic field. In a magnetic profile comparing them to surrounding rock, these igneous bodies produce an outlying field strength value which does not conform to the predicted pattern of natural variation. That outlying value is a magnetic anomaly. The

susceptibility and natural remnant magnetization of concealed basic igneous rocks allows their detection from remote locations through the examination of the magnetic anomalies they produce.

Throughout geologic time, there have been time intervals during which the magnetic poles have had a *reverse* orientation relative to the modern orientation which is conventionally called *normal.* This pattern is best recorded at mid-ocean ridges where the crystallization of basaltic magma is continuous on a geologic time scale. Upon crystallization, the basaltic rock records the location of the magnetic pole and, thereby, the orientation of the magnetic field. During marine surveys, a striped pattern in the magnetic orientation of seafloor rocks emerged allowing the establishment of a polarity time scale (Appendix A). The most recent reversal to normal polarity occurred 780 Ka. Thus, a rock which yields a strong negative anomaly was aligned with a reversed magnetic field at the time of its formation and pre-dates 780Ka. (Musset and Kahn, 2001) Igneous bodies with strong remnant magnetization may thus have a positive anomaly (where the remnant magnetization is 'normal' and adds to the Earth's field) or a negative anomaly (where the remnant magnetization is 'reverse' and substracts from the Earth's field).

Treatment of Magnetic Data

Magnetic data over Franklin Volcanic Field was extracted in a series of east-west profiles from the data set for NBP 04-01. To map magnetic signatures of geological bodies, it is necessary to process magnetic field values measured during a survey. First, the values attributable to the Earth's magnetic field must be removed. This is done using

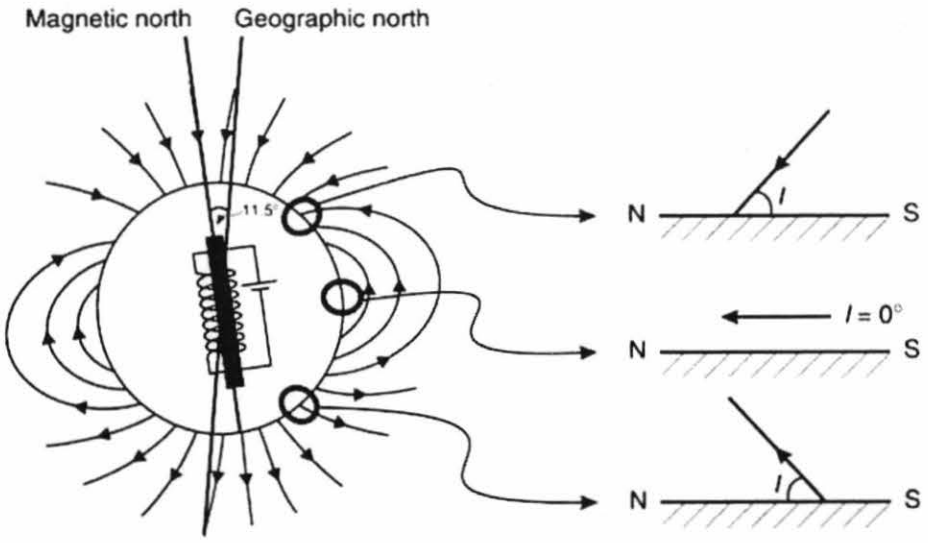

Figure 21: Change in inclination angle with geographic latitude. Inclination Angle is 90 degrees at magnetic poles and zero degrees at the equator. (Reynolds, 1997)

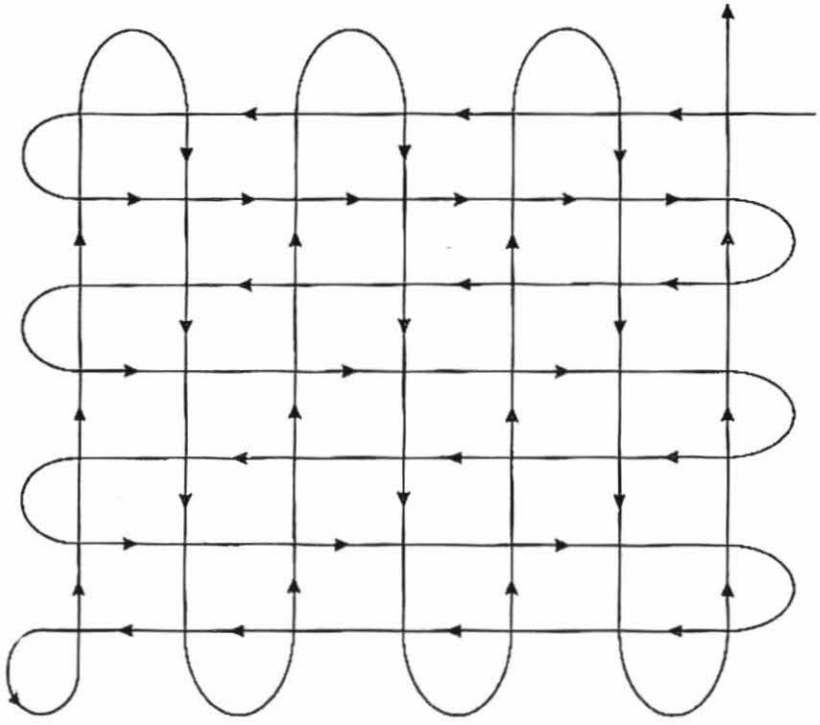

Figure 22: Ideal survey grid for an aeromagnetic survey (Reynolds, 1997)

the IGRF model for the survey region. For this study, the author provided the FVF data to Dr. Beata Csatho at the Byrd Polar Research Center, who removed the IGRF from the data using the Geosoft magnetic data processing software package. Second, contributions from other sources of natural magnetic variation (i.e. diurnal variation or magnetic storms) must be removed. There are many available methods to accomplish this correction; however, none have yet been applicable to the Franklin Volcanic Field for reasons discussed below.

Surveys designed primarily for detection of magnetic anomalies generally are carried out in a series of relatively closely spaced, parallel survey lines, linked by perpendicular 'tie lines' (Figure 22). In the presence of a constant field, the value at each crossover point would be the same over time. By observing the variation between the first and second readings at crossover points, one can calculate the change in field strength, which is then directly attributed to fluctuations in the magnetic field. Since a tie line crosses all the lines in the region, it allows the calculation of variation over time, thereby modeling the natural fluctuation of the magnetic field (Kearey and Brooks, 1984). These data are also later compared to readings at a local base station in order to identify natural variation in the values.

For shipborne surveys where the primary goal is to collect magnetic data, two magnetometers are commonly used. Each is towed behind the vessel, with a mutual spacing which corresponds to the scale of features which are being observed so that as one magnetometer passes over a feature of interest, the other does not and provides a reference value. The proximity of the two magnetometers is sufficient to allow the inference that there is a direct correlation between the total magnetic field at one

magnetometer and the expected total magnetic field at the other. Thus, any differential field measured between the two magnetometers can be interpreted as a local anomaly and used to calculate that anomaly's magnitude.

During the NBP 04-01 cruise, a single magnetometer was towed and neither of these common survey modes was used. The original intent of the research expedition was more dependent on the identification of seafloor hills as volcanic features based on seafloor morphology and seismic profiling. The magnetic data was aimed at detecting the signature of basaltic volcanic bodies at or beneath the seafloor by identifying relative highs or lows in the magnetic data, compared with local background values. Problems arose in trying to remove contributions from non-geological sources of natural magnetic variation from the survey data. A first approach to identify and remove diurnal variation and magnetic storm components planned to use data from geomagnetic observatories in the region as base stations for the surveys. Data was obtained from the Scott Base from http://www.intermagnet.org, courtesy of Stuart Henrys, and from the Terra Nova Bay Magnetic Observatory courtesy of Dr. Domenico Di Mauro (Istituto Nazionale di Geofisica e Vulcanologia, Rome, Italy). These data were graphed together with NBP 04-01 profile data for identical time intervals. This revealed significant differences between magnetic intensity between the base stations (Figure 23), indicating that the base stations could provide information about the general magnetic conditions during a given time, but were not useful for removing diurnal variations from the NBP data.

Using local observations where tie lines provide crossover points to level the magnetic field values for the area is commonly used in well-gridded aeromagnetic surveys but has not been possible for the Franklin Volcanic Field due to the nature of the

Figure 23

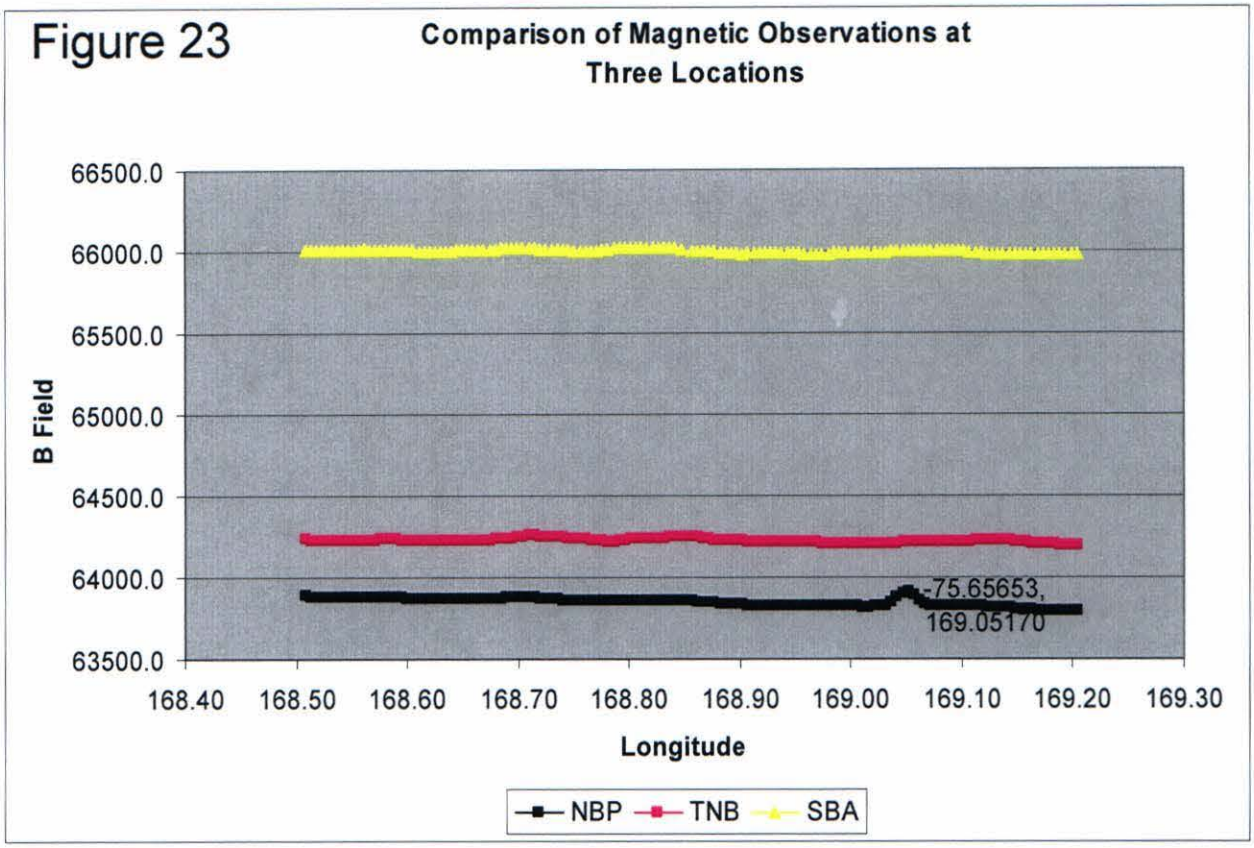

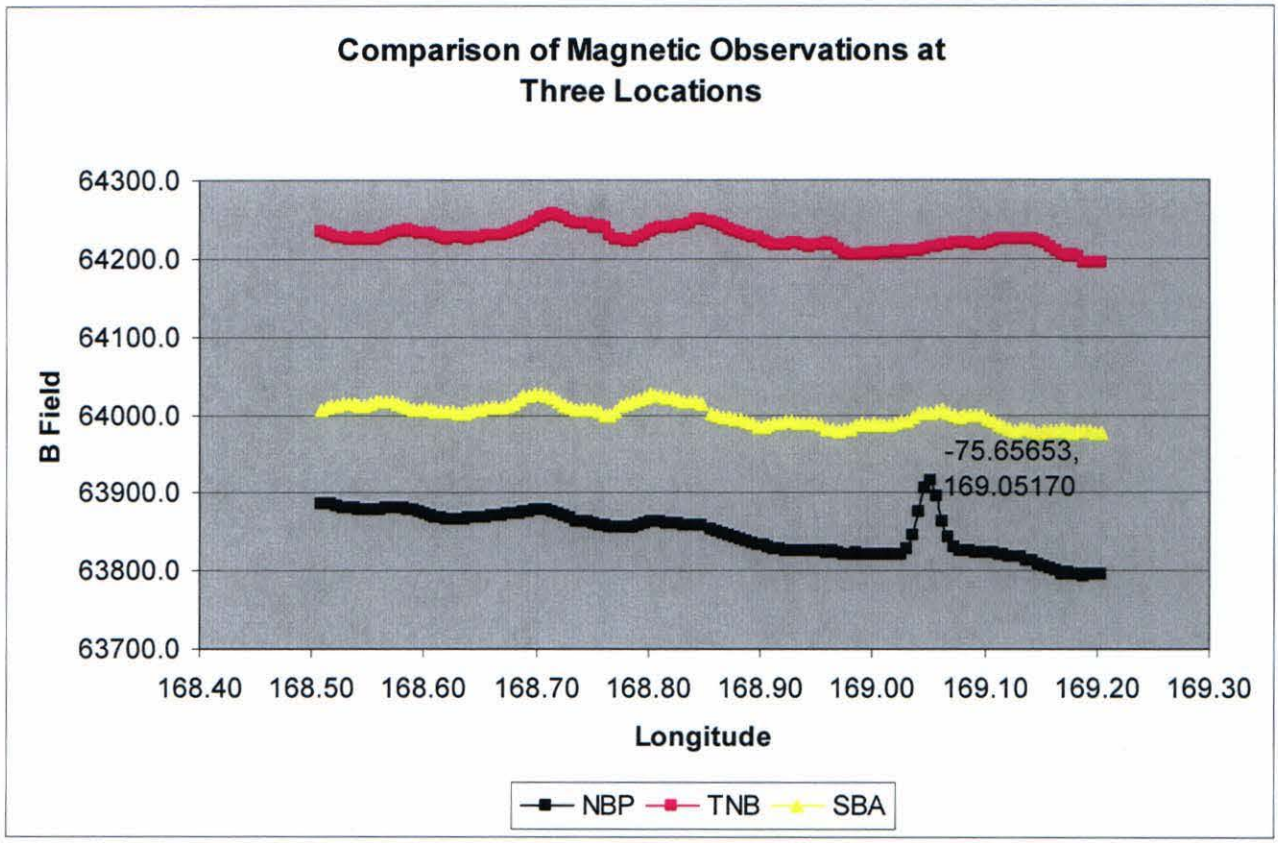

A) Data along the N1 profile. Longitude is the location of the NBP. Contrasting magnitude of observations for time equivalent magnetic data prevents direct subtraction of base station values to calculate magnetic anomaly magnitude at NBP. B) Same data, rescaled to show detail. Note that general conditions of the magnetic field are analogous.

survey. The Franklin Volcanic Field and its adjacent low lying areas were surveyed on various days over a month-long period. Data were obtained in the region on the 20, 23–25th and 27- 29th of January and on the 6, 7, and 12th days of February. In the case of NBP 04-01, data along the tie lines were collected days or weeks after the original parallel grid lines were observed. The time expansive nature of the NBP survey makes the classic grid technique inadequate because the time in which the magnitude of variation can be modeled using the cross over points is limited. Furthermore, the tie lines provide clusters of data which skip entire days and therefore entire cycles of diurnal variation and potential magnetic storms.

Because of the aforementioned limitations, profile analysis was applied instead of producing an anomaly map from gridded values. The observed magnetic anomaly value for each minute was plotted against the corresponding position as recorded by the vessel's GPS. Once the series of parallel profiles is complete, the anomalies observed in each individual line can be correlated to magnetic anomalies in other lines which cross the same feature. In order to ease spatial correlation of the profile data, data were imported into the GIS and color coded according to the calculated anomaly magnitude. The resulting map is included in the descriptive section below. In order to enhance the quality of the data display, anomaly values along profile N30 and other extreme maximum and minimum values were removed. The correlation of anomalies across two-dimensional space in map view allows the anomalies to be directly attributed to sea floor features mapped from the bathymetry data.

Gravity Data

The following section incorporates background information on the origin and collection of gravity data. This material is referenced from Reynolds (1997) unless otherwise noted.

The Gravity Field

According to Newton's universal law of gravitation, gravity acts to pull two massive objects toward each other. The magnitude of this attraction depends on the mass of the two objects as well as the square of the distance between them (See Figure 24 for equations governing magnitude of gravity force). The magnitude of the force of gravity is proportional to the acceleration that it causes between two objects. By convention, the acceleration of an object due to the Earth's gravity field is denoted g which is approximately 980cm/s^2 (1 cm/s^2 = 1 Gal) at the surface of the Earth. Measurements of g are taken with respect to the geoid, a surface which is always perpendicular to the gravity field and connects all points of equal field strength. If the Earth were a smooth, homogeneous sphere sitting motionless in space, the geoid would be aligned exactly along its surface. However, in addition to its rotation, the Earth is flattened at its poles, has an uneven distribution of mass and uneven surface topography, all of which act to warp the geoid and produce long wavelength anomalies. (See Figure 25) Superimposed on the long wavelength anomalies are shorter wavelength anomalies due to near surface variations in mass distribution and surface morphology.

Gravimeters, which measure changes in the gravity field, respond to variable mass distribution or density of the material in the subsurface. Commonly, the gravimeter

Figure 24: Equations governing gravitmetric forces

$$\text{Force} = \text{gravitational constant X } \frac{\text{mass of Earth (M) X mass (m)}}{(\text{distance between masses})^2}$$

$$F = \frac{G \times M \times m}{R^2}$$

$$G = 6.67 \text{ X } 10\text{^-}11 \text{ N m}^2 \text{ kg}^{-2}$$

A) Newton's law of universal gravitation governs the gravity pull between an object of mass m and the Earth .

$$\text{Force} = \text{mass (m) x acceleration (g)}$$

$$F = m \times g$$

B) Newton's second law of motion.

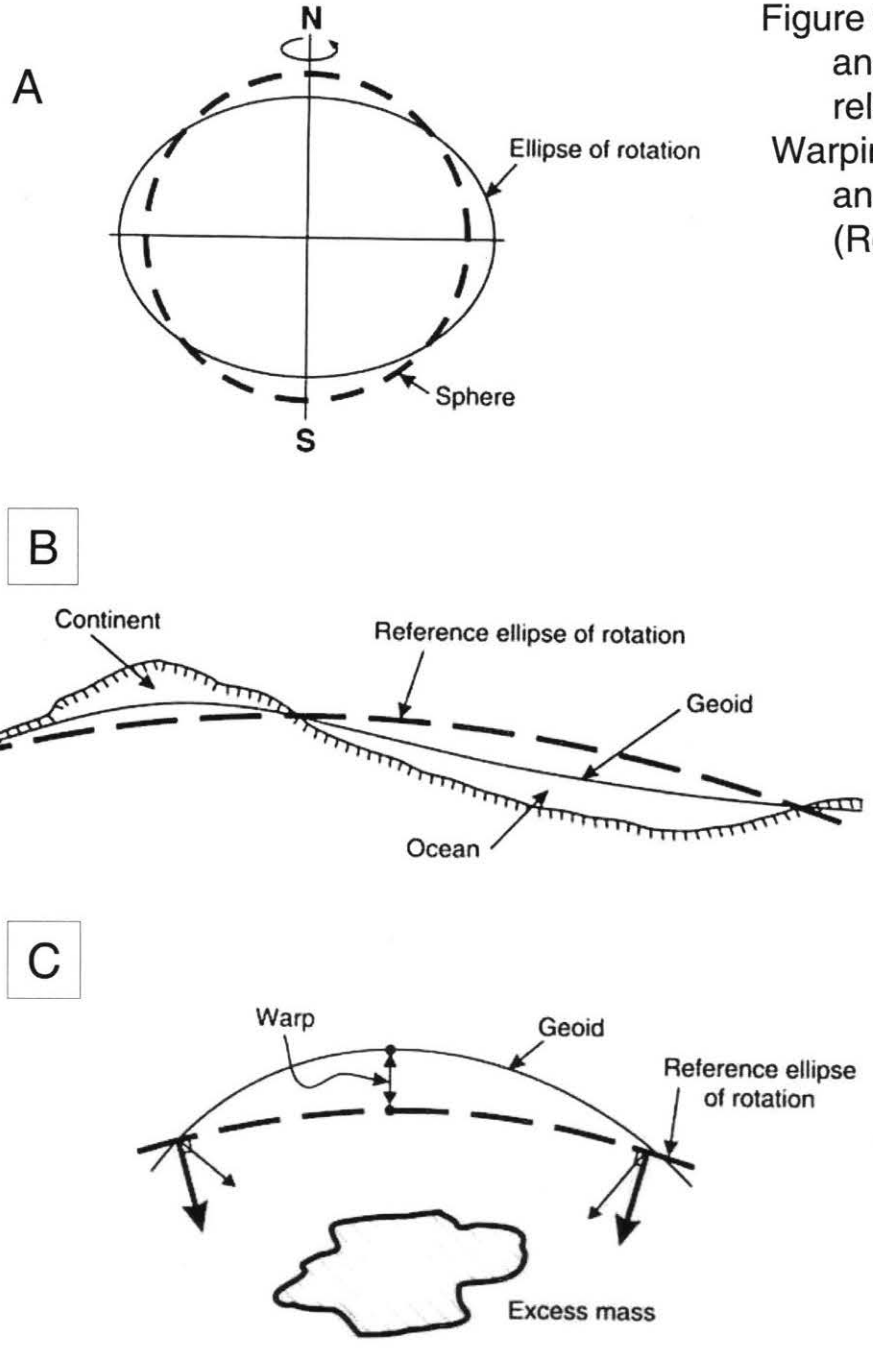

Figure 25: Origin of long wavelength gravity anomalies. A) The true shape of Earth relative to ideal sphere.
Warping of the geoid due to B) topography and C) relatively dense body of rock. (Reynolds, 1997)

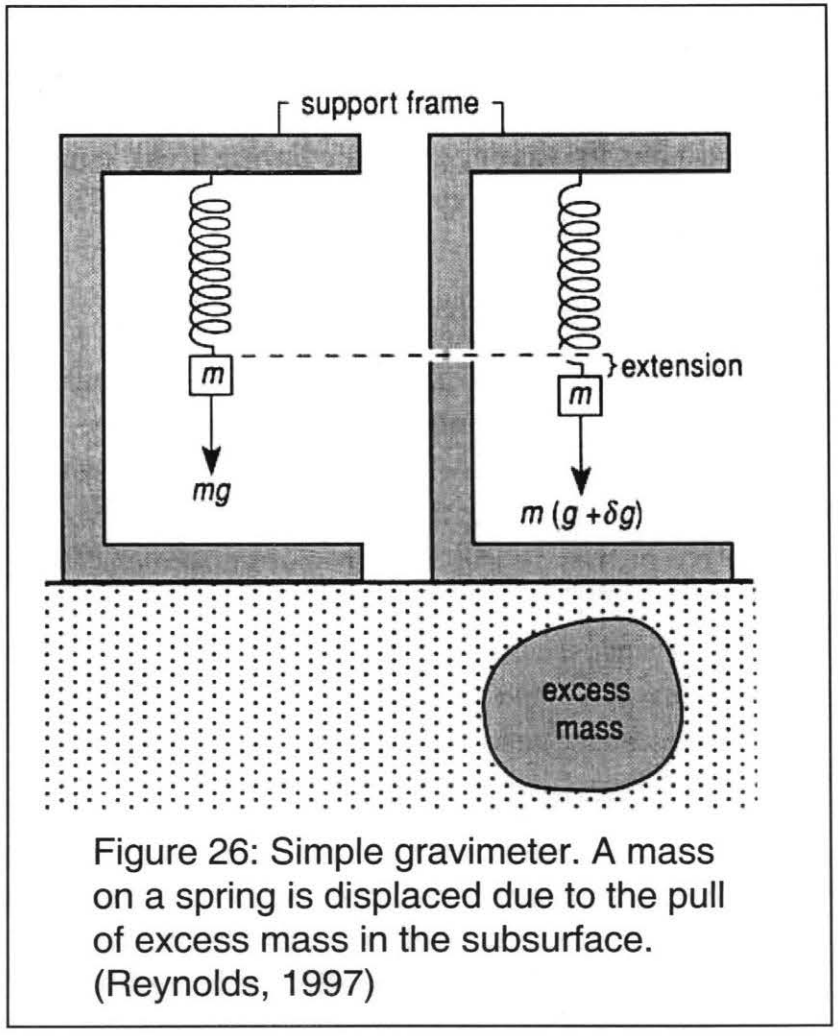

Figure 26: Simple gravimeter. A mass on a spring is displaced due to the pull of excess mass in the subsurface. (Reynolds, 1997)

uses a mass and spring system based on the principle that displacement of the spring is directly proportional to the local change in g resulting from a change in mass distribution (Figure 26). The magnitude of gravity anomalies, which can be either high or low, are measured with respect to the value expected from the location of the geoid in the area of interest. When surface elevations are sufficiently constrained, modern gravimeters are sophisticated enough to measure the variation in gravimetric acceleration on the order of microGal (10^-6 Gal).

In geologic settings, variable rock types and crustal thicknesses are common causes of gravimetric anomalies. Rocks, depending on their origin and composition, have a characteristic density (mass per unit volume). As a general rule, sedimentary rocks are less dense than igneous rocks (See Figure 27). Thus an igneous rock will appear more massive than a sedimentary rock of the same volume. The local thinning of crust allows the mantle to rise up closer to the surface. Since the mantle is a denser layer than the crust (3.3 g/cm^3 as compared to 2.75 g/cm^3), this upwelling increases the local pull of gravity. Thus areas of extensional tectonism, like WARS, are commonly gravimetric highs relative to their surroundings, meaning that acceleration due to gravity is locally enhanced. In contrast, during mountain building, contractional deformation produces crustal thickening and thereby lowers the level of the crust-mantle boundary, called the Moho, toward the center of the Earth. Depression of high density mantle material creates a relative gravimetric low corresponding to a local decrease in g (See Figure 28). (Barret et. al, 1995; Reitmayr, 1997)

On a broad scale, the regional gravity signature of the TAM-WARS system conforms to these predictions. The TAM are associated with a broad gravity low,

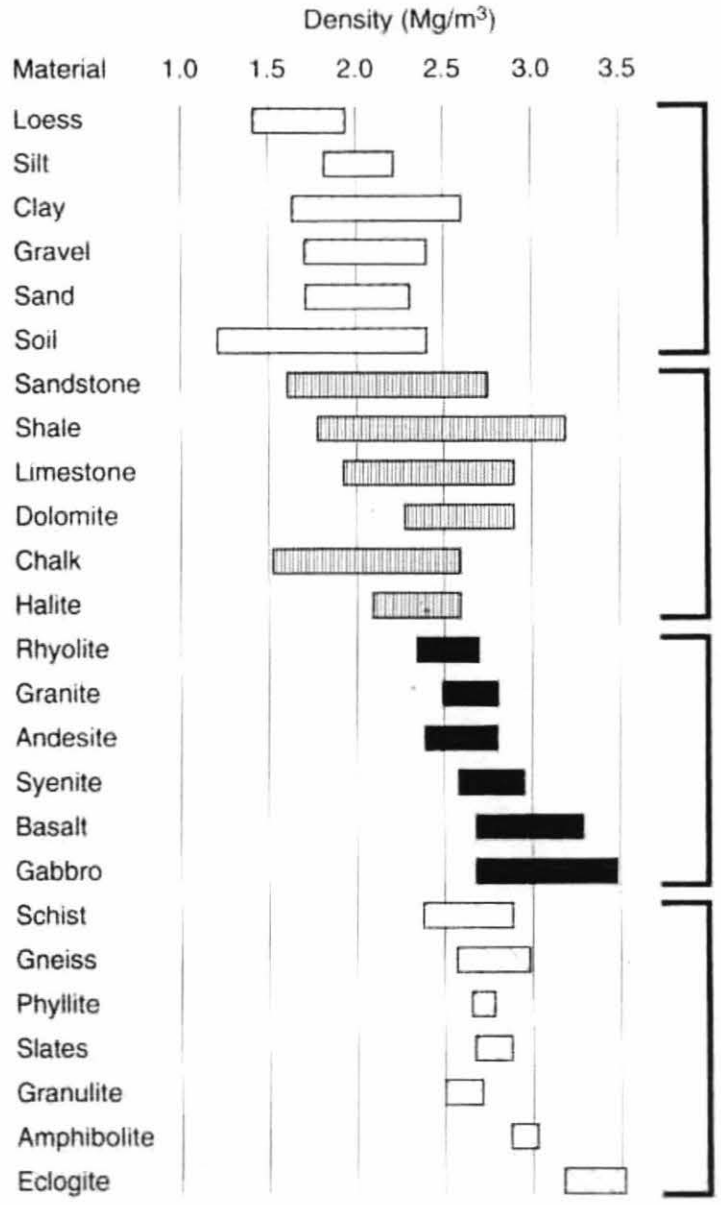

Figure 27: Densities of common rocks and sediments. (Reynolds, 1997)

Figure 28

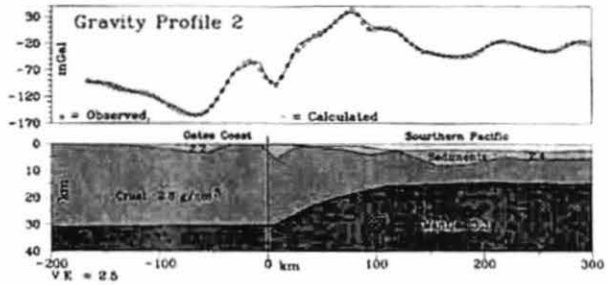

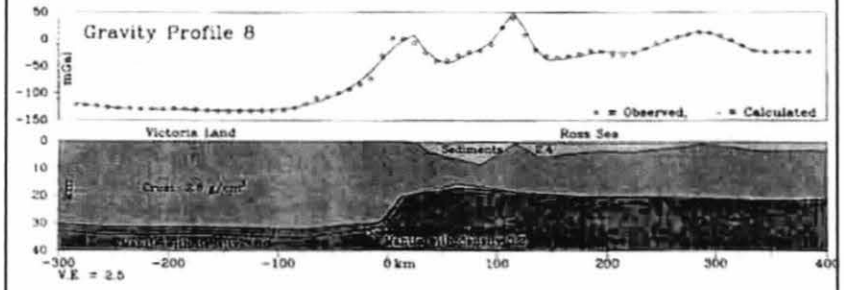

Gravity profiles over the TAM and Ross Sea illustrate the relationship between crustal thickness and long wavelength gravity anomaly value. Smaller wavelength anomalies are superimposed due to near surface lithologic contrasts. (Reitmayer, 1997)

whereas the region of the WARS under the Ross Sea has relatively higher gravity values (Reitmayer, 1997). Sediment-filled rift basins are expected to be marked by gravity lows, and some Ross Sea basins are anomalous in having relatively higher gravity than adjacent basement block uplifts. This may relate to underplating by magmatic intrusions, from mechanical flexure of the crust, or other, as yet unidentified, sources. On a local scale, shorter wavelength anomalies are superimposed on the regional trends, reflecting the distribution of mass within the upper crust. Where short wavelength anomalies are greater than the regional mean, they indicate the presence of relatively dense rock types such as the basaltic igneous rocks of the McMurdo Volcanic Group. Short wavelength anomalies with values less than the regional mean are indicative of sediment infilling of surface depressions.

Treatment of Gravity Data

Gravity data from the NBP 04-01 cruise was obtained using a gravimeter mounted in the ship. A tie between the shipboard gravimeter and a land-based gravity station at McMurdo Station was made prior to the cruise. Before the end of the cruise, values were corrected using the EOTVOS subtraction which accounts for the motion of the ship relative to the rotation of the Earth. Additional correction for depth of the features relative to the gravimeter has not yet been undertaken. The anomaly values obtained from the cruise were plotted along tracklines in the FVF using the location given by the ships GPS. The resulting map is included in the descriptive section below.

Seismic Reflection Data

The following section incorporates background information on the origin and collection of seismic data. This material is referenced from Musset and Khan (2001) unless otherwise noted.

Seismic surveying

Seismic reflection surveying uses ground penetrating energy pulses, or 'seismic waves', to map a cross section through the Earth's crust (Figure 29). The ability of a rock unit to transmit the acoustic energy signals varies with its density, and hence its lithology, as well as with its structure. As the seismic waves pass through the subsurface they are reflected at boundaries between units with different acoustic impedance. These boundaries commonly correspond to lithologic changes in the subsurface. The cross section produced shows the geometric relationship of rock units throughout the underlying area. Sedimentary basins, characterized by thick accumulations of approximately horizontal sedimentary layers, are well-suited for seismic analysis because horizontal and gently-dipping layers produce the most coherent reflections. Through the study of the geometry and lateral continuity of the reflectors, post-depositional disturbances to strata within basins can be identified and mapped.

The Franklin Volcanic Field is developed within the Victoria Land rift basin, characterized regionally by flat-lying or dipping strata. Lateral disruptions or truncations of sedimentary layers could be the result of faulting, glacial erosion, paleotopography, or volcanic intrusions. Faults produce offset of otherwise continuous strata across a linear zone. This is observed in the seismic lines as a truncation and change in the position of a

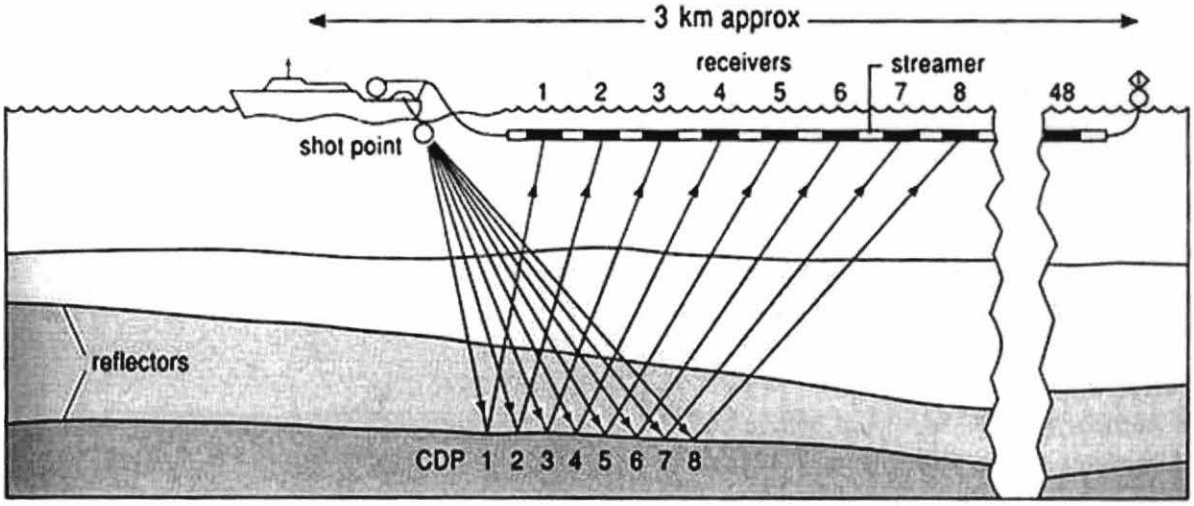

Figure 29: Cartoon of seismic surveying shows streamer in tow behind the vessel

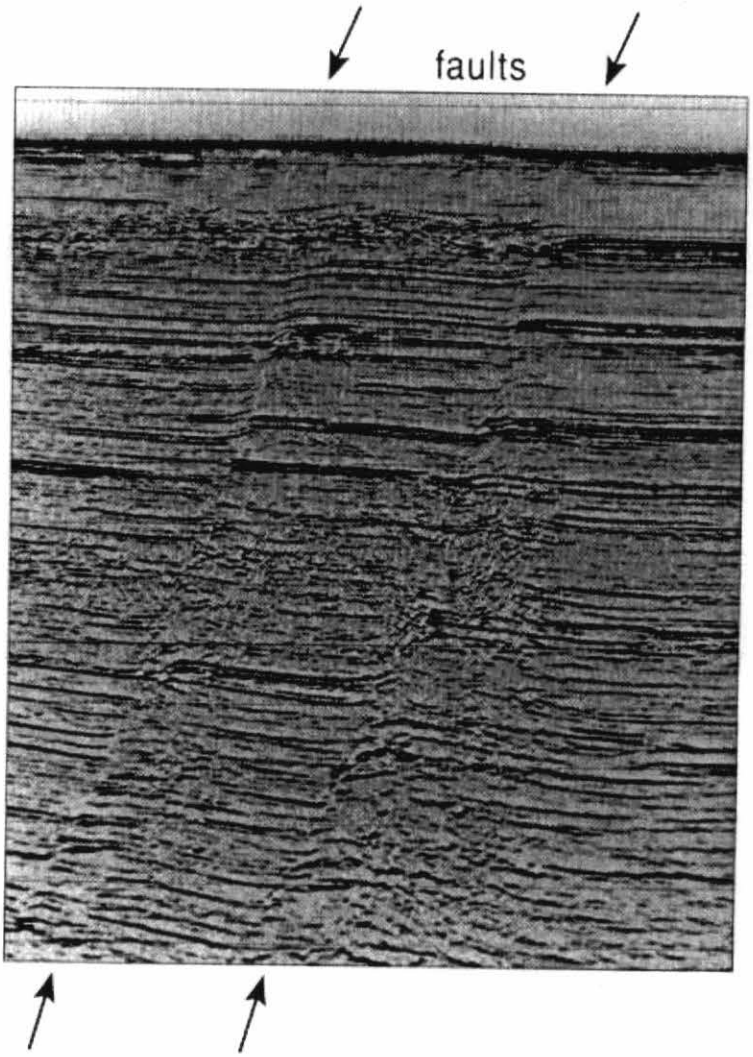

Figure 30
Truncation and offset of strata across a fault zone as seen in seismic section.

reflector across a dipping, planar surface, the fault (Figure 30). Glacial erosion alters surface morphology and can reduce the thickness of the rock units it scours. Receding glaciers can create unconformable contact surfaces in the stratigraphic column and can spawn stream channels that carve into the substrate. Paleotopography created by past glaciations or tectonic movements is filled in by later stage sedimentary strata which are deposited horizontally. Deposition on top of pre-existing structure and dipping layers creates a change in bedding orientation across the contact. Since the contact represents a significant geologic time gap between the units it is referred to as an angular unconformity. Volcanic intrusions cut upward through pre-existing layers and so appear as zones of interrupted reflector patterns. Dike intrusions have contacts that are at a high angle to the general bedding dip. Morphology of intrusion contacts and patterns within volcanic bodies can be variable. Some units have internal stratification which differs from that of the surrounding rock, some units lack stratification and other units do not seem to inhibit the passage of very bright reflectors at all.

Treatment of seismic data

During the NBP 04-01 cruise, seismic data were collected along tracks perpendicular to the general trend of the Franklin Volcanic Field (Figure 31). During optimal conditions, the system operated 6 GI Air Guns which used compressed air to generate the necessary acoustic energy wave. The streamer, which was towed in the water at near constant depth, contained hydrophones which recorded small local changes in pressure as the energy waves returned to the surface. Initial processing was conducted onboard the ship by members of the science team to produce seismic profiles showing

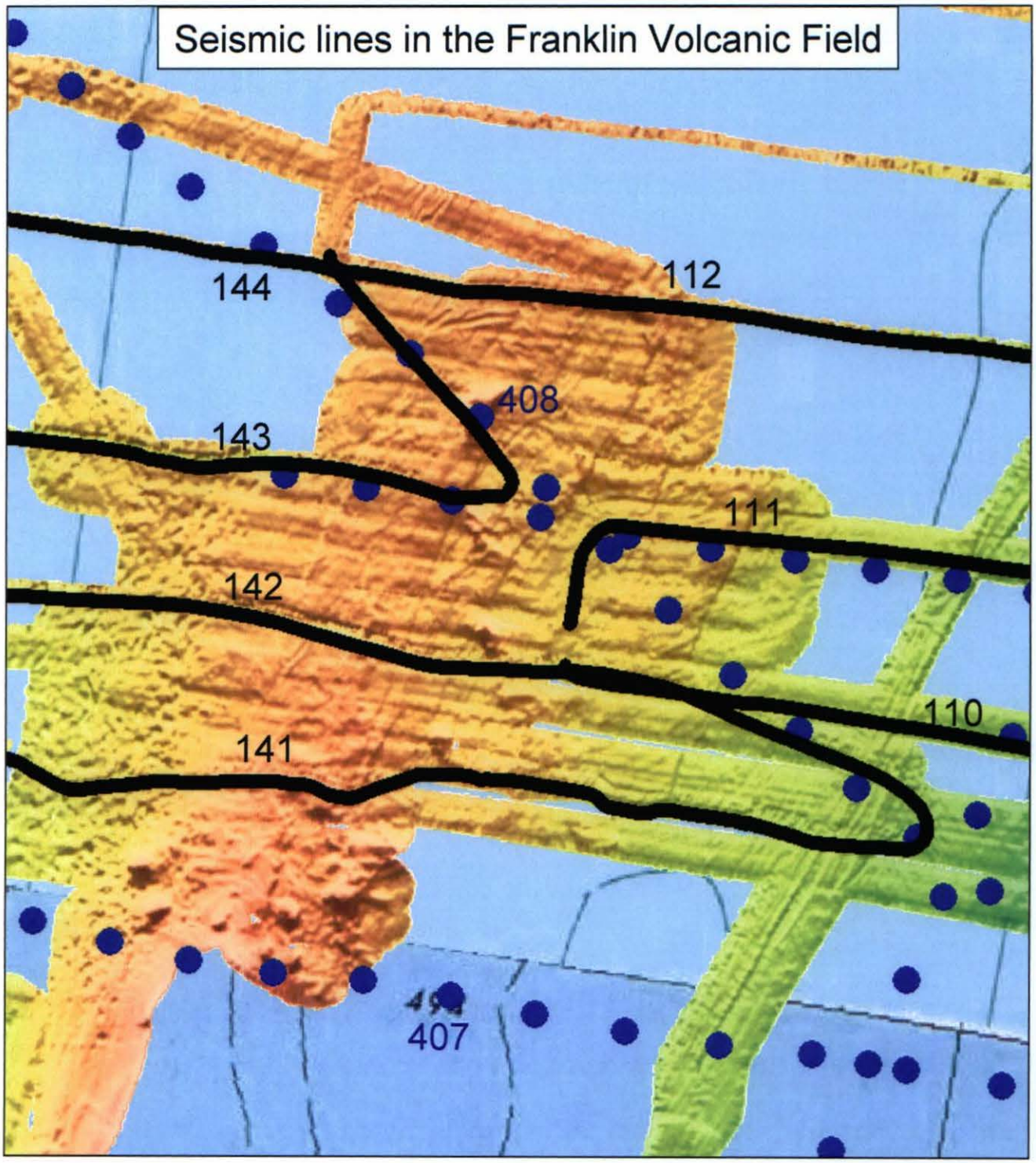

Figure 31: Seismic lines in the Franklin Volcanic Field. NBP 04-01 lines are in black. Lines from Cooper et al. (1987) are in blue.

subsurface reflector position relative to two-way travel time. Additional processing is being conducted at the Institute of Geological and Nuclear Sciences in New Zealand (Stuart Henrys). Since rock units have a wide range of acoustic velocities, converting the units of a seismic profile from two-way travel time to depth is an involved process which has not yet been undertaken for the NBP 04-01 seismic data. This study focuses on the subsurface shape of features and their spatial correlation with seafloor topography, so that their absolute depth is inconsequential.

Processing of the seismic profiles is ongoing. At this time, only single channel seismic data are available for profiles 141, 142, 143 and 144. The current single channel seismic profiles have high vertical exaggeration which stretches vertical disruptions while compressing and obscuring the horizontal dimension. Very narrow dikes and steep, small-offset fault zones are particularly hard to distinguish on such lines. Current interpretations of small features from seismic data are tentative, and must rely on the integration of other geophysical data sets to draw conclusions about their mode of origin. In addition, it appears that the geographic location recorded for seismic shot points is not correctly registered spatially with the bathymetric maps. Thus, the bathymetric expression of the seismically observed features is consistently to the west of the locations given by the seismic profile's shot point numbers. Finally, the resolution of the seismic data is such that features with less than 15 meters vertical expression may not be observed.

Results

Bathymetric Maps: Description and Initial Interpretation

Based on the bathymetric maps, the Franklin Volcanic Field is divided into three north-south trending terrains with distinct morphological characteristics: the western terrain is marked by hummocky topography and abundant surface depressions, the central terrain is dominated by conical bathymetric highs and long, branching linear features, and the eastern terrain is characterized by a closely-space fabric of linear traces (See Figure 32). The contrasting morphology of each terrain provides a basis for interpreting their respective mechanism(s) of formation as the result of different geologic processes.

Western Hummocky terrain

The hummocky terrain occupies the western slope of the Franklin Island Ridge. The slope is shallow, dropping from 440 meters to 500meters below sea level in approximately 8 km. For the length of the slope, there are randomly distributed surface depressions up to 1 km in diameter and 30 meters deep. The depressions show variable shapes from oval to round. The negative relief and frequency of these features suggests a glacial rather than volcanic origin however, the depressions are unique within the Ross Sea Floor and lack a submarine analog. Two modes of formation have been suggested by Julia Wellner via e-mail correspondence. The depressions could be kettle holes formed by deformation of sedimentary layers under the weight of a large ice block or they may be depositional structures formed as sediment is deposited around blocks of partially grounded ice. Both hypotheses agree that the features formed under stationary blocks of ice which were left by the ice sheet during its retreat.

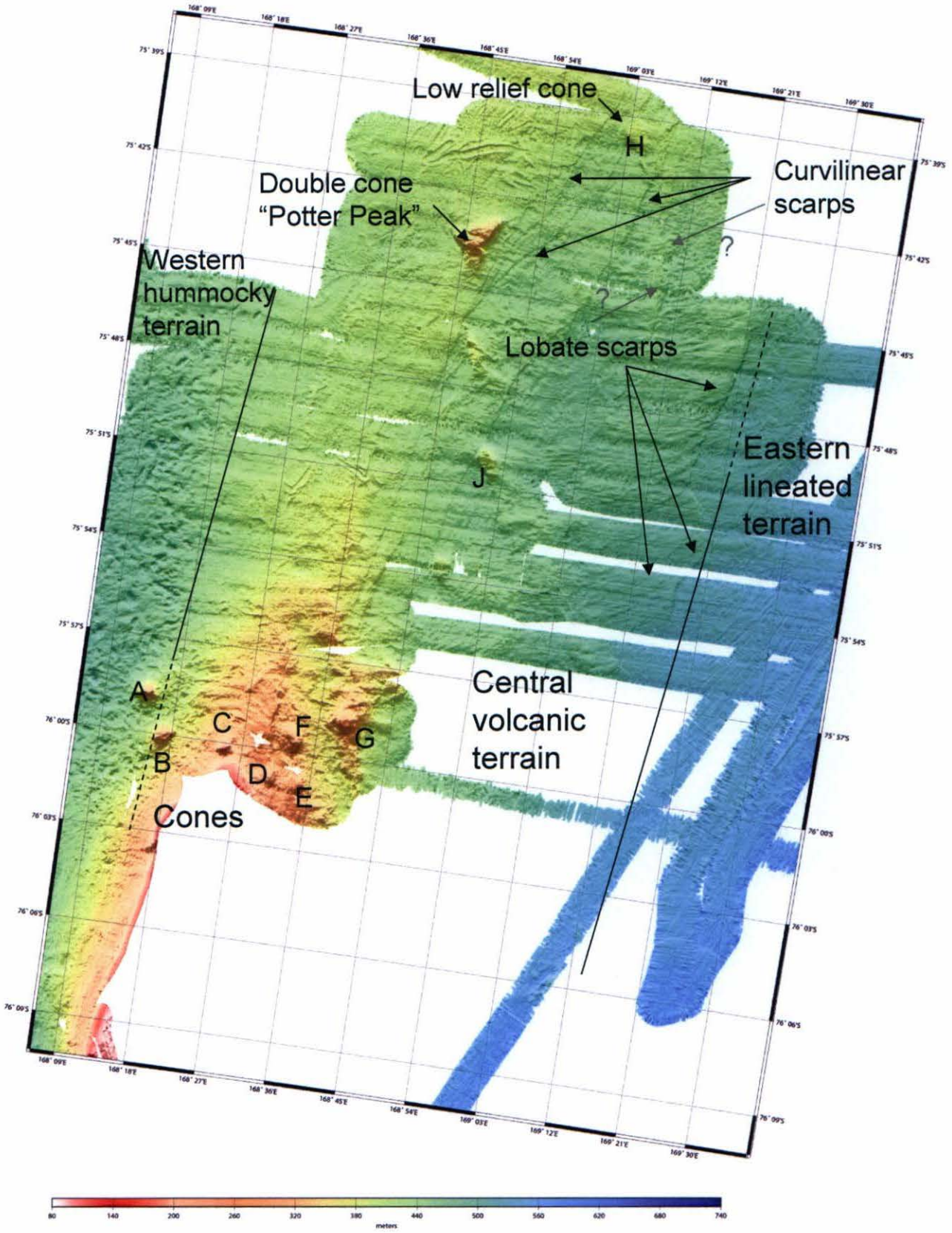

Figure 32 : Bathymetrically defined terrains and nomenclature of features North of Franklin Island. Image illumination from the West and North.

Central Volcanic terrain

The Franklin Island Ridge has a regional N-S trend which curves toward the northeast near Franklin Island. The raised topography of the ridge, its association with Franklin Island, and the broad magnetic anomaly over it were early indications of its volcanic origin. The origin of cones A, C, G and Potter Peak was determined during the NBP 04-01 cruise through the collection of samples from the sides of these edifices. Through dredging, basalt, hyaloclastite and tuff from the four hills were obtained for geochemical analysis and age dating. The presence of basalt on each points to a volcanic origin. Based on their similar morphology and spatial association, the cones B, D, E, and F are also interpreted as volcanic cones. The morphological characteristics of cones A-G are summarized in Table B.

Cone A sits on the margin between the hummocky and volcanic terrains. Its symmetric shape prevents definitive correlation with other volcanic features. The trend of the long axis of cone B is parallel to the trend of the regional volcanic ridge. Cone C has a more easterly elongation than any other volcanic feature and sits very near the axis of the regional ridge. Cones D, E and F are clustered just east of the central ridge axis. Each of the cone bases has a north-south elongation; craters on cones D and F have north-south and northwest elongations, respectively, which are all different than the northeast elongation of the cones to the west of the central ridge axis. Cones E and F sit on a superimposed ridge which trends northwest. Cone G is the most prominent topographic high, and is positioned on a northwest trending ridge, R1. R1 is surrounded by lobate ridges extending outward from its flank at a high angle. These lobate ridges are

Table B	Dimensions	Basal morphology & elongation; cone symmetry	Crater morphology and elongation
A (west)	1.34 km long 1.34 km wide 110m total relief	Circular cone base with steep pyramidal sides	Round
B	1.34 km long 1.09 km wide 60m total relief	Stubby oval shape, NE-SW elongation Steep western flank	Oval, elongated to the northeast
C	1.43 km long 0.71 km wide 50m total relief	Stubby oval shape, NE-SW elongation Steep western flank	no visible crater
D	1.64 km long 0.88 km wide 30m total relief	Oval shape, N-S elongation Steep eastern flank	Oval, elongate in north-south direction
E	1.18 km long 0.80 km wide 30m to 90m total relief	Oval shape, N-S elongation Steep eastern flank	no visible crater
F	2.02 km long 1.18 km wide 35m to 70m total relief	Oval shape, N-S elongation Steep eastern flank	Oval, elongate to the northwest
G (east)	1.30 km long 1.09 km wide 50m total relief	Nearly round with slight N-S elongation	no visible crater

interpreted to be lava flows that were extruded from a vent (or vents) coevally with the formation of the ridge itself.

Further north from the steep slope of Franklin Island, there are two additional northwest trending ridges named R2 and R3, a prominent double cone named 'Potter Peak', and by long, curvilinear escarpments E1, E2 and E3. R2 and R3 have superimposed cones which are elongate to the northwest. The cones have relatively shallow flanks and are up to 50 meters tall. Depending on the perspective, these two ridges may look to be parts of the same northwest trending ridge. However, since bathymetric linkage between the two is lacking, they have been interpreted as separate but parallel volcanic ridges forming an *en echelon* pattern. 'Potter Peak' is a triangular edifice with the largest dimension in the area, having a maximum cross section of 3.3 km. The cone has a total relief of 75 meters. The triangular morphology is in part due to a flanking lava flow which extends from the southern face of the cone. At the northern limit of the mapped area, there is a low relief cone, cone H, which is approximately 20m high on its steep western side. Its ovate morphology is elongate to the northwest. The curvilinear scarps E1, E2 and E3 are at least 10 m high, step down to the east, and extend north-northeast for 25km in the mapped region. The westernmost scarp, E1, appears to link Franklin Island with Potter Peak, however, it branches into three traces (E1a, E1b, and E1c) that curve to the northeast adjacent to Potter Peak. From bathymetry alone, the origin of the curving scarps is not clear. They could represent volcanic ridges, fault scarps, or glacial lineations.

The eastern margin of the volcanic terrain is defined by a set of lobate scarps LS1 and LS2. Each steps down-to-the-east with a drop of approximately 10 meters. To the

south and east of LS2, there are a series of subparallel, curving low-relief escarpments, all stepping down to toward the east. The lobate form of these scarps (LS1, LS2 and related features), and the overall setting within a volcanic province, suggests they may be the margins of lava flows.

Superimposed on the volcanic terrain are sharp, elongate depressions of 10 to 15 meters with distinctive angular bends. These are only observed where the seafloor is above about 400 m depth. The sharp, steep sides suggest they were formed where iceberg keels dragged across the seafloor. Although lineations are also carved by the motion of grounded ice sheets, the sudden change in movement direction recorded by these features, their lack of continuity, and their development only in the shallow portions of the region, are indicative of iceberg movement.

Eastern lineated terrain

The lineated terrain shows some overlap with the eastern edge of the volcanic terrain. The lineations in this zone have 5 to 20 meters of vertical relief, 5 per kilometer frequency of spacing, and can be traced nearly continuously across the eastern terrain. Across the region, the lineations show a systematic change in trend from east-west over the volcanic region, to northeast in the eastern terrain. The traces are continuous for 6 km before crossing over the lobate escarpments interpreted as the margins of lava flows. The lineations are much more pronounced in the easternmost part of the mapped region where single ridges can be traced for 8 km before leaving the extent of the mapped area.

The contrast in total relief, frequency and lineation direction of these features point to a different mode of formation than that of the volcanic cones and ridges. The

Figure 33
Nomenclature of features for use with seismic, magnetic and gravity observations

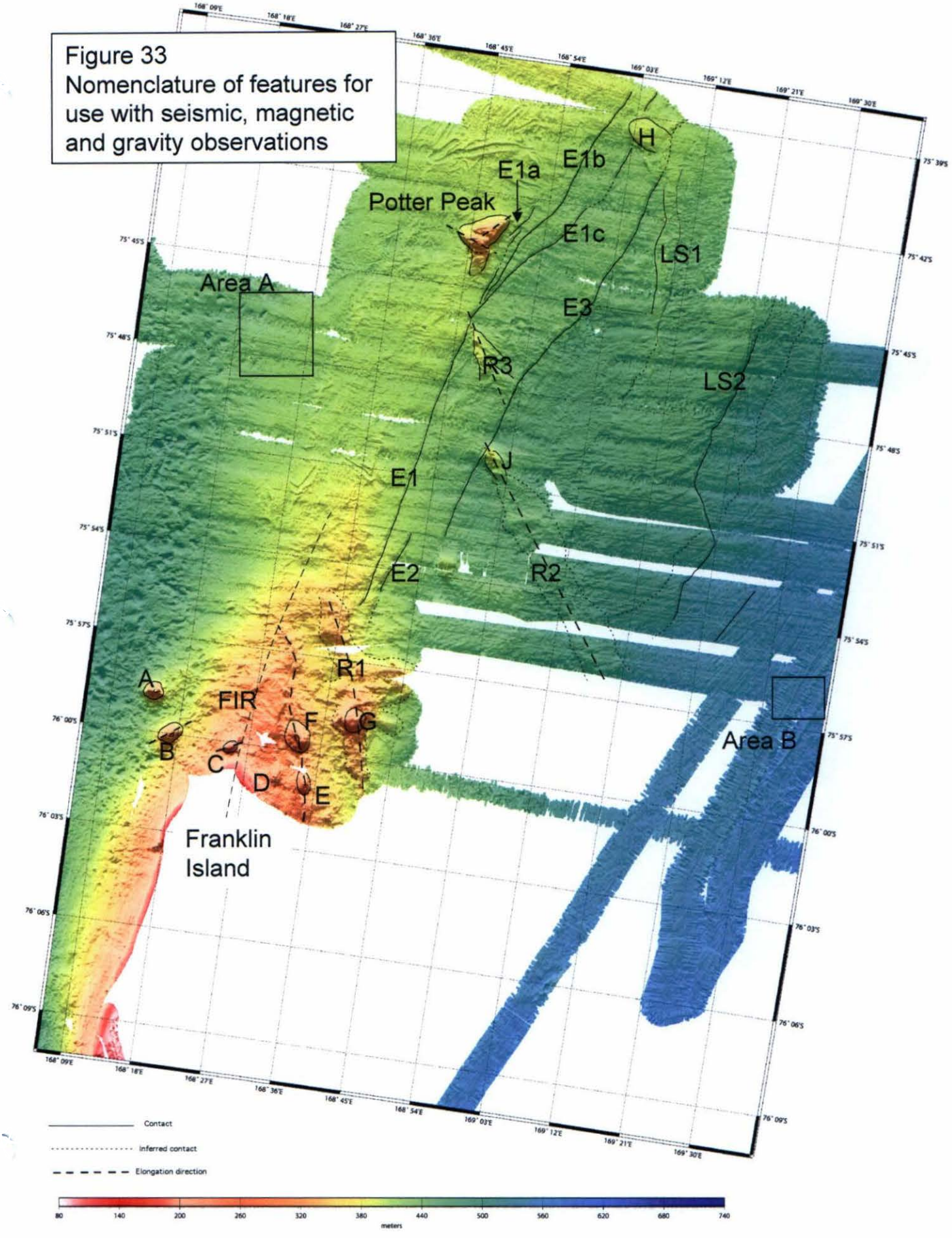

Figure 34: Magnetic anomalies of the Franklin Volcanic Field

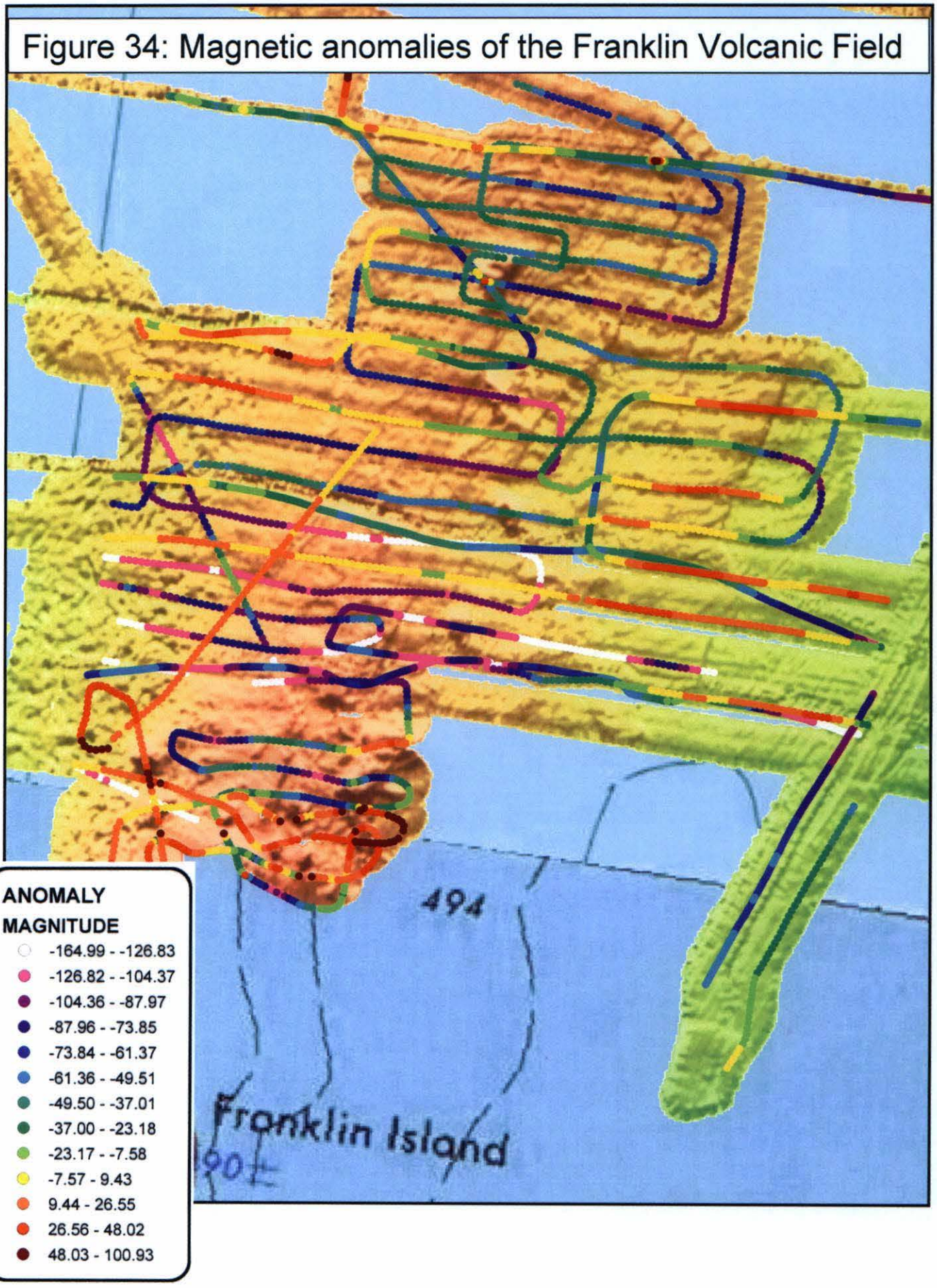

lineations are interpreted as glacial lineations formed by the passage of grounded ice across the region during the Last Glacial Maximum because they are similar to those previously mapped throughout the Ross Sea Embayment. These glacial scours are evidence of a unidirectional flow regime which diverts from the norm around bathymetric highs such as Franklin Island. (Anderson and Shipp, 2001; Anderson and Wellner, 1997). The fact that they are superimposed across the lava flow margins indicates the lineations post-date volcanism, consistent with formation during LGM. The prominence of glacial lineations at the eastern extent of the mapped region is an indication that this area has a softer surface lithology (i.e. unlithified sediment) and provides further evidence that the curving escarpments to the west are the edges of lava flows.

Magnetic Data

Throughout this section the stated value of a magnetic anomaly is taken with respect to the magnetic anomaly values that are immediately adjacent on either side.

Observations

Figure 34 displays the magnetic anomalies of the Franklin Volcanic Field. Discrete positive anomalies overlie Potter Peak and Cones A-H, with Potter Peak and cone H having the largest magnitude anomalies. The trace of R1 is characterized by a positive anomaly. R2 lacks an anomaly signature but Cone J which sits on its northwestern end is a positive anomaly. Three of the four lines crossing escarpment E2 show a drop in the anomaly values from West to East but escarpments E1 and E3 lack a strong signature. There are two conflicting observations over the northernmost part of E3.

One profile shows a short wavelength positive anomaly but the line immediately north of it has an asymmetric anomaly which increases on the eastern side of the scarp trace. The area west of LS2 has a series of broad positive anomalies which cannot be correlated to an individual seafloor feature. Some tracklines show a drop in the magnetic anomaly from west to east across LS2 and LS1, however, the majority of profiles across each lobate scarp lack a signature. Although Area 1 does not have a bathymetrically observed feature, each of the three profiles which cross over it show broad positive anomalies.

Due to the color scale used to plot the magnetic anomaly values, small magnitude anomalies may not be observable if they occur within one of the anomaly value intervals. In order to refine or confirm the observations, profile data across the escarpments and lobate scarps was examined. Some sample profile plots are provided in Appendix B. The profiles show that magnetic values across E1 and E3 generally show variation of about 10 nT on either side of the median value. Lobate scarp 1 and 2 (LS1 and LS2) lack discrete anomalies but each correlates to a change in flexure along a nearly linear trend.

Interpretation

The occurrence of a positive anomaly indicates that the corresponding feature contains iron bearing rocks which formed during a period of normal magnetic field polarity. Thus cones A-H and J as well as Potter Peak are composed of normally oriented volcanic rocks. Based on the time scale for magnetic reversals, this constrains their age to be within the last 780 Ka or older than 1 My. The escarpments E1 and E3 lack a magnetic signature both in the raw NBP observations and the corresponding anomaly values. The anomaly signature of E2 on the map indicated a systematic drop in the

magnetic field value to the east of this escarpment however, profiles failed to produce any measurable anomaly across the feature and thus the corresponding color change may be due to the level slicing of the color scale. The profiles of LS2 show a decreasing trend across the escarpment which has a slight change in flexure across the contact. The absence of an anomaly in this case does not discredit the original hypothesis that these lobate scarps are the edges of successive lava flows. It could simply be that the layer east of the contact is also magnetic and similar in age and therefore produces analogous anomaly values. The general decrease of anomaly values may be the result of the changing depth of the seafloor surface.

It is well known that the McMurdo Volcanic Group has both high magnetic susceptibility and natural remnant magnetization and produces short wavelength magnetic anomalies of 100-1300nT (Behrendt, 1987). The cones and ridges which proved anomalous in the Franklin Volcanic Field were expressed as anomalies of approximately 50nT. This divergence from the expectation can be explained by the noise of diurnal variation which remains in the data set, from the similar magnetic properties of adjacent material, a sediment cover which obscures the natural remnant magnetization of the features, or a combination of these and other effects.

Gravity Data

Figure 35 displays the gravity anomalies of the Franklin Volcanic Field. Throughout the next two sections, anomalies are described as positive meaning positive relative to the immediately adjacent values or negative, meaning negative relative to

Figure 35: Gravity anomalies of the Franklin Volcanic Field

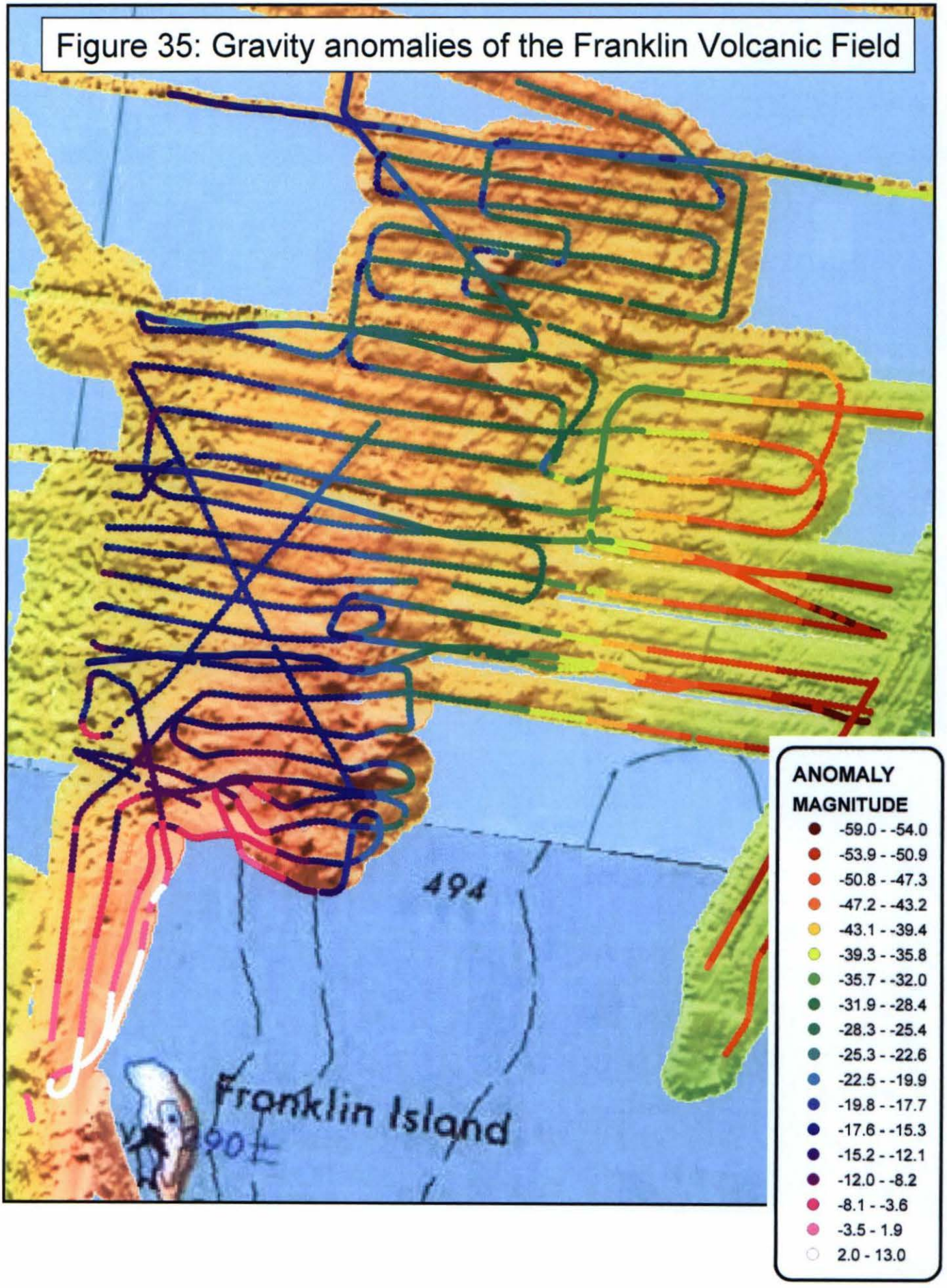

immediately adjacent values. The term *discrete gravity high* is reserved for only those values which are framed by lower anomaly values on both sides.

Observations

Gravity anomalies are greatest along the Franklin Island Ridge and decrease to the North and East of it. The gravity values, as depicted in 'level slices' by the color scale, define subparallel bands across the area which trend to the northwest in the western sector and trend NNE in the eastern sector. The high gravity values of Franklin Island ridge itself extend out to the adjacent cones, A and B, as well as encompassing the superimposed cones C, D, E and F. Cone G lacks a discrete gravity high but is part of the broader high associated with R1. Cone H and Potter Peak are the largest discrete gravity highs relative to their surroundings but are still negative anomalies with reference to the geoid. The southern portion of LS2 shows some indication of increasing gravity anomaly magnitude across the contact; however, this pattern is not seen in the North, which may be due to the 'level slices' of the color scale. Escarpments E1, E2 and E3 lack notable signatures. Where track lines curve, there are strong variations in gravity field values which do not correlate to seafloor features.

Interpretation

The trend of the relative positive gravity anomalies suggest an overall trend of northwest for the magmatic bodies underlying Franklin Island Ridge whereas the bathymetric expression trends more directly north to northeast. The overall trend of decrease out from the ridge may correspond to a thinning of volcanic bodies overlying or

within the sedimentary sequence. Superimposed on the regional trend, Ridge 1, cones A-H, and Potter Peak are all short wavelength positive gravity anomalies which indicate a local concentration of relatively dense, igneous rock. The drop in gravity values across LS2 is subtle but systematic. This change can be explained with the initial hypothesis that the lobate scarps are the edges of lava flows. At the edge of a lava flow, the ratio of sedimentary to volcanic rock increases causing a decrease in the local gravity field. Furthermore, as the topography steps down, the gravity anomalies measured should also step down due to the increased distance between the seafloor and the ship which is filled by low density saltwater. If the units are of significantly different density, the step will be large. In the case of overlapping lava flows, each of basaltic composition, it is expected that the step is decidedly smaller and depends only on the changing depth of the bodies. The anomalous gravity values coincident with sharp ship turns suggest that the EOTVOS correction is incomplete and that the anomaly values on the turns are due to the changing orientation of the ship and not geological bodies.

Seismic Data

Observations

The NBP 04-01 expedition produced four parallel seismic tracks across the northern part of the Franklin Volcanic Field. In addition, an earlier survey reported by Cooper et al. (1987) provides two additional seismic lines, one just North of Franklin Island and the other trending southeast through Potter Peak. Figure 36 shows the location and subsurface expression of prominent seismic features in the Franklin Volcanic Field.

Figure 36: Location of select seismic features

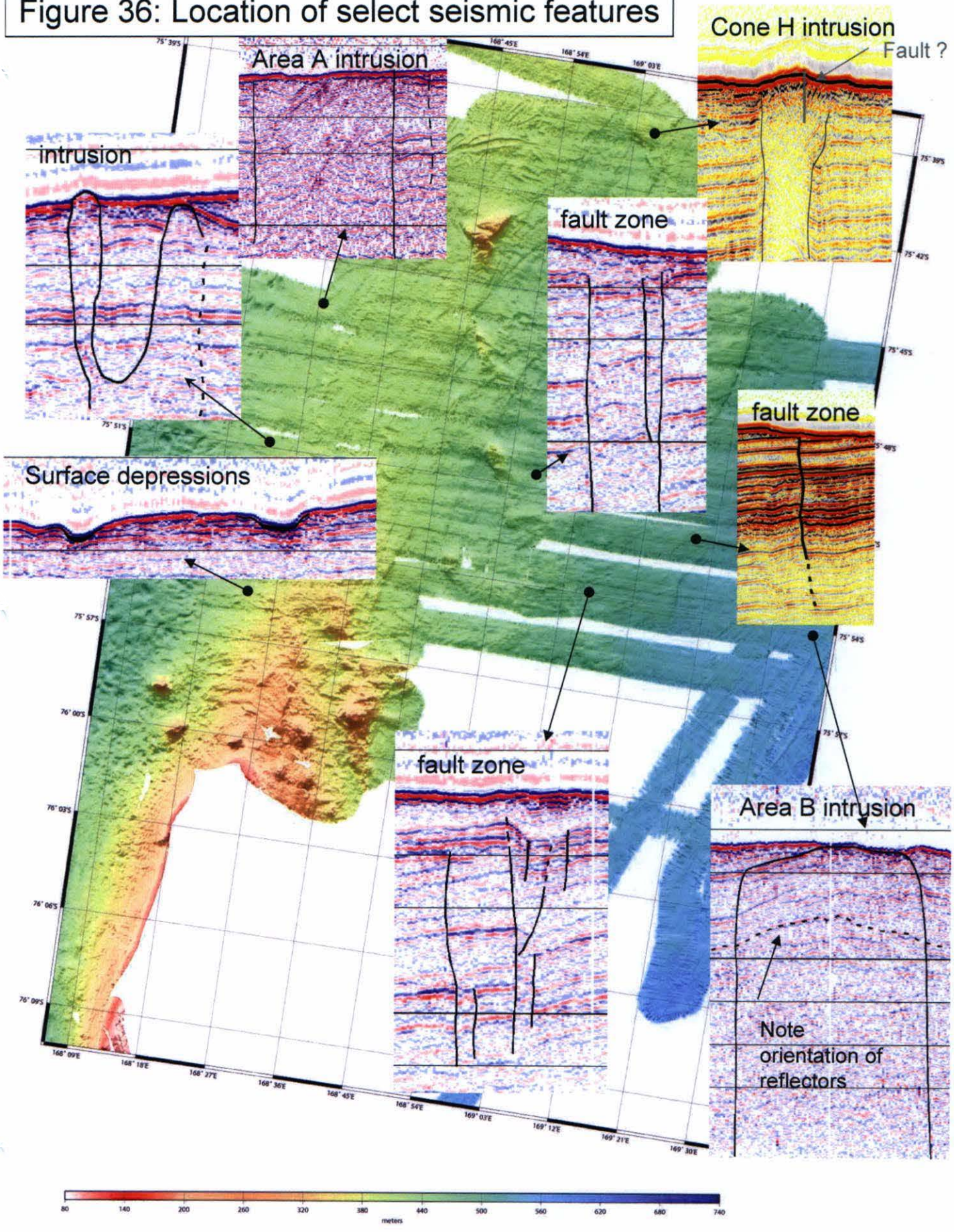

The three bathymetrically defined terrains show a strong degree of contrast in the seismic sections. Common features observed on the seismic lines in the region include an unconformable surface between the gently dipping reflectors of the substrate and the bright near-surface reflectors, vertical zones of blurred and/or arched reflections which are interpreted as igneous intrusive bodies, and steeply dipping lines or linear zones of truncation and offset of reflectors, interpreted as faults.

The regional pattern of reflectors across the Franklin Volcanic Field defines a broad syncline in sedimentary basin strata. In the west, east-dipping strata are truncated and overlain by subhorizontal layers, whereas in the east the west-dipping strata of the syncline are truncated at the seafloor. Along the Franklin Island ridge there is a superimposed central arch overlying the broad syncline. Layers which comprise the arch dip and thin away from the central axis suggesting that it has been built up by successive volcanic intrusions.

Western Hummocky terrain

The substrate of the hummocky terrain consists of subhorizontal or gently east-dipping planar reflectors. The surface is marked by sparse depressions under which the reflectors on either side are downwarped toward the center of the depression and the uppermost reflector thickens at the base. Near the northern limit of the western terrain, in the area labeled Area A, there is a broad, steep-sided zone of near-complete disruption of reflectors. This feature lacks surface expression. Inside this feature, near the surface, linear zones of possible reflections or diffractions dip steeply into the zone. To the south,

in the same region, there are two closely spaced features which also have steep sided contacts and internal zones with strongly arched reflectors.

Central Volcanic terrain

Lines 112, 141, 142, 143 and 408 transect the curvilinear escarpments (E1, E2 and E3) which extend the length of the northern FVF. Due to the current state of data processing, their subsurface character is obscure on lines 141, 142 and 143. On line 142, a narrow zone that has sharp boundaries and is associated with abrupt dip changes of reflectors is co-located with E2. Line 112 shows minimal evidence of E1 and E2 on surface topography and in cross section. Line 408 shows a zone of closely spaced offsets just east of Potter Peak that appear to coincide with the branches of the E1 escarpment, and a plane with offset and truncation which correlates with the E3 escarpment.

Zones of closely spaced, steeply dipping lines of truncation and offset can be observed on lines 141 and 142. The western margin of these zones is an east dipping line which shows truncation and down-to-the-east offset of reflectors. The eastern margin of these zones dips steeply west and has down-to-the-west offset of reflectors. In between the zone boundaries, reflector geometry is irregular.

Cone H is underlain by a broad zone with nearly vertical contacts surrounding near completely disrupted reflectors. Reflectors immediately adjacent to the contacts dip steeply away from the zone. Within the zone, bright reflectors dip toward the center. Escarpment LS1, which shows some topographic linkage with Cone H, is underlain by a narrow zone of arched reflectors, seen on profile 111.

Near the border between the volcanic and lineated terrains there is a sharp line of offset and truncation of reflectors along profiles 142 and 110 with strata displaced down to the east. The offset and truncation observed in these sections is not evident on lines 141 and 112 therefore this feature has limited lateral extent.

Eastern Lineated terrain

The lineated terrain has an irregular surface topography consisting of low relief ridges and grooves. In the north, the subsurface reflectors are gently west dipping and uninterrupted. Although not distinctive bathymetrically, Area B shows a zone that is either characterized by disrupted or strongly arched reflectors on lines 141, 142, and 408. Reflectors adjacent to the contacts dip steeply away from the zone margins. Correlation of this feature between the seismic lines indicates it has a northeast trend. Projection of this trend southwestward intersects line 407 where a similar, but less well defined, zone occurs. The top of the zone of arched reflectors reaches the surface and is truncated by a plane of ridge and groove morphology much like the areas to the north.

Interpretation

Based on examples from Bally (1983), steep sided zones in which reflectors are strongly disrupted and/or arched upward are common signatures of intrusive bodies. Normal faults are indicated by steeply dipping lines or zones of truncation and offset. Using the seismic expressions of these features as analogues, the following hypotheses were formed.

Western hummocky terrain

The dip of surface reflectors into the depressions suggests either downward collapse or deposition over an existing low point. The thickening of the unit that underlies the base of the depression points to localized deposition in a depression. These are probably glacial depositional features, presumably associated with retreat of grounded ice from the region.

The broad, near vertical disruptions or reflectors are interpreted as dike intrusions. The two steep arched features of line 142 are two dikes and a broader dike intrusion is interpreted on line 143.

Central volcanic terrain

The layered arch along the axis of the Franklin Volcanic Field is interpreted to be constructed of extrusive volcanic layers. Along line 407 (Cooper et al, 1987) there is a broad, near vertical intrusion corresponding to the location of Franklin Island ridge (Figure 37). This is presumably part of the main feeder system for the volcanic field. In addition to the magmatic body under the main ridge, line 407 shows dike intrusions are vertical feeders below volcanic cones D and E. Both line 407 and Line 141 show a narrow dike-like body below ridge R1, just east of the Franklin Island ridge axis. This intrusion supports the previous hypothesis that this ridge is the result of magmatic intrusion and that its flanking lobate morphology is due to extrusive lava flows.

The geometry and offset seen in the zone of truncation and offset on lines 141 and 142 is typical of a graben downdropped between normal faults, a tectonic structure typical of extensional settings. The boundaries of this feature are indicative of faulting

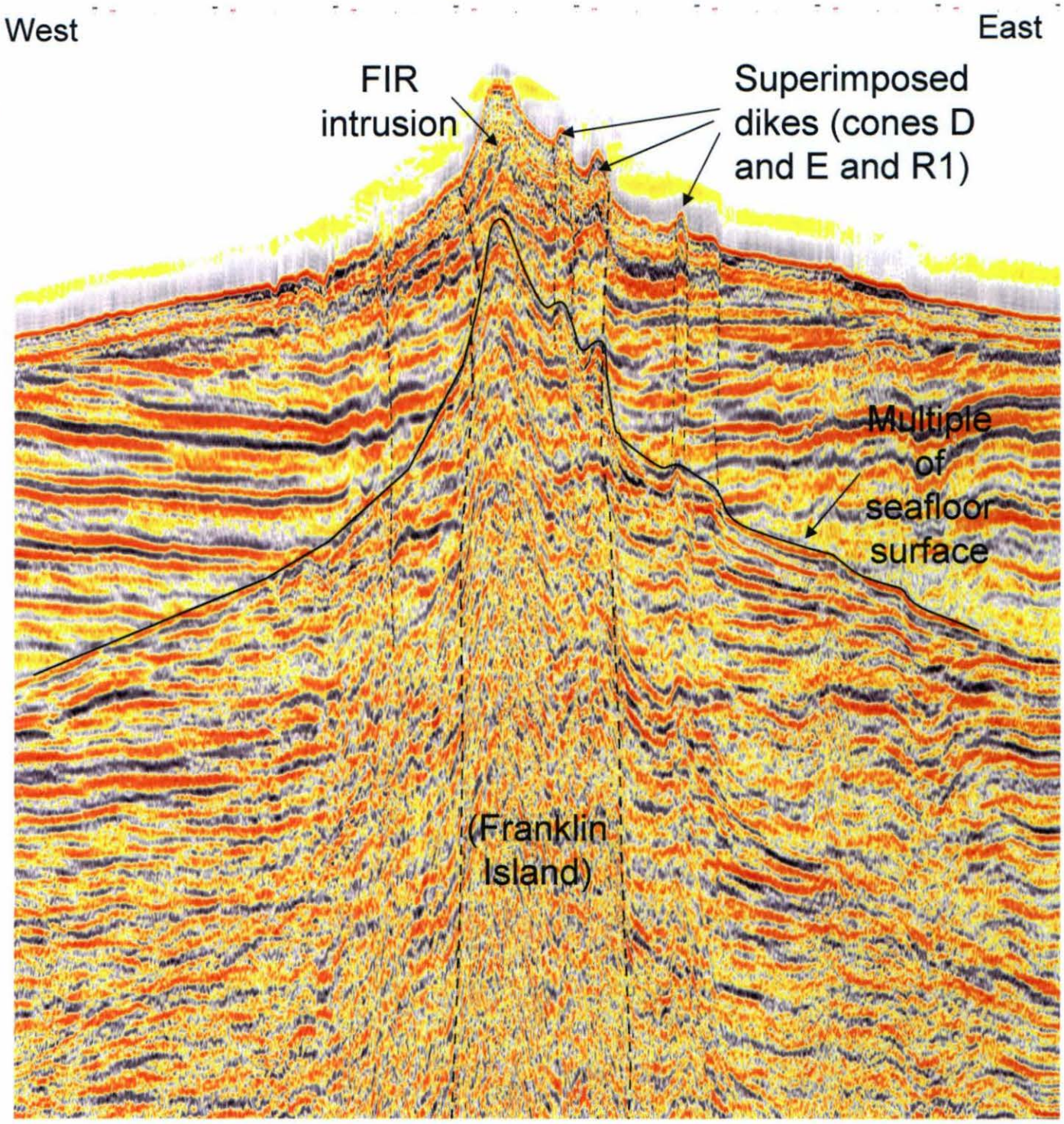

Figure 37: Volcanic intrusions of seismic line SP Lee 407 (Cooper et al., 1987)

whereas the disruption of strata implicates a magmatic origin. Although some seismic lines are shifted from their true location, the positive relief of R2 can be observed on the seismic lines and does not correlate with the graben.

The subsurface structure below escarpments E1, E2 and E3 is difficult to observe on most seismic sections. The underlying strata are in fact disturbed but the nature of that disturbance is difficult to discern, and could mark faults or intrusive bodies. However, the fact that there is subsurface expression does suggest that the features are not formed by glacial erosion. Line 408 best displays the cross sectional view, showing three closely spaced truncations which correlate to the E1a, E1b and E1c branches and an additional truncation at E3 (Figure 38). The truncated geometry points to faults with normal displacement underlying the E1 scarps. Based on their close association in trend and morphology, all the escarpments appear to most likely be normal faults.

Cone H is volcanic in origin, and is underlain by a dike intrusion. The apparent dip of internal reflectors may be an indication that there is a cap on the surface of the intrusion which is harder than the surrounding lithology.

LS1 sits halfway between the edge of the E3 escarpments and lobate escarpments defining the margins of the central terrain as defined here. Its origin was in question because of its intermediate location, orientation and morphology in comparison to escarpments on either side. In the seismic section, LS1 is underlain by a volcanic intrusion which is much wider than the scarp itself. This intrusion points to a more ridge like geometry for the escarpment which is not well defined bathymetrically.

The eastern margin of the volcanic terrain (vicinity of LS2), was preliminarily interpreted as the edges of successive lava flows. This region shows a stair case pattern in

Figure 38: USGS Seismic Line 408 (Cooper et al., 1987)

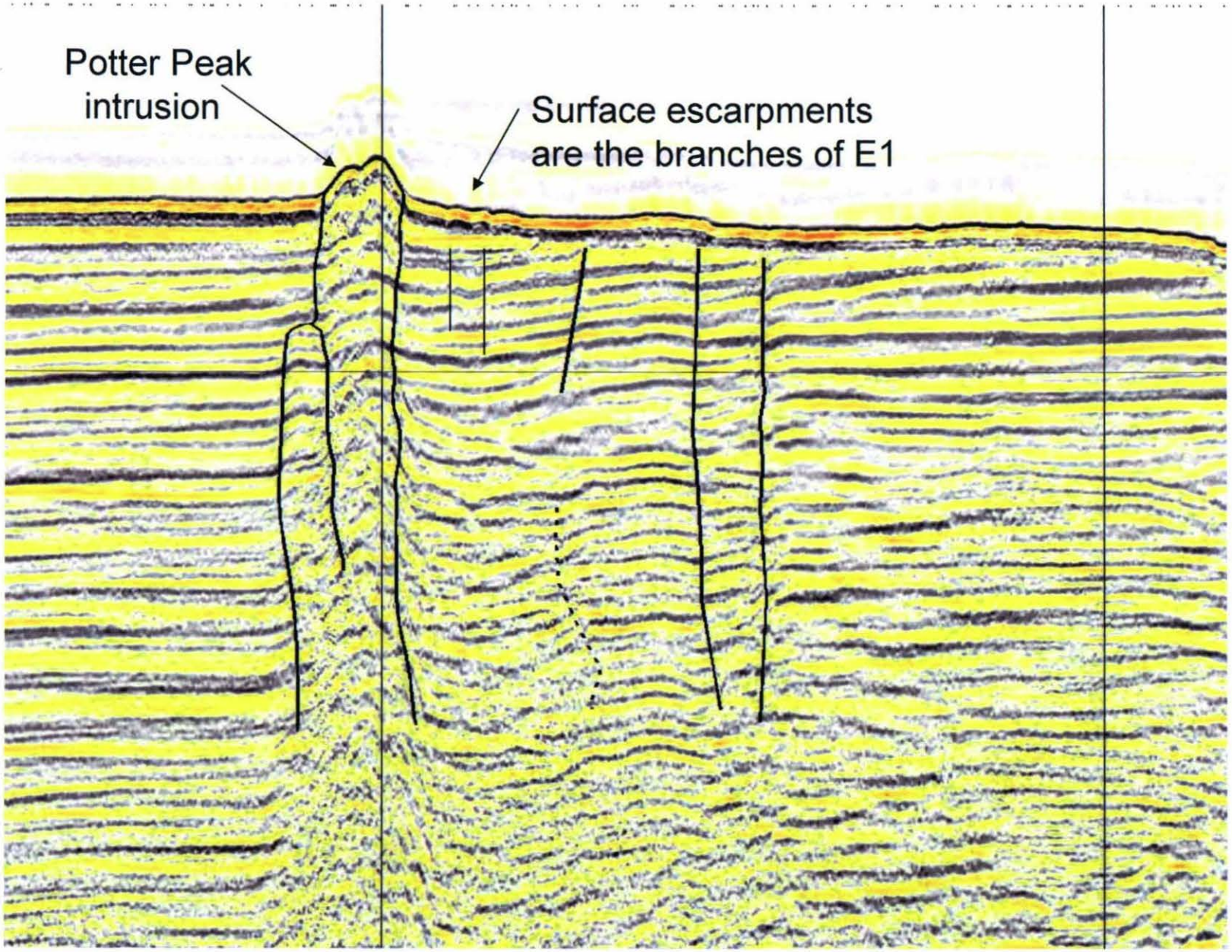

cross section on the seismic profiles. Along line 141, the staircase 'steps' occur where west-dipping layers intersect the seafloor. This is compatible with the lobate escarpments marking the margins of lava flows, although some erosional truncation of the volcanic layers may also have occurred.

Eastern Lineated terrain

The overall ridge and groove morphology points to erosional processes. Individual ridges and grooves appear to lack any associated subsurface structure, which is consistent with their formation by glacial erosion of the seafloor. Area B has either the disrupted reflectors or the arched reflector geometry which is commonly seen in volcanic intrusions. The truncation of the arch at the surface is an indication that post depositional erosion leveled off this feature. Thus the current surface morphology is a combination of volcanic and glacial processes.

Discussion

Combining the observations made in the magnetic, gravity and seismic data sets the features can be divided into three classes of different origin. The class of volcanic features includes the FIR, cones A-J, R1, R2, the lobate scarps (LS1, LS2 and LS3) as well as the intrusive bodies under Area A and Area B. The most likely interpretation for the long escarpments, E1 including its branches, E2 and E3 is that they are tectonically formed normal faults with displacement down to the east. The glacial features include the surfaces depressions of the western hummocky terrain, the ridge and groove morphology of the eastern lineated terrain and the ice berg scours throughout the central volcanic terrain. The classification of these features is depicted spatially in Figure 39.

Within the each class of origin, the trends of surface and subsurface features can be mapped. Surface features are mapped by lateral continuity whereas subsurface features, such as the intrusion under Area A, are mapped by correlation between seismic lines or consistent trends in both the seismic and bathymetric data. The map reveals two volcanic trends. The northeast orientation is expressed on the surface by the Franklin Island ridge, the curvilinear escarpments and the elongation of cones B and C. In the subsurface, this trend is paralleled by the intrusions under Area A and Area B. The northwest trend is expressed on the surface by ridges R1, R2 and R3; cones H and J; and the elongate crater of cone F. The number of associated features and greater continuity of the northeast trend suggest it is the primary trend of the Franklin Volcanic Field. A radial pattern, which is commonly associated with large magma conduits, is not observed in the cones near Franklin Island, indicating that the regional stress field was stronger than the magmatic pressure built up by the intrusives.

Figure 39: Features of the Franklin Volcanic Field distinguished by origin

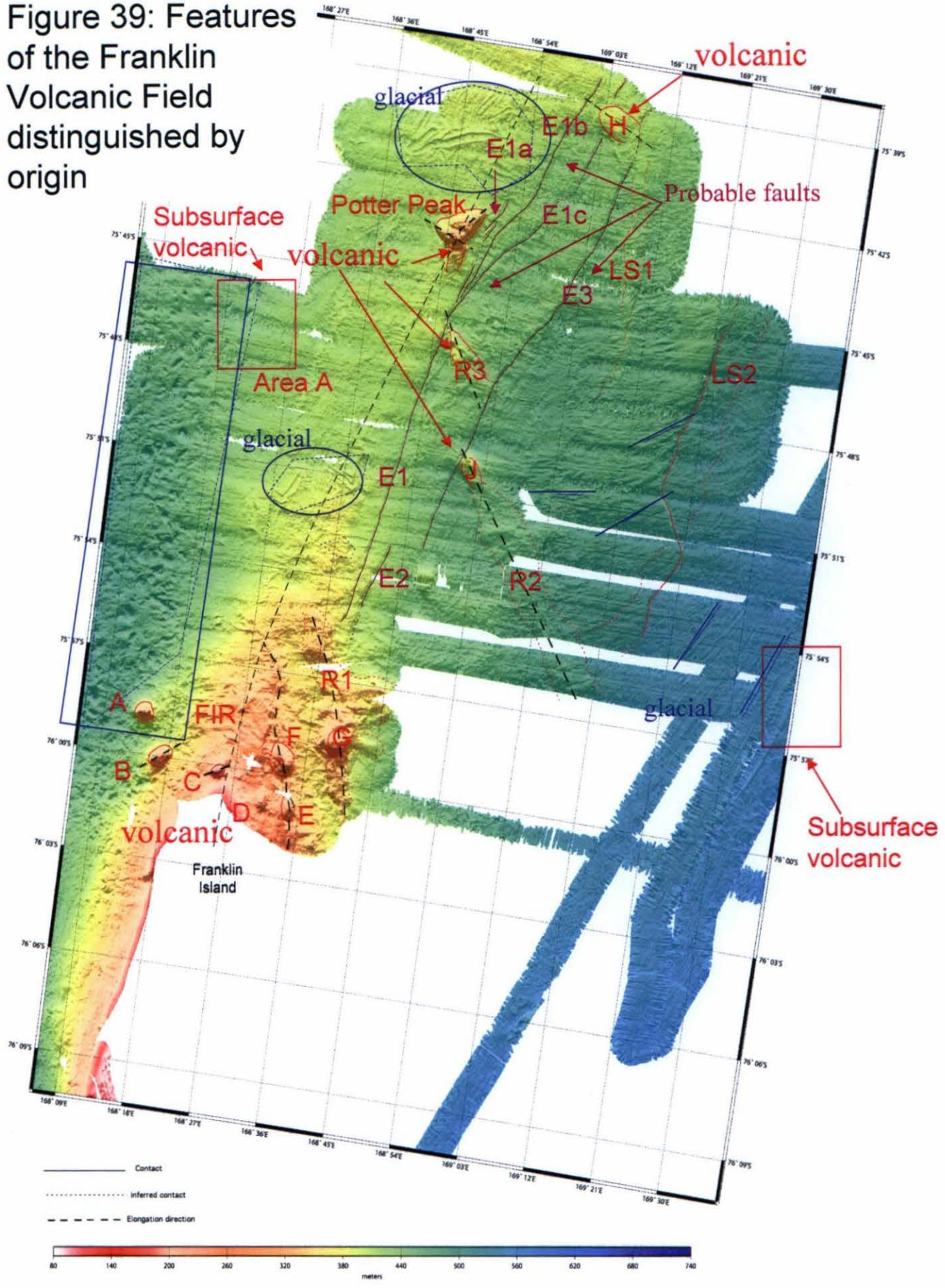

The bathymetric and seismic superposition of the cones suggests that they formed at a later date than the ridge on which they sit. The subsurface dikes, which may be feeders for the cones or sources of the local lava flows, may be either coeval or younger than the FIR. The E1, E2 and E3 escarpments cross cut features of volcanic origin, including cone H and R2, pointing to a younger age for the tectonic features. However, there is also evidence that lava flows of R1 and FIR may overly the escarpments. The fault observed on seismic line 110 cross cuts substrate reflectors but appears to be truncated by the bright surface reflectors which are currently interpreted as lava flows. This indicates that this fault preceded the extrusion of the most recent lava flow which is defined by the LS2 escarpment. Given that the volcanic and tectonic features show evidence of temporal overlap, it is reasonable to consider them two modes of response to the same stress regime. The regional occurrence of two volcanic trends suggests that one of the trends is either controlled by pre-existing structure or formed by a different stress regime acting at a different period of time.

Glacial flow reconstruction

The frequency and regular spacing of the lineations of the eastern lineated terrain suggests they formed in the direction of ice sheet movement. The ridge and groove fabric trends approximately 25 degrees east of North. Although the measure of lateral continuity is limited by the extent of the mapped region, the features may be additional mega-scale glacial lineations like those mapped throughout the Ross Sea by Shipp et al. (1999). These lineations form as soft sediment is deformed at the basal contact of a grounded ice

sheet and parallel the direction of ice flow. Figure 40 compares the local flow direction observed in the eastern lineated terrain with regionally mapped patterns.

The features of the western hummocky terrain lack an indication of glacial flow direction. However, they support the current reconstruction which calls for a grounded ice sheet throughout the embayment during the Last Glacial Maximum.

Stress reconstruction

Based on the geometry of the FIR and trend of the escarpments, it is concluded that the length of these features parallels the maximum horizontal stress whereas the underlying feeder system has opened perpendicular to the long axis and parallels the minimum horizontal stress. The observation of faults in the seismic profiles constrains the magnitude of the third, vertical stress direction which is perpendicular to the surface of the Earth. According to Anderson's theory of faulting, the normal displacement along the curvilinear escarpments formed in response to the maximum principal stress, S1, being oriented vertically while the direction of downdropping points to extension, in response to S3, in the east-west direction. Thus, in the Franklin Volcanic Field, S2, the intermediate compressive stress is oriented 11 degrees east of North, with S3 perpendicular in the horizontal plane and S1 perpendicular in the vertical dimension (Figure 41).

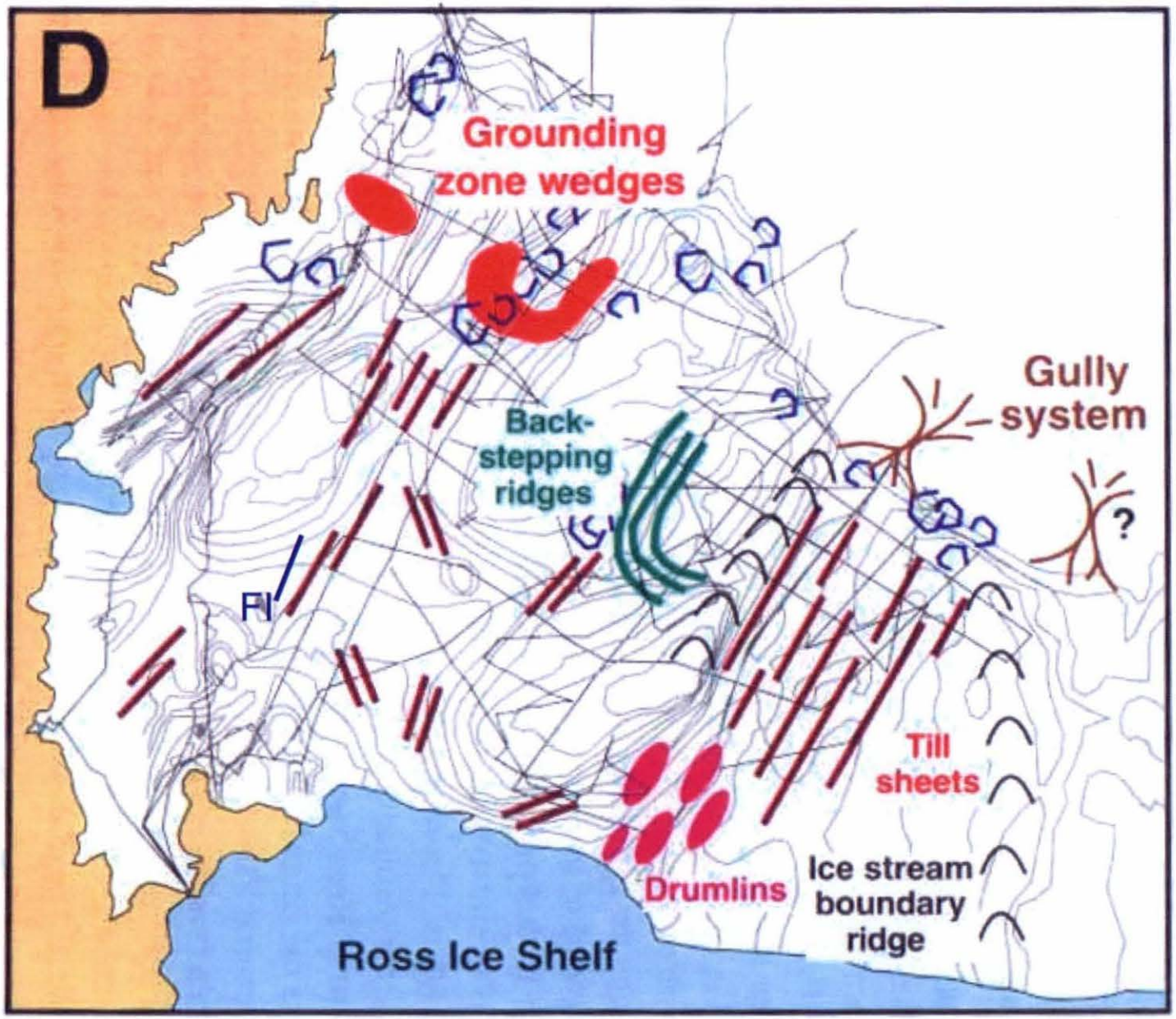

Figure 40: Local ice flow directions as indicated by 25 East of North trend of the eastern lineated terrain

Figure 41
Orientation of principal stress directions in FVF

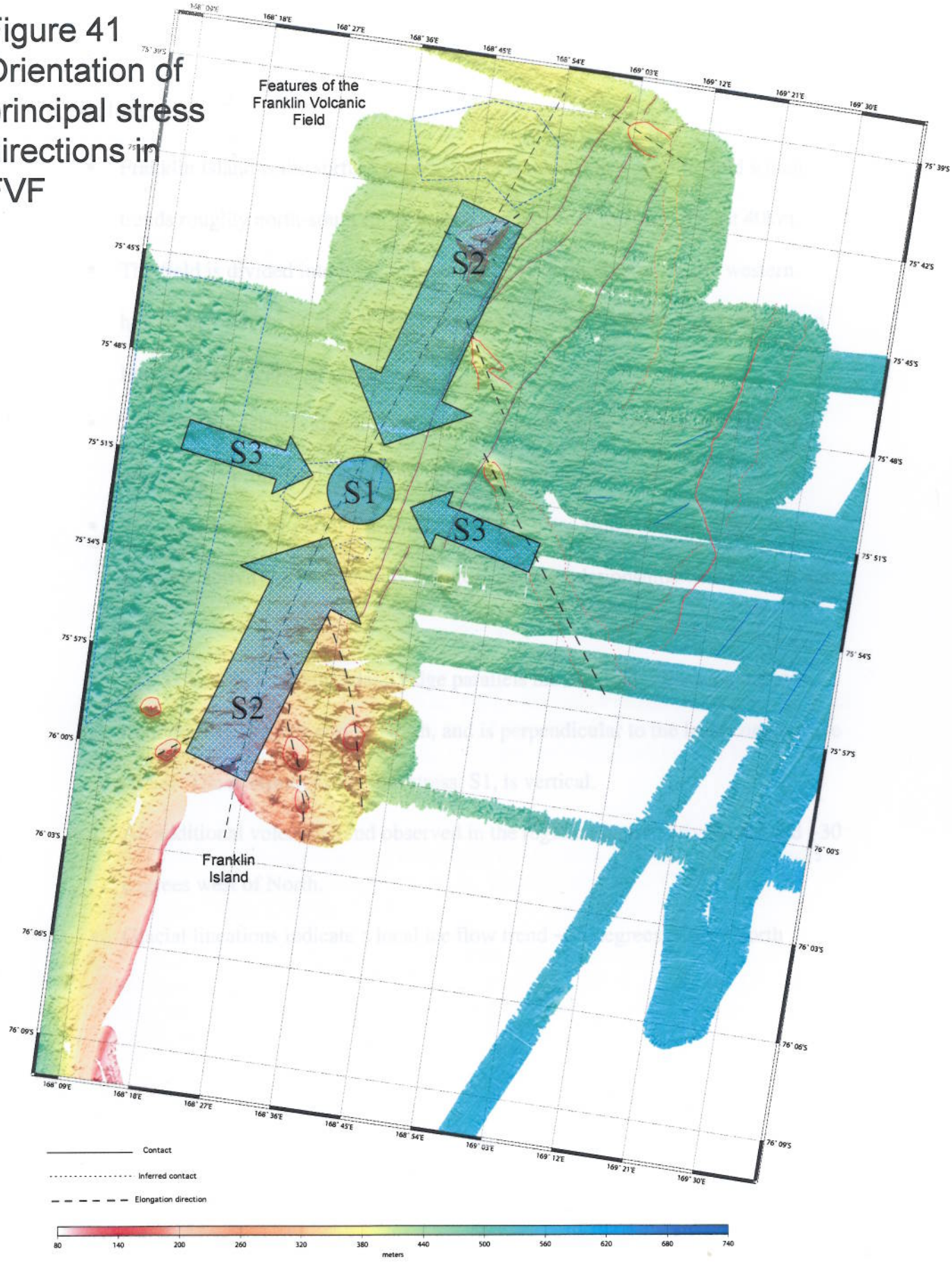

Conclusions

- Franklin Island is the surface expression of a submarine volcanic field which trends roughly north-south for at least 80km and east-west for at least 40km
- The field is divided into three morphologically defined terrains, the western hummocky terrain of glacial origin, the central volcanic terrain, and the eastern lineated terrain, also of glacial origin.
- The Franklin Island ridge formed during multiple phases of volcanic intrusion, producing a prominent ridge with superimposed volcanic cones
- The ridge is cut by parallel normal faults which are either coeval or post date volcanic activity as indicated by the cross cutting relationships with Cone H and Ridge 1.
- The axis of the Franklin Island ridge parallels the maximum horizontal stress, trending ~11 degrees east of North, and is perpendicular to the least compressive stress. The maximum principal stress, S1, is vertical.
- An additional volcanic trend observed in the regional bathymetry is oriented ~30 degrees west of North.
- Glacial lineations indicate a local ice flow trend ~25 degrees east of North

References

Anderson, John B., 1999. Antarctic Marine Geology Cambridge University Press, New York pp. 29, 65-70, 241

ANTOSTRAT Project, 1995. Seismic stratigraphic atlas of the Ross Sea, Antarctica. In: A.K. Cooper, P.F. Barker, and G. Brancolini (Editors), Geology and Seismic Stratigraphy of the Antarctic Margin. American Geophysical Union, Antarctic Research Series, 68: Plates.

Bally, A.W. (editor) 1983, Seismic expression of structural styles: A picture work atlas Vol. 1. The American Association of Petroleum Geologists

Barrett P.J., Henrys S., Bartek L.R., Brancolini G., Busetti M., Davey F.J., Hannah M.J. & Pyne A.R., 1995. Geology of the margin of the Victoria Land basin off Cape Roberts, southwest Ross Sea. In: Cooper A.K., Barker P.F. & Brancolini G. (eds.), *Geology and Seismic Stratigraphy of the Antarctic Margin, Antarctic Research Series*, **68** AGU, Washington, 183-208.

Cape Roberts Science Team, 1999. Studies from the Cape Roberts Project, Ross Sea, Antarctica – Initial Report on CRP-2/2A. Terra Antarct., vol. 6, p. 1-173.

Chiappini, M., Ferraccioli, F., Bozzo, E., Damaske, D., 2001. Geomagnetic investigations and regional aeromagnectic anomaly map over the Transantarctic Mountains – Ross Sea sector of the Antarctic. Tectonophysics

Cooper, A.K., Davey, F.J. and Behrendt, J.C. 1987. Seismic stratigraphy and structure of the Victoria Land Basin, Western Ross Sea, Antarctica. **in** Cooper, A.K. and Davey, F.J. *The Antarctic Continental Margin: Geology and Geophysics of the Western Ross Sea.* CPCEMR, **5b,** Houston, Texas. p27-77.

Cooper, A.K., Davey, F.J., Behrendt, J.C. 1987. Seismic Stratigraphy and Structure of the Victoria Land Basin, Western Ross Sea, Antarctica in The Antarctic Continenetal Margin: Geology and Geophysics of the Western Ross Sea, CPCEMR Earth Science Series, v. 5b pp. 27-76

Davey, F.J. And Brancolini, G., 1995. The Late Mesozoic and Cenozoic structural setting of the Ross Sea Region. In: A.K. Cooper, P.F. Barker and G. Brancolini (Editors), Geology and seismic stratigraphy of the Antarctic Margin, Antarct. Res. Ser., AGU, Washington D.C., vol. 68, p.167-183.

Dalziel, I.W.D. and Elliot, D.H., 1982. West Antarctica: Problem child of Gondwanaland. Tectonics, 1: 3-19.

Fitzgerald, P., 2002. Tectonics and landscape evolution of the Antarctic Plate since the breakup of Gonwana, with an emphasis on the West Antarctic Rift System and the Transantarctic Mountains. Royal Society of New Zealand Bulletin 35: 2002, pp453-469

Hambrey, M., 1994. Glacial Environments. UVC Press, Vanvouver. pp. 81-109

Kearey, P., and Brooks, M., 1984. An Introduction to Geophysical Exploration Sec Ed. Blackwell Scientific Publications. Ch 7 pp. 148-171

Kyle, P.R., 1990. McMurdo Volcanic Group, western Ross Embayment: Introduction, in LeMasurier, W.E. and J. W. Thomson, (eds.), Volcanoes of the Antarctic Plate and southern Oceans. AGU Antarctic Res. Ser., vol. 48, p. 19-25.

Kyle, P.R. 1990. The Erebus Volcanic Province. **in** LeMasurier W.E. and Thomson, J.W. (eds) 1990.*Volcanoes of the Antarctic Plate and Southern Oceans.* Washington D.C. American Geophysical Union. p81-88.

Kyle, P.R., 1990. Chapter A.13 Franklin Island in LeMasurier, W.E. and J. W. Thomson, (eds.), Volcanoes of the Antarctic Plate and southern Oceans. AGU Antarctic Res. Ser., vol. 48, p. 91-93.

McClay, Ken, 1987. The Mapping of Geologic Structures. John Wiley and Sons Publishers New York, 161 pp.

Musset, A.E., and Khan, M. A., 2000. Looking into the Earth: An introduction to geological geophysics. Cambridge University Press, New York, 470 p

Nakamura, Kazuaki., 1977. Volcanoes as possible indicators of tectonic stress orientation- principal and proposal. Journal of Volcanology and Geothermal Research., vol 2: 1-16

Park, R. G., 1989. Foundations of Structural Geology. Chapman and Hall, New York, 148 pp.

Rocchi, S, Armieti, P, D'Orazio, M., Tonarini, S., Wijbrans, J. R., Di Vincenzo, G. 2002 Cenozoic magmatism in the western Ross Embayment: Role of mantle plume versus plate dynamics in the development of the West Antarctic Rift System. Journal of Geophysical Research, Vol. 107 No B9, 2195

Salvini, F., and Storti, F., 1999, Cenozoic tectonic lineaments of the Terra Nova Bay region, Ross Embayment, Antarctica. Global and Planetary Change, 23: 129-144.

Shipp, S.S. and Anderson, J.B., 1997. Lineations on the Ross Sea Continental Shelf, Antarctica in Glaciated Continental Margins: an Atlas of Acoustic Images. Davies, T.A editor. Chapman and Hall. London 315 p.

Shipp, S.S. and Anderson, J.B., 1999.Late Pleistocene-Holocene retreat of the West Antarctic Ice-Sheet system in the Ross Sea: Part 1-Geophysical result. Geological Society of America Bulletin vol. 111, no 10. pp.1486-1516

Suppe, J., 1985. Principals of Structural Geology. Prentice-Hall Inc. Englewood Cliffs, New Jersey. 537 p. : ill. ; 29 cm

Verosub, K.L., 2000. Paleomagnetic Dating in Quaternary Geochronology: Methods and Applications. Noller, J.S., Sowers, J. M. and Lettis, W. R. (editors) American Geophysical Union

Wellner, J., Lowes, A.S., Shippe, S.S. and Anderson, J.B., 2001. Distribution of glacial geomorphic features on the Antarctic Continental shelf and correlation with substrate: implications for ice behavior. Journal of Glaciology, vol 47, No158 pp.397-411

Appendix A: Relevant Time scales

Geologic time scale for the Phanerozoic

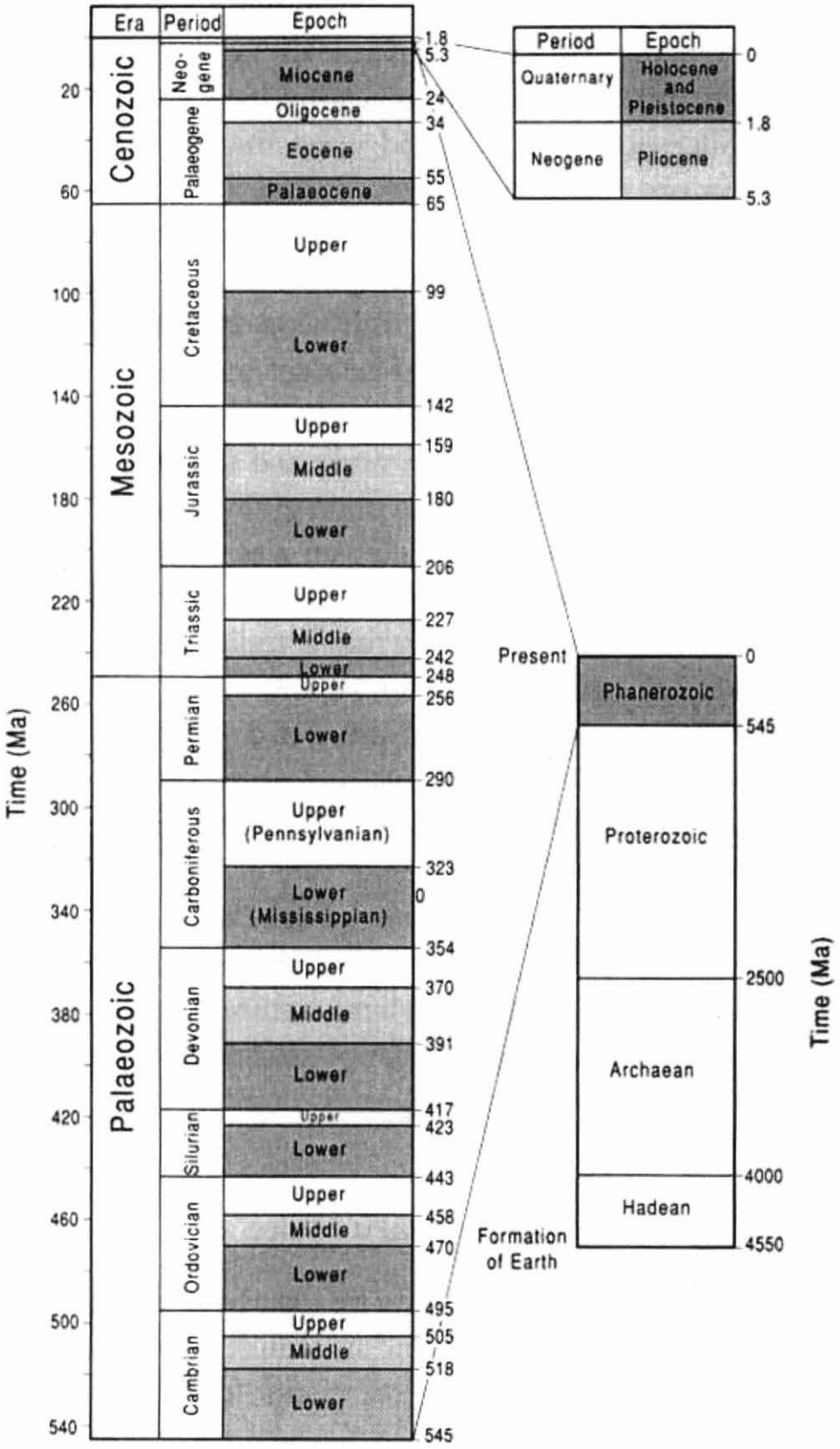

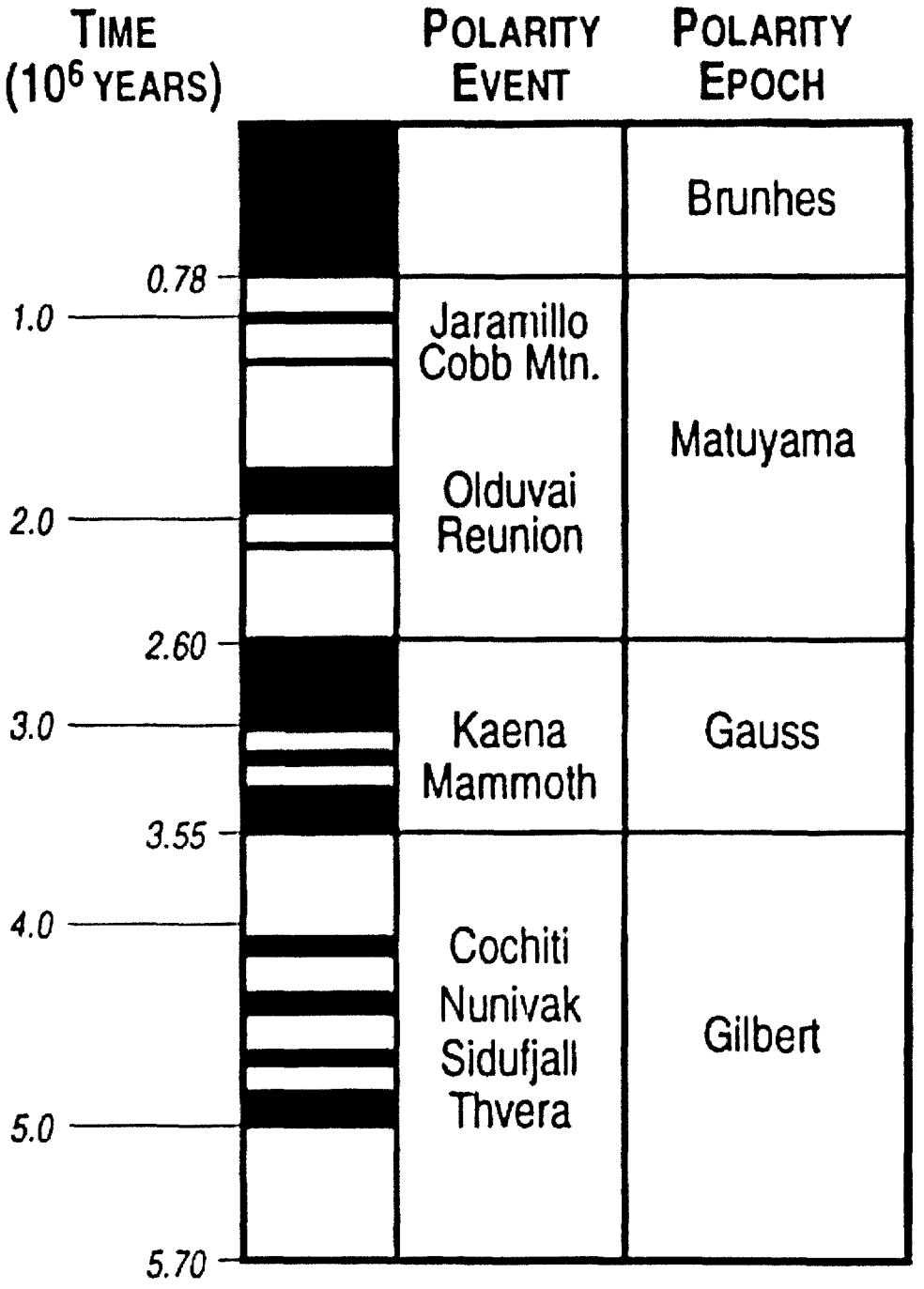

Magnetic polarity time scale. Periods of normal polarity are shaded. (Noller et al., 2000)

Appendix B: Magnetic Data Addendum

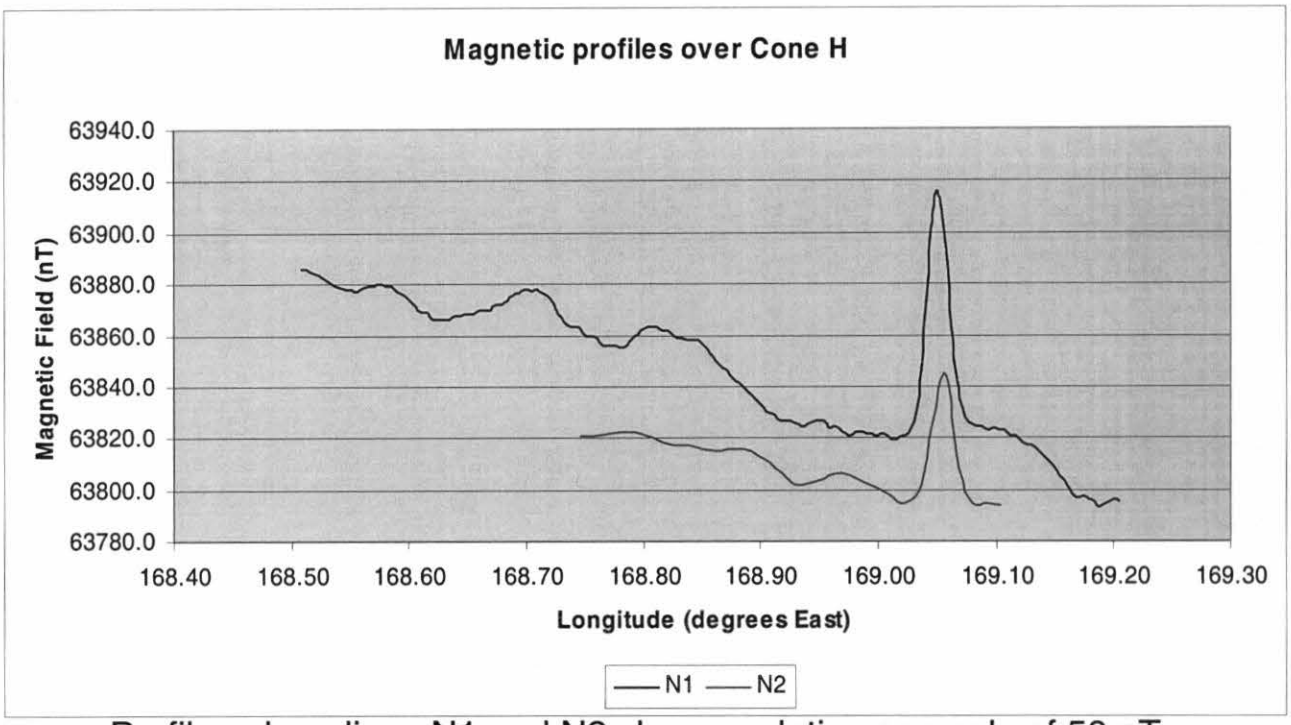

Profiles along lines N1 and N2 show a relative anomaly of 50 nT to 70 nT over cone H. Note contrast to profiles for scarps.

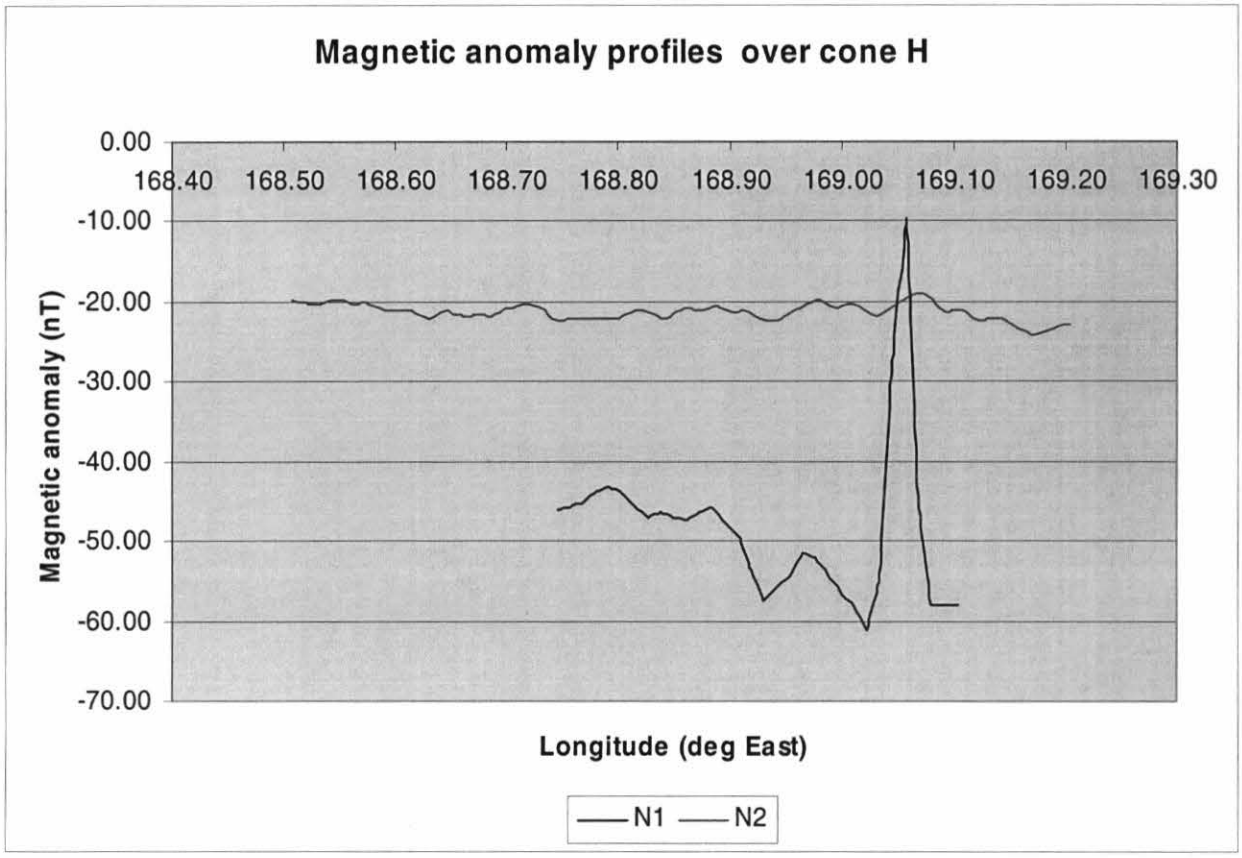

Corresponding magnetic anomaly profiles over the same cone. The absence of a relative anomaly in the N2 anomaly values is suspect.

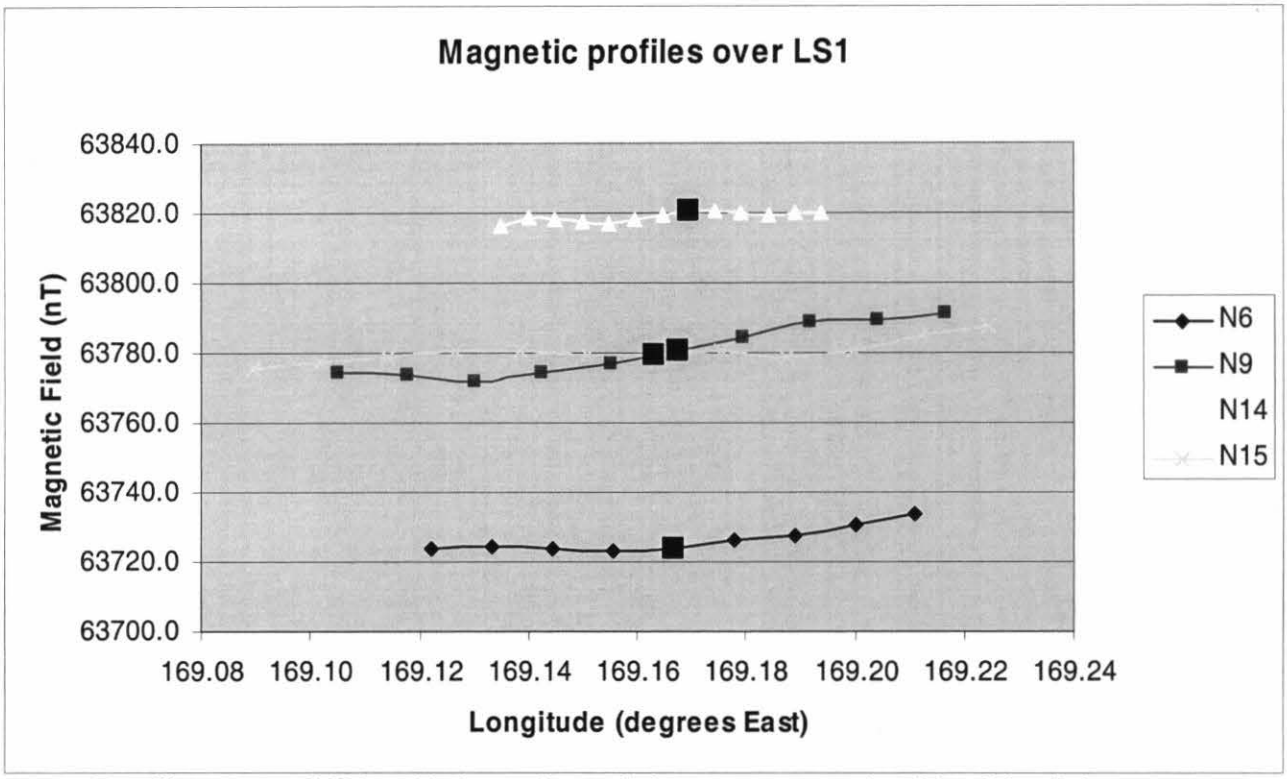

Profiles over LS1 with location of the scarp marked by black boxes. There is a slight change in flexure observed on 3 of the 4 profiles.

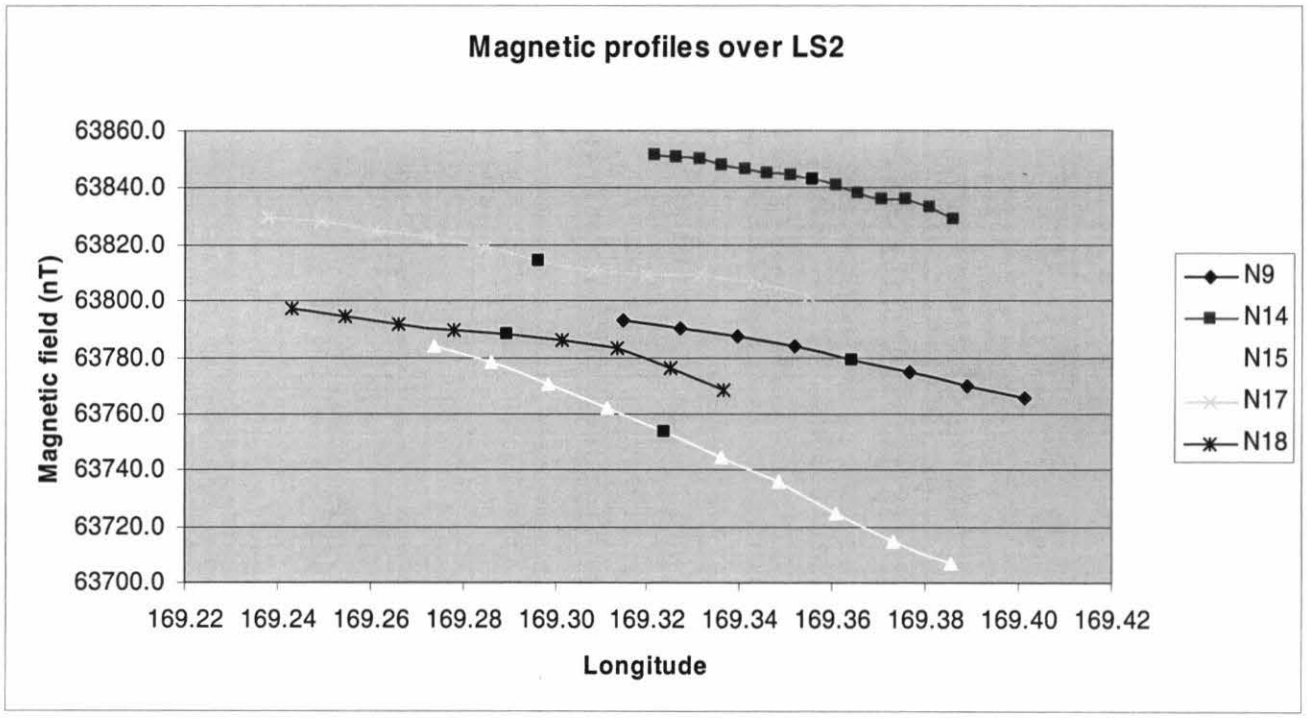

Profiles over LS2 with location of scarp marked in black. 3 of 5 lines show a small change in flexure at the location of the scarp.

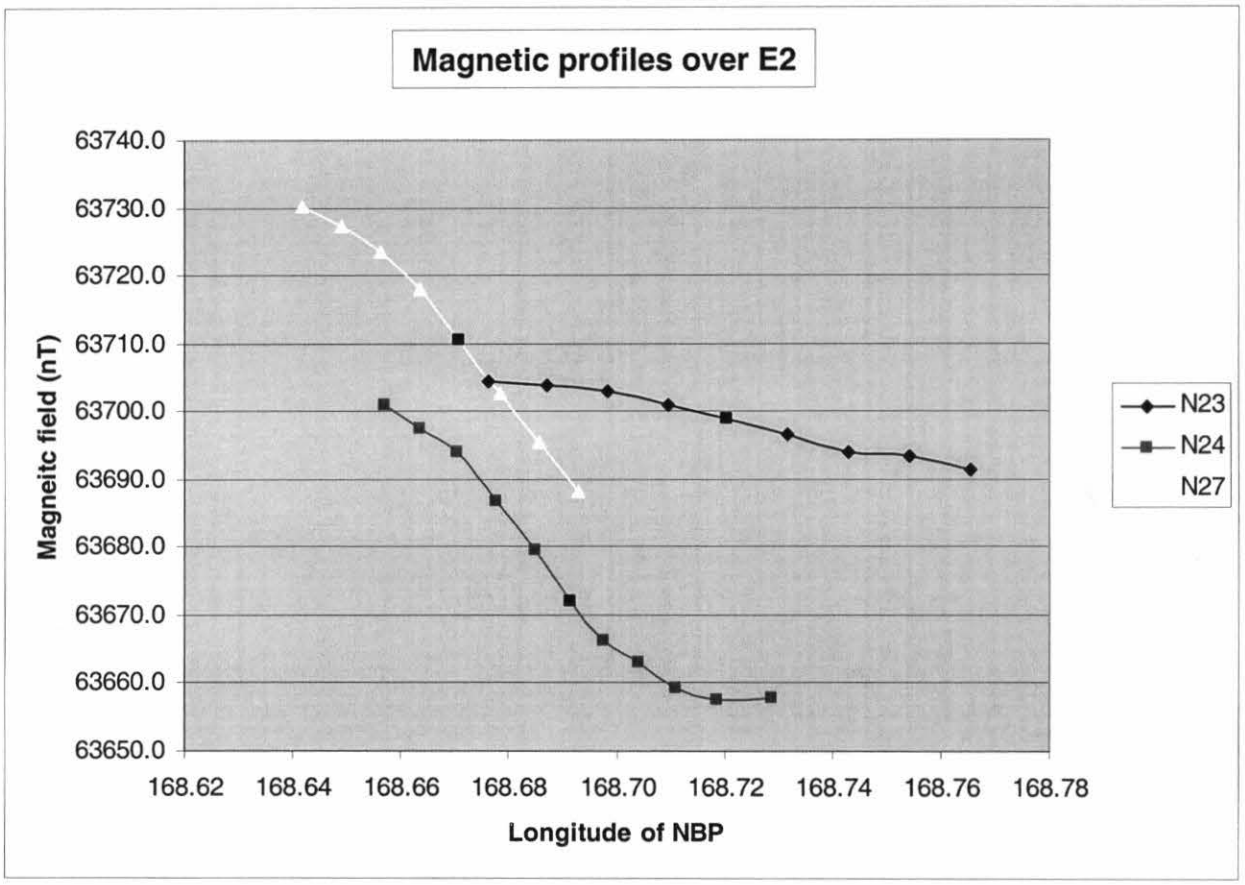

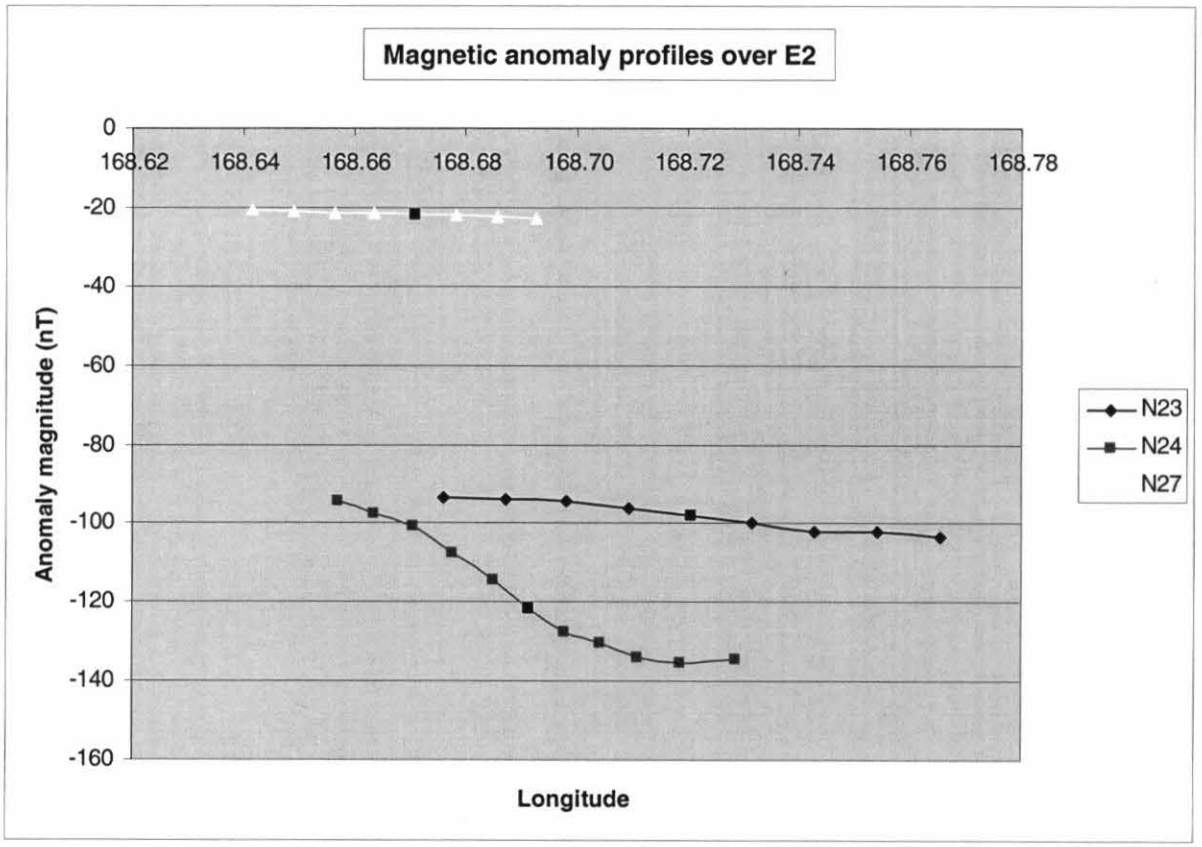

Both magnetic and magnetic anomaly profiles over the E2 escarpment lack evidence of a discrete anomaly.

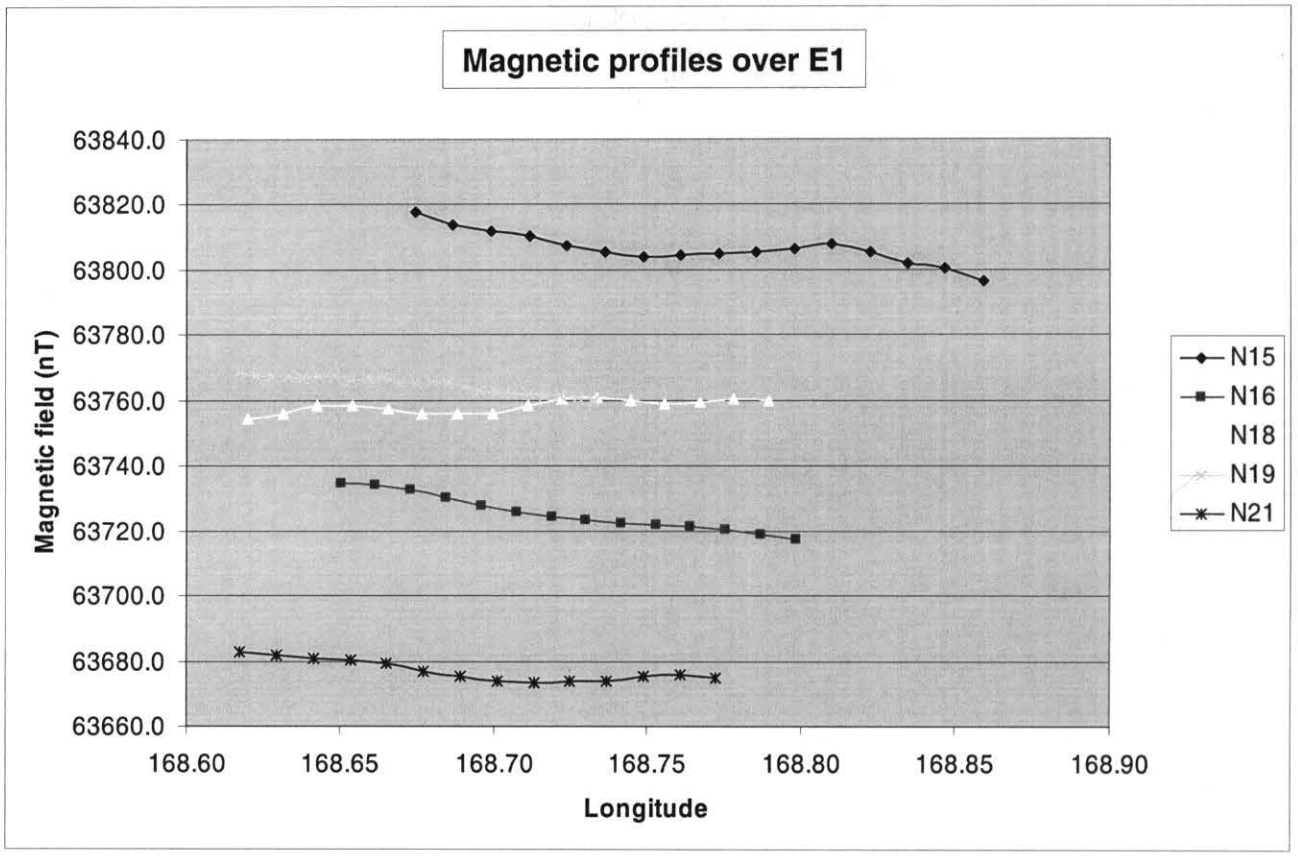

Magnetic profiles across escarpment E1 at varying latitudes. No anomalies are observed.

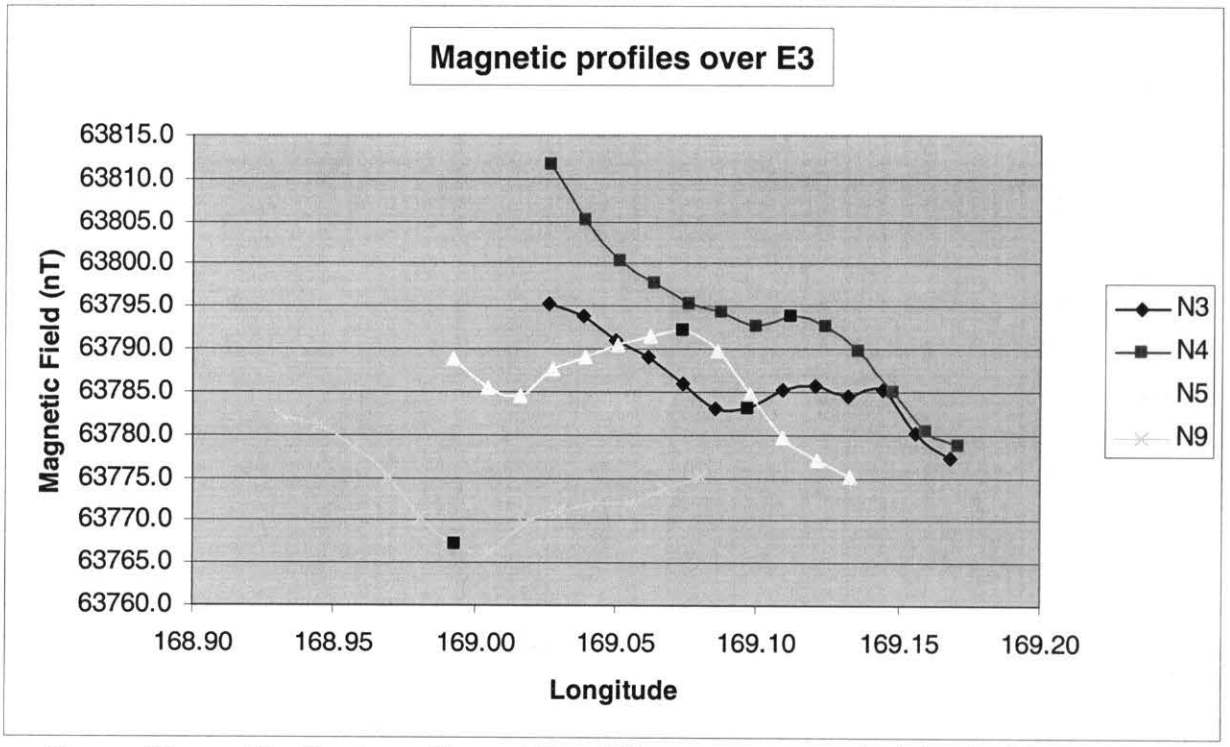

Magnetic profiles with the location of the E3 escarpment in black. Note that variations are only on the order of 15 nT as opposed to the 50nT anomaly seen at cone H.